Tampere University

Ville Raittinen

DESIGN OF A UPS INTEGRATED HEAT EXCHANGER

Product development process utilizing CPM/PDD, DRP, Taguchi method and CFD simulation

Master of Science Thesis
Faculty of Engineering and Natural Sciences
Associate Professor (tenure track) Tero Juuti
University Lecturer Timo Lehtonen
September 2022

ABSTRACT

Ville Raittinen: Design of a UPS Integrated Heat Exchanger
Master of Science Thesis
Tampere University
Master's Degree Programme in Mechanical Engineering
September 2022

Thesis objective is to study how CPM/PDD, DRP, Taguchi methods and CFD simulation integrate to each other. Study is done by using a case study which is developing prototype for a proof of UPS integrated heat exchanger concept. This thesis uses a CPM/PDD method for a framework to product development and integrates DRP and Taguchi methods and approximate calculations and CFD simulation tools to it.

Thesis goes through a little bit of a background of UPS and case study's subject. Before diving into subject, thesis determines the research methodology and opens how research is made. After principal information of research, thesis presents the theory behind the CPM/PDD, DRP, Taguchi methods, thermal and flow calculations and CFD simulation. Last parts of thesis present how theory is applied to case study and proposes results of each of them.

Development starts with project planning using a DRP method, goes on to collecting a list of required properties of UPS integrated heat exchanger and opens CPM/PDD method's applying to case study. Opens available initial information where heat exchanger's dimensioning is based on. Presents results of calculations and CFD simulation. Presents how prototype's testing is made and what are the results of test measurements. Collects all of designer's knowledge to DRP map of product development to use in further product development.

Results for thesis objectives are promising. All of methods and tools integrated to each other. Only inconvenience is that Taguchi method couldn't applied to practice. CPM/PDD and DRP methods nature is kind a same and they fit to each other well. CPM/PDD method is designed to suit tools which determine properties of characteristics, such as calculations and CFD simulation. Case study's subject, a proof of UPS integrated heat exchanger concept, is functional even though every required properties isn't fulfilled.

Keywords: CPM, PDD, characteristics, properties, product development, DRP, design reasoning pattern, heat transfer, pressure drop, heat exchanger, fan, CFD, turbulence, Taguchi, prototype testing, UPS

PREFACE

This thesis addresses the subject of development work behind the UPS integrated heat exchanger. Topic of thesis came from the Eaton Power Quality Oy. They wanted a proof of concept of a working cooling device designed straight to UPS's or at minimum how it should be designed. With a helpful assistance of Associate Professor (tenure track) Tero Juuti thesis got its development methods and boundaries where to start working.

I would like to thank Eaton's Manager of Mechanical Engineering, Juha Manninen, and Mechanical Engineer, Tuomas Alapassi for such an interesting subject and patience during progression of the thesis. I am also grateful for all Eaton's employees who helped me and from whom I learned about UPS devices, building a test bay and prototypes test set-up.

Also, I like to thank University Instructor Niko Niemelä for his advices and help with managing such a complex subject, how to do a CFD simulation from start to finish. Without his help, simulation results wouldn't be reliable or readable.

Tampere, 21.7.2022

Ville Raittinen

CONTENTS

LIST OF FIGURES

LIST OF TABLES

LIST OF ABBREVIATIONS AND SYMBOLS

Abbreviations

AC	Alternating current
ANOVA	Analysis Of Variance
C_i	Characteristics of product
CAD	Computer-Aided Design
CFD	Computational Fluid Dynamics
CPM	Characteristics-Properties Modelling
CPU	Central Processing Unit
CRAC	Computer Room Air-Conditioning
CRAH	Computer Room Air-Handling
CV	Control Volume
D_x	Dependencies between characteristics
DNS	Direct Numerical Simulation
DC	Direct current
DOE	Design Of Experiments
DOF	Degrees Of Freedom
DRP	Design Reasoning Pattern
Eaton PQ	Eaton Power Quality Oy
EC_j	External Conditions
GB	GigaByte
IFM	Information Flow Modelling
ISBM	Integrated System Bypass Module
IT	Information Technology
MSD	Mean Square Deviation
OA	Orthogonal Array
P_j	Properties of product
PDD	Property Driven Development
PR_j	Required Properties of product
R_j	Relation between product characteristics and properties
R_j^{-1}	Relation between product properties and characteristics
RAM	Random Access Memory
RANS	Reynolds-Averaged Navier-Stokes equations
SN	Signal-to-Noise ratio
SST	Shear-Stress Transport
UPM	Uninterruptible Power Module
UPS	Uninterruptible Power Supply
ΔP_j	Deviations between required properties and product properties

Latin symbols

a	Coefficient (eq.64)
$\mathbf{a_c}$	Component vector [-]
a_1	Model specific constant [-]
A	Cross-sectional area of control volume face [m^2]
A_{ep}	Filter's effective pass area [m^2]
A_f	Fin surface area [m^2]
A_{he}	Heat transfer surface area [m^2]
A_i	Normalized dot product of area vector of face [m^2]
A_{in}	Inside surface of tube [m^2]
A_o	Total outer surface of fin and tube [m^2]
A_s	Air inflow smallest cross-sectional area [m^2]
A_{t0}	Surface area of bare tube between fins [m^2]
A_0	Air inflow cross-sectional area [m^2]

b_f	Width of rectangular fin [m]
C	Factor (eq. 13)
C.F.	Correlation factor [-]
c_i	Vector from the centroid of the control volume to the centroid of adjacent control volume that shares that face [m]
d_i	Inner diameter of tube [m]
d_o	Outer diameter of tube [m]
E	East side node [-]
E_{ie}	Internal energy [J]
f_e	DOF of error term [-]
f_i	Vector from centroid of control volume to centroid of to that face [m]
f_{Fn}	DOF of each factor [-]
f_T	Total DOF [-]
F	External body forces [N]
F_{Fn}	Variance ratio [-]
F_{nm}	Factor number and level [-]
F_1	Coefficient (eq. 55)
F_2	Coefficient (eq. 52)
$F(M_t)$	Compressibility function (eq.62)
g	Gravitational magnitude [m/s^2]
G_k	Production of turbulent kinetic energy [J/kg]
G_ω	Generation of dissipation rate [1/s]
h_j	Specific enthalpy [J/kg]
J_j	Mass flux [kg/m^{2}s]
L_n	Array [-]
m	Number of factors [-]
m_{air}	Air flow rate [kg/s]
m_w	Water flow rate [kg/s]
M_t^2	Coefficient (eq. 63)
M_{t0}	Model specific constant [-]
n	Total number of tests [-]
n_n	Test [-]
n_{fp}	Filter's pressure loss coefficient [-]
$\mathbf{n}_{out}$	Normal of outward vector [-]
N	Number of tests or designs [-]
NC	Number of tube columns [-]
Nu_d	Nusselt number for tube bank [-]
NR	Number of tube rows [-]
k	Turbulent kinetic energy [J/kg]
k_{ht}	Overall heat transfer coefficient [W/m^2 K]
K	Loss coefficient for cross flow in tube bank [-]
l_f	Length of rectangular fin [m]
L	Number of levels for each factor [-]
p	Static pressure [Pa]
$p_{dry\ air}$	Partial pressure of dry air [Pa]
$p_{sat.water}$	Pressure of saturated water [Pa]
p_{tot}	Pressure of dry air and water vapor mixture [Pa]
$p_{water\ vapor}$	Partial pressure of water vapor [Pa]
p_0	Pressure at inflow [Pa]
p_1	Pressure at outflow [Pa]
P	Center node [-]
P_{IN}	UPS input electrical power [W]
P_{OUT}	UPS output electrical power [W]
P_{UPS}	UPS power losses [W]
Pr	Prandtl number [-]

$\dot{Q}$	Heat flow [W]
r	Number of repetitions [-]
R	Gas-law constant [$3.314447*10^3$ J/kmol K]
R_β	Model specific constant [-]
R_ω	Model specific constant [-]
Re_d	Reynolds number for heat exchanger's air side [-]
Re_t	Turbulent Reynolds number [-]
RH	Relative Humidity of Air [%]
S	Modulus of mean rate-of-strain tensor [1/s]
S_{diff}	Source term of diffusion [-]
S_e	Error sum of squares [-]
S_{ij}	Mean rate-of-strain tensors [1/s]
S_h	Source term [J]
S_m	Source term [kg]
S_{mean}	Mean sum of squares [-]
S_T	Total sum of squares [-]
S_u	Function of dependent variable [-]
S'_e	Pure sum of squares of error [-]
S'_{Fn}	Pure sum of squares of 1 factor [-]
t	Time [s]
T	Temperature [K]
T_n	Test number [-]
u_i	Average velocity scalar [m/s]
$\bar{u}_i$	Reynolds averaged mean velocity component [m/s]
$\tilde{u}$	Favre averaged mean velocity component [m/s]
u_i'	Fluctuating velocity component is Reynolds averaging [m/s]
u''	Fluctuating velocity component is Favre averaging [m/s]
v	Velocity [m/s]
V_e	Error variance [-]
V_{Fn}	Factor variance [-]
V_T	Total variance [-]
w_s	Air velocity in the smallest cross section of heat exchanger [m/s]
w_{sT}	Temperature corrected air velocity in the smallest cross section of heat exchanger [m/s]
w_0	Air inflow velocity [m/s]
w_1	Air outflow velocity [m/s]
W	West side node [-]
y	Distance to next surface [m]
$\bar{Y}$	Average value [-]
Y_i	Measured value [-]
Y_k	Turbulence dissipation of turbulent kinetic energy [J/kg s]
Y_0	Target value [-]
Y_ω	Turbulence dissipation of specific dissipation rate [J/kg s]
z_0	Inflows height from receiver point [m]
z_1	Outflows height from receiver point [m]

Greek symbols

α	Coefficient (eq. 50)
α^*	Coefficient (eq. 52)
α_i	Heat transfer coefficient in the inner tube [$W/m^2 K$]
α_m	Mean heat transfer coefficient for tube and fin [$W/m^2 K$]
α_v	Virtual heat transfer coefficient [$W/m^2 K$]
α_0	Model specific constant [-]
α_∞	Coefficient (eq. 53)
$\alpha_{\infty,1}$	Coefficient (eq. 58)

$\alpha_{\infty,2}$	Coefficient (eq. 59)
β	Coefficient (eq. 62)
β_i	Coefficient (eq. 55)
$\beta_{i,1}$	Model specific constant [-]
$\beta_{i,2}$	Model specific constant [-]
β^*	Coefficient (eq. 63)
β_i^*	Coefficient (eq. 64)
β_∞^*	Model specific constant [-]
γ	Ratio of specific heats [-]
Γ_k	Effective diffusivity of turbulent kinetic energy [J/kg]
Γ_φ	Diffusion coefficient [-]
Γ_ω	Effective diffusivity of specific dissipation rate [1/s]
δ	Kronecker delta [-]
δ_f	Fin thickness [m]
δx_{Pe}	Distance between east side face and center node [m]
δx_{PE}	Distance between east side node and center node [m]
δx_{we}	Control volume width from west face to east face [m]
δx_{wP}	Distance between west side face and center node [m]
δx_{WP}	Distance between west side node and center node [m]
ΔV	Volume of control volume [m^3]
$\Delta\Theta_{LM}$	Logarithmic mean temperature [K]
Δp_{tb}	Pressure drop in tube bank [Pa]
Δp_{filter}	Pressure drop in air filter [Pa]
ζ^*	Model specific constant [-]
η_f	Fin efficiency [-]
η_{UPS}	UPS efficiency [-]
Θ_e	Angle for equiangular face or control volume [°]
Θ_{max}	Largest angle in face or control volume [°]
Θ_{min}	Smallest angle in face or control volume [°]
Θ_{in}	Air temperature at inlet [K]
Θ_{out}	Air temperature at outlet [K]
Θ_{surf}	Inside surface temperature of heat exchanger’s tube [K]
Θ_{tube}	Fluid temperature inside tube [K]
κ	Model specific constant [-]
λ_{air}	Thermal conductivity of air [W/m K]
λ_c	Thermal conductivity of copper [W/m K]
λ_f	Thermal conductivity of fin [W/m K]
λ_t	Thermal conductivity of tube [W/m K]
μ	Dynamic viscosity [Pa*s]
μ_t	Turbulent dynamic viscosity [Pa*s]
ν_{air}	Kinematic viscosity of air [m^2/s]
ν_t	Turbulent kinematic viscosity [m^2/s]
ρ	Fluid density [kg/m^3]
ρ_{air}	Density of air [kg/m^3]
σ_k	Turbulent Prandtl number [-]
$\sigma_{k,1}$	Model specific constant [-]
$\sigma_{k,2}$	Model specific constant [-]
σ'_f	Ratio of pitch of fin and diameter of tube [-]
σ''_f	Ratio of height of fin and diameter of tube [-]
σ_ω	Turbulent Prandtl number [-]
$\sigma_{\omega,1}$	Model specific constant [-]
$\sigma_{\omega,2}$	Model specific constant [-]
σ^2	General variance [-]
$\varphi\_$	Average component scalar [-]
φ	Mean component [-]

φ'	Fluctuating component [-]
Φ	Diffusion of property [-]
Φ_1	Thiele modulus [-]
Φ_2	Coefficient (eq. 56)
φ_{op}	Operand (eq. 11)
φ'_{op}	Operand (eq. 12)
X	Operand (eq. 10)
ω	Specific dissipation rate [1/s]
ω_n	Specific humidity of air [$kg_{H2O}/kg_{dry\ air}$]

1. INTRODUCTION

This thesis was made in cooperation with Eaton corporation and its Finnish department Eaton Power Quality (Eaton PQ). Eaton PQ's factory locates at Espoo along the national road 50 (ring three). They have research and development, pre and after sales support, product marketing and management, and test departments, but also manufacturing of large 3 phase uninterruptible power supplies (UPS) from 8 up to 1,200 kilowatts (kW) all under same roof (Alapassi, 2021). In this chapter is presented the thesis background and motivation, and a structure of the study.

1.1 Background and motivation of the research

Electrical components produce heat when they are under operation. Sometimes heat produced in electrical components can be used in advantage, like in sauna stove or underfloor heating cable. In other hand, devices which main operation is processing or storing data, provide back-up power and so on, produced heat is unwanted side effect. If produced heat can't be use in advantage, the heat must be transferred elsewhere or cooled down, so room ambient temperature doesn't rise too much and harm electrical components (ASHRAE Inc., 2015, p. 283). For example, device which was selected for this study's base, Eaton large tower UPS 9395P maximum allowable temperature range is 0 to 35 °C at elevations up to 1,000 meters (m) from sea level without derating (Eaton Corp., 2022, p. 197).

Usually, room temperature control is done with air conditioning or separate cooling unit. In data center these separate cooling units are called computer room air-conditioning (CRAC) or computer room air-handling (CRAH) units (ASHRAE Inc., 2015, p. 287). In typical data center layout, UPS and its related back-up power equipment are in separate room with cooling units (Yogendra & Pramod, 2012, pp. 1-2). Footprint of these equipment needs to take account when building is planned and it's increasing costs of building facility or it's away from customers main operation which is, in data centers, information technology (IT). Eaton PQ has been developed higher power density UPSs to reduce customers footprint used to ensure power supply and for same reason cooling unit's development came in question. UPS's produce heat in operation, and it must be cooled down somehow so why not integrate UPS and cooling device into same footprint used.

This research tries to find the best UPS integrable heat exchanger unit concept which uses least material, parts, and footprint. On the way to the best concept, this study uses Property Driven Development (PDD) as a frame of development process, Characteristics-Properties Modelling (CPM) to develop the product, Design Reasoning Pattern (DRP) to model development decisions and project planning, Computational Fluid Dynamics (CFD) to model concept virtually before real prototype, and Taguchi method to optimize prototype tests in laboratory. As a result of the research there should be understanding how PDD, DRP, CFD, and Taguchi methods and tools like approximate calculations and CFD fit together in this kind of product development, but also the concept which can be taken to further productize.

1.2 Structure of the study

This study is divided into 7 phases. This first chapter, the introduction, includes background and motivation, and thesis structure. Second chapter represents how this research is done. The second chapter includes research objectives and questions, research strategy and methods, and how literature and patent review are done. After those study presents used base device of the case study in chapter 3 and dives to theory part in chapter 4. Theory part represents main theory behind the research questions and thesis subject. Before introduction of development process chapter number 5, structure of this study is presented in Figure 1.

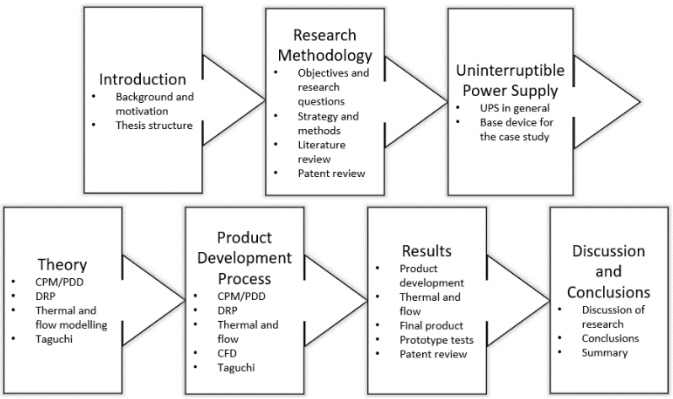

Figure 1. *Structure of the study.*

Chapter 5 represents what have been done and how it's applied in development process towards to final product. Chapter is divided to PDD, DRP, CFD, Taguchi, thermal and flow, and CFD parts. After presentation of development process is time to present results of research and development project in chapter 6. Last chapter, number 7, includes discussion and conclusions. It discusses how this research is made and how methods worked out, what didn't go as planned and summary of main points of this study.

2. DESCRIPTION OF THE RESEARCH

In this chapter, aim is to give holistic view how this thesis research is made. Chapter opens research objectives, what are the research questions, and what strategy and research methods were chosen. Also, this chapter introduces how literature and patent review were done. Literature review represents used databases, keywords, and sources. Patent review part goes through keywords and related patents of UPS cooling which were found from patent database Espacenet.

2.1 Research objectives

This research has 2 objectives. First objective of research is to integrate CPM/PDD, DRP, and Taguchi methods into each other and test the usability of them in heat exchanger unit's development project. Second objective is to design a functioning UPS integrated heat exchanger unit by utilizing a thermal and flow calculations, CFD simulation, and prototype testing. As the end result of research, there should be knowledge how mentioned development process methods and tools work within each other in such case and how a functioning prototype of the heat exchanger unit is designed.

Heat exchanger unit's technical objective is to find required properties of UPS integrated heat exchanger unit, find appropriate solutions which fulfils required properties, the needed cooling power of the heat load and doesn't have effect on the normal operation of UPS. Heat exchanger unit's development is delimited into 1 UPS model and initial values for dimensioning is obtained from it.

The CPM/PDD method shall be used to guide through development and DRP method to model decision making and project planning. Taguchi method, calculations and CFD simulation are used to determine the characteristics and properties of characteristics.

This study's heat exchanger unit development theory is related to thermal and flow modelling. So, a part of research is to investigate how to model thermal and flow by calculations, investigate air flow behaviour by using CFD simulation tool and how heat exchanger unit effects on UPS behaviour by prototype testing.

Also, this study includes building and testing a prototype. Prototype tests can be time consuming because the number of tests done. To shorter the time used to prototype tests, one part of the research is to investigate how use of Taguchi method could improve prototype tests efficiency with a smaller number of experimental test runs.

2.2 Research questions

Research project was started by outlining what are necessary questions behind the research. Some of the questions were formulated during the study, but the main idea of original research questions is still there. Research questions of CPM/PDD, DRP, Taguchi methods, and thermal and flow modelling were:

1. How to integrate CPM/PDD, DRP, and Taguchi methods to each other in heat exchanger unit's product development?
    a. How DRP model suits development project flow modelling?
    b. How CPM/PDD method suits to heat exchanger unit's concept development project?
    c. How to use DRP model to model heat exchanger unit development project decision making?
    d. How prototype tests should be done?
2. What should be considered when designing a heat exchanger unit to UPS?
    a. What are the primary parameters when dimensioning heat exchanger unit to UPS?
    b. How much cooling capacity heat exchanger needs to prevent ambient room temperature rise?
    c. How large heat exchanger's surface area should be to cool down air heated in UPS?
    d. How the pressure drops in the flow?
    e. How heat distribution can be equalized?
    f. Whether there are related patents to this kind of UPS cooling solution?

2.3 Research strategy and methods

Research strategy is set of research methodological choices which drives research project through in theoretical and practical level. Strategy should be chosen to serve the subject, not the other way around, to fit subject on certain strategy. Choosing suitable strategy for research subject will help researcher identify what is this research expected to fulfil and focus on methods which are important for the progress of the project. (Blessing, 2004)

Strategy to this research was chosen multi-methodical empirical case study. Empirical method is experimental way to do research, and it leans on concrete observations, calculations, and measurements on study's subject (Lähdesmäki, et al., 2009). Empirical method was chosen because research objective is to test how certain development methods support on this kind of development project and how they could be integrated on each other. Also desired results of project support empirical method because they show up as a researcher's experience, but also in the light of numerical data.

Multi-methodical study is a mix of qualitative and quantitative methods. Qualitative method methodology is trying to understand study's subject meaning and characteristics holistically. In qualitative method, theory and information isn't normally detailed or numerical and focus on this method is trying to understand phenomenon. As against quantitative method normally focuses on detailed, computational, or statistical theory and tries to understand subject in the light of collected or produced data. (Lähdesmäki, et al., 2009)

Qualitative method was chosen because the development methods aren't numerical or mathematical measurable when development group is just one developer and product under development is built from scratch without any earlier data on development time, money spent etc. Also, when combining few development methods, main objective is to understand meaning and usability holistically. Quantitative method was chosen because study also covers measurements on digital and physical prototype of product. After all, desired results support each other because numerical data tells success or unsuccess of development work and give a perspective on researcher's experience.

Case study is an empirical method which examine the real-world context and tries to understand it (Yin, 2018, p. 15). In case study focus on research is only in one or few subject or object (Lähdesmäki, et al., 2009). According to Yin (2018, pp. 10-11) case study can be chosen when research questions are "how" or "why" questions and study tries to explain how something works or not. Single-case study focuses on the 1 individual subject, object, or context, such as 1 individual person as a study subject. Whereas multiple-case study includes few or more cases. Single-case study designs can be divided into 2 basic types which are holistic and embedded. Holistic type contains a single unit analysis and embedded type contains multiple units analysis in 1 case (Yin, 2018, pp. 53-55).

The case study type was chosen to be holistic single-case study. That's because this research focuses on developing only 1 object and almost all research questions are "how" questions which are trying to explain how particular thing works and tries to find challenges or extension to theory under examination.

Whole research strategy is presented in Figure 2. Research is divided in 2 parts, collecting, and analysing theory and apply theory to practical development work. 2 parts also divine research strategy in half. In first qualitative part is where to acquire theory and competence and second quantitative part is where theory applies to practice. Second part of research is strongly iterative and include multiple developing rounds before product is in desired form.

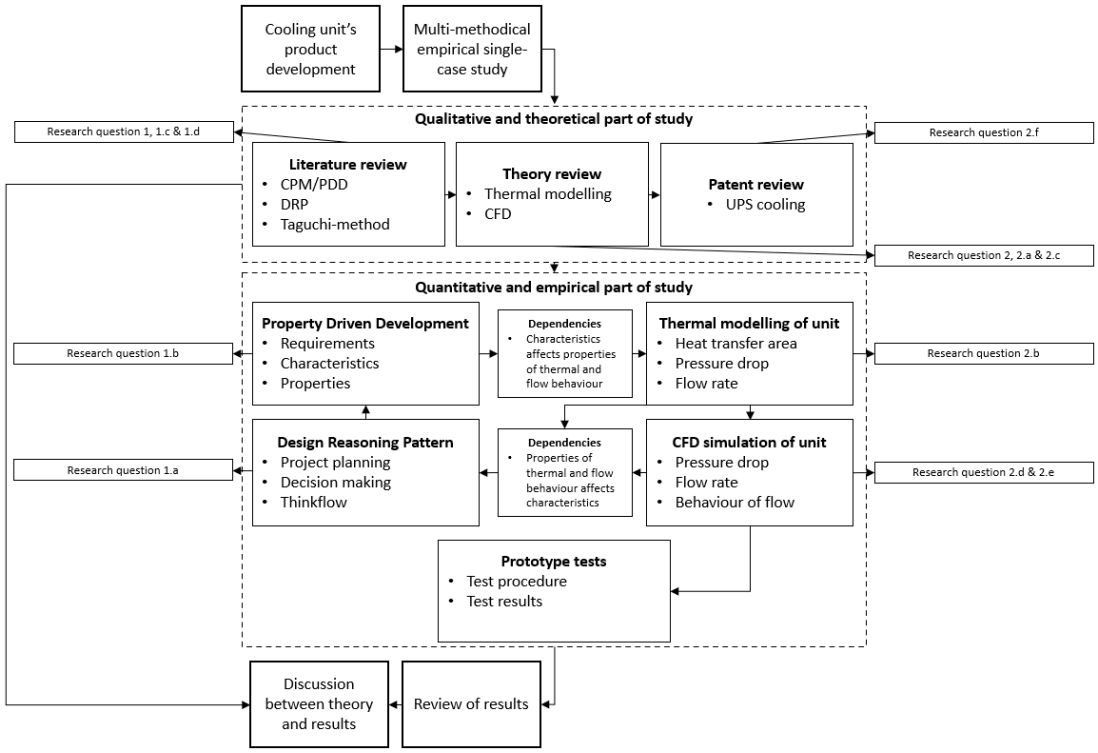

Figure 2. *Research strategy.*

At the end of product development is time to collect results and experiences, review what has been done and how chosen methods work in practice. Success or unsuccess of product development tells how project went. Last part of research is review how theory applied to practical research and what should be improved or changed to the next project.

2.4 Literature and theory review

Literature review was implemented as a traditional review for product development methods. In traditional literature review main goal is to answer questions:

- What do we already know about the selected topic?
- What do we not know yet?

Theory review was implemented as a search for latest and generally accepted equations and correlations for heat transfer and CFD in heat transfer air to fluid solutions and UPS cooling solutions. Also, the review mapped ambient conditions in most common use of Eaton large tower UPS devices.

Literature and theory review started mapping databases and initial keywords which are most relevant for the research subject and produce best results. After evaluation of most comprehensive results of keywords and databases, review moved to imposing limitations

on searches to help find relevant and latest releases to the subject. Literature review and theory review databases, initial keywords, and limitations are shown in Table 1.

Table 1. *Literature and theory review databases, keywords, and limitations.*

Literature review definitions	
Databases	Andor, Eaton Corp. intranet, SpringerLink, ScienceDirect, Scopus, Tampere University Library
Keywords	”CPM AND PDD”, ”CPM”, “PDD”, ”product driven development”, “characteristics-properties modelling”, “DRP”, “design reasoning pattern”, “Taguchi”, “Taguchi method”, “Taguchi method” “UPS”, “uninterruptible power supply”, “data center*”, “data center* AND cooling”, “cooling”, “heat exchanger”, “UPS AND “heat exchanger””, “pressure drop”, “finned heat exchanger”, “air-liquid exchanger”, “”fin tube” AND “pressure drop””, “”fin tube” AND “air side” AND “pressure drop””, “CFD”, “computational fluid dynamics”
Content types	Articles, Books, Chapters, Conference papers
Language	Finnish, English
Limitations	Peer-reviewed, Engineering, Energy, Engineering Design, Thermodynamics, Engineering Thermodynamics
Years	2000–2021

There were plenty of literature in databases for these subjects of study. Literature and theory review was started to go through all titles of search results and select topics which are related to study and are eligible for this research. As a title selection criterion was used relation on engineering design, mechanical product development, and heat transfer design. After title-based selection of literature, review moved to read abstracts and reduce usable sources with like same criterion as titles, but more detailed if an article or book is relevant for this study’s subjects. Last selection of usable literature was made by reading through found articles and chapters which are related to research. Source selection protocol as an example of keyword “CPM AND PDD” is presented in Figure 3. Same source selection protocol was applied to all keywords and databases mentioned in Table 1.

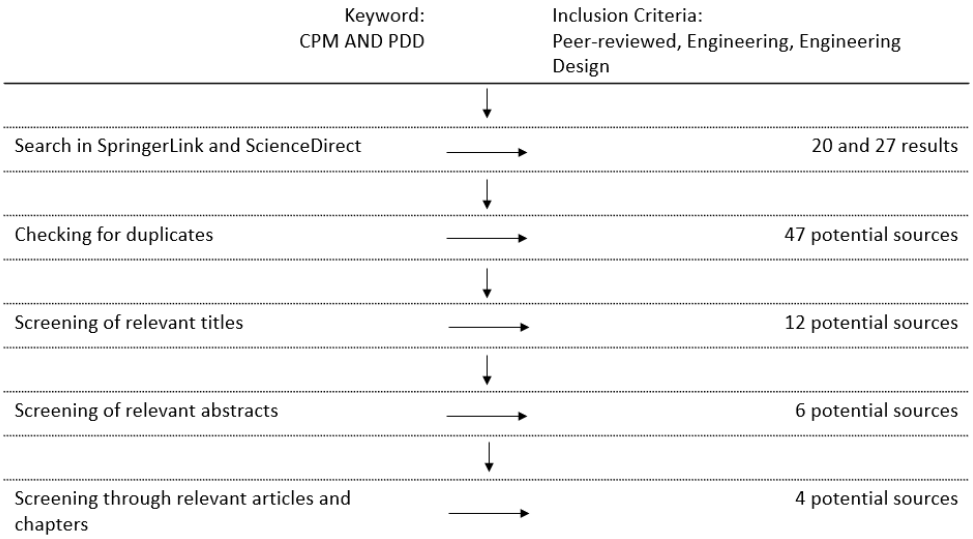

Figure 3. *Source selection protocol.*

Main sources which were selected from found potential sources for this research are shown in Table 2. However, this study uses some literature as a background study sources which aren't mentioned on the table.

Table 2. *Main sources of research.*

Title	Writers and year
Looking at "DFX" and Product Maturity" from the perspective of a New Approach to Modelling Product and Product Development Processes	Weber C.; 2007
What is Design Knowledge from The Viewpoint of CPM/PDD?	Conrad J., Köhler S., Wanke S. & Weber C.; 2008
Modelling Products and Product Development Based on Characteristics and Properties	Weber C.; 2014
Impacts of making design decision sequence explicit on NPD project in forest machinery company	Halonen N., Lehtonen T. & Juuti T.; 2014
Challenges and Opportunities in Capturing Design Knowledge	Lehtonen T., Halonen N., Pakkanen J., Juuti T. & Huhtala P.; 2016
Formalization of Information Flows to Support Lean Manufacturing Implementation – Study of High-Variety, Low-Volume Manufacturing in a High-Cost Country	Adlin, Nillo; 2022
A Primer on The Taguchi Method	Roy R.; 2010
Taguchi's Quality Engineering Handbook	Taguchi G., Chowdhury S., Wu Y.; 2005
VDI Heat Atlas	Stephan P. et al.; 2010
Thermodynamics: An Engineering Approach	Çengel & Boles; 2015
Boilers and Burners	Basu P., Kefa C., Jestin L.; 2000
An Introduction to Computational Fluid Dynamics	Versteeg H. & Malalasekera W.; 2007
ANSYS Fluent Theory Guide 19.2	Ansys Inc.; 2018

2.5 Patent review

Patent review was made to be sure that concept to be developed isn't already patented. The review was made in Espacenet database which includes valid patents, patentable, and patent applications of inventions, devices, and systems over hundred countries (European Patent Organisation, 2016). Patent review definitions are shown in Table 3.

Table 3. *Patent review definitions.*

Keywords	Limitations	Results	Evaluation
ntxt = "UPS" AND ntxt = "Heat ex-changer" AND nftxt = "cooling" AND pd >= "2001""	Language: English	41	6 related patents
ta = "ups" AND (ntxt = "heat ex-changer" OR ntxt = "cooling") AND pd >= "2001"	Language: English	603	63 related patents

As seen in Table 3 there were plenty of patents in relation to UPS cooling. Year 2001 was chosen to start year for search, because there weren't earlier publication dates and publicised patents had almost an exponential rise after year 2011. Patents publication date graph is represented in Figure 4 (European Patent Organisation, 2016). Patents was first shorted reading titles and abstracts through to pick up eligible patents for further examination.

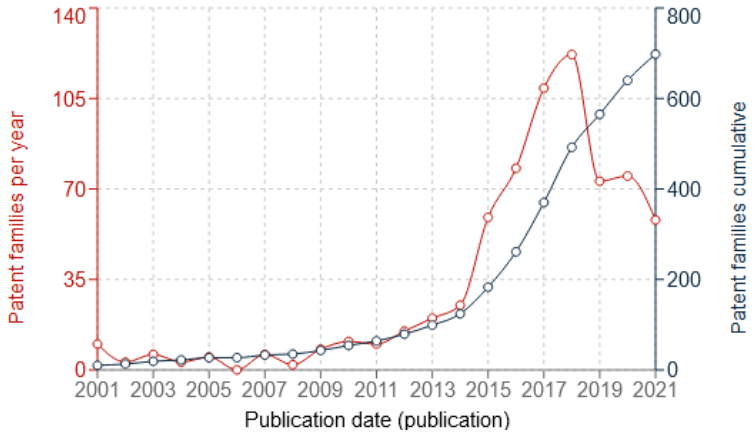

Figure 4. *Patent publication dates (European Patent Organisation, 2016).*

3. UNINTERRUPTIBLE POWER SUPPLY (UPS)

This chapter represents basics of UPS devices and introduces Power Xpert 9395P UPS, which was selected to use as a base of development and dimensioning to this study's heat exchanger unit development case. UPS device itself isn't main part of development work, but it's important understand what factors should be taken into consideration for successful development of UPS integrated heat exchanger.

UPS is electrical device which is connected between electrical power supply and critical equipment. It provides back-up power to critical equipment long enough to shut it down normally or as long as generator reach power high enough to keep equipment in operation. UPS devices also keeps quality of power supply high and prevents harms caused by power problems (Eaton Corp., 2011, pp. 2-3). There are nine power problems described in Table 4 that could be preventable by using a UPS device (Eaton Corp., 2020, p. 28).

Table 4. *The nine power problems (Eaton Corp., 2020, p. 28)*

#	Power problem	Definition
1.	Power failure	A total loss of utility power
2.	Power sag	Short-term low voltage
3.	Power surge (spike)	Short-term high voltage more than 110 percent of normal
4.	Under-voltage (brownout)	Reduced line voltage for an extended period of a few minutes to few days
5.	Over-voltage	Increased line voltage for an extended of a few minutes to a few days
6.	Electrical line noise	High power frequency power wave caused by radio frequency interference (RFI) or electromagnetic interference (EMI)
7.	Frequency variation	A loss of stability in the power supply's normal frequency of 50 or 60 Hz
8.	Switching transient	Instantaneous under-voltage in the range of nanoseconds
9.	Harmonic distortion	The distortion of the normal power wave, generally transmitted by unequal loads

There are multiple different ways to categorize UPSs, for example 1-phase or 3-phase or form factors like desktop and tower, wall-mount, rackmount, and large tower device. Selecting between them depends on various needs and environmental factors of a customer (Eaton Corp., 2020, pp. 6-14). The content of this study focuses only 3-phase large tower UPS, so only the relevant factors of it is briefly described.

There are three major varieties of UPS which are also known as topologies. Topologies are single-conversion, double-conversion, and multi-mode systems. Different conversions describe how many times UPS converts alternating current (AC) power to direct current (DC) power and vice versa in normal power supply. As the topology names suggests, single-conversion doesn't convert AC power to DC power at all when using normal power flow route through UPS and double-conversion converts AC to DC twice. Multi-mode system is again combination of single- and double-conversion systems. Although all topologies convert AC to DC when charging UPS batteries and vice versa when AC input supply fails, and power supply is using only battery power. UPS model 9395P is a double-conversion topology and only that topology is described in detail. (Eaton Corp., 2011, pp. 2-4)

Double-conversion system, as mentioned earlier, converts power twice. First power source feeds AC power to rectifier as an input. Rectifier converts AC power into DC power and feeds it to inverter and batteries. Inverter converts DC power back to AC power before feeding it to power supply of critical equipment. This double-conversion system protects equipment from raw utility power and ensure equipment gets only clean and reliable electricity. Double-conversion system is demonstrated in Figure 5. (Eaton Corp., 2011, p. 3)

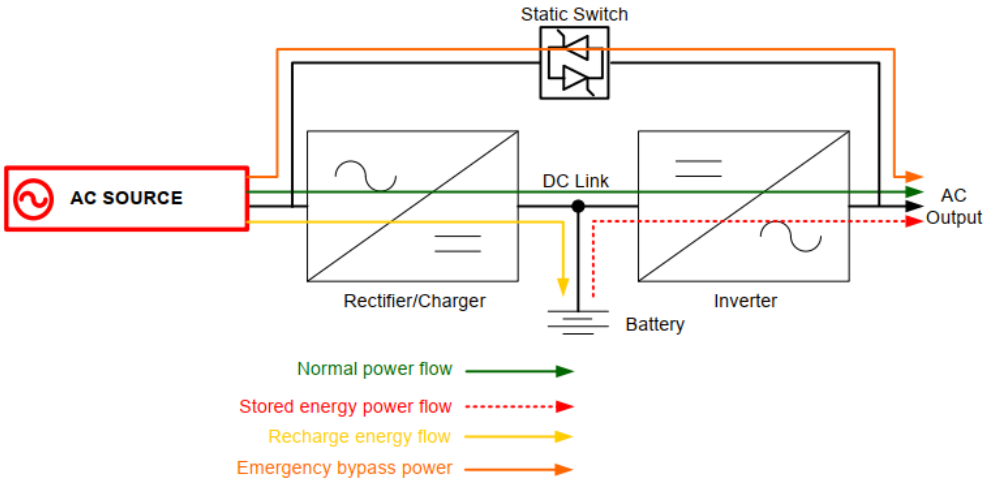

Figure 5. *Design of a double-conversion system (Eaton Corp., 2011, p. 3).*

In normal operation, double-conversion system continually processes power twice in rectifier and inverter as green line presents in Figure 5. When AC source falls out of predefined limits or shuts down completely rectifier shuts off and inverter begins to take power from the battery. UPS keeps power input to equipment alive until AC source returns to normal tolerances or batteries run out of power. After AC source returns to normal tolerances UPS continues to feed power in normal mode and recharges batteries at same

time. In emergency case where rectifier or inverted fails or inverter has severe overload, UPS turns quickly static bypass switch on to support output loads. (Eaton Corp., 2011, p. 3)

3.1 Power Xpert 9395P 300 kVA / 300 kW UPS

This study's base device for heat exchanger unit's development case was selected Power Xpert 9395P 300 kilovolt-ampere (kVA)/300 kW UPS, which is currently Eaton PQ's newest large tower 300 kW UPS in market. 9395P UPS is modular back-up power UPS to support most common customer needs, scalability, and maintenance. In 9395P feeding power is scalable from 250 kW up to 1,200 kW just adding uninterruptible power modules (UPM) and scalable back-up time from 120 ampere (A) up to 480 A. Also, back-up time could be increased with external battery cabinets. 9395P 300 kVA/300 kW UPS voltage (V) models are 380 V, 400 V, 415 V, and 480 V. (Eaton Corp., 2018)

Factory configuration can be divided in to two sections, integrated system bypass module (ISBM) and UPM as demonstrated in Figure 6 (Eaton Corp., 2022, pp. 20-21). Main components of the ISBM section are UPS input and output connections, static switch, control boards, control panel, and air filter. Main components of the UPM section are rectifier, inverter, redundant aux power supplies, control and interface boards, fans, batteries, and air filters. (Alapassi, 2021)

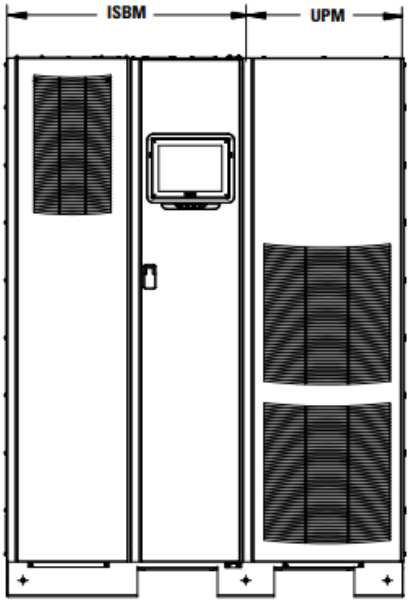

Figure 6. *9395P 300 kVA/300 kW configuration (Eaton Corp., 2022, p. 21).*

As mentioned earlier, electronic devices produce heat in operation and UPS isn't an exception. Most of the heat losses in UPS comes from UPM section where most of electrical components are located and more specifically in rectifier and inverted where most of power goes through in normal operation (ASHRAE Inc., 2015, p. 286). Cooling of UPM section uses fans to create forced convection to fulfil needed heat transfer efficacy. When ISBM section cools down enough with natural convection. UPM section's air inlet is on lower half on front panel and outlet is at top of device. Forced convection section aka UPM airflow route is demonstrated in Figure 7. This study's delimitation is on product development of heat transfer device, so it focuses on UPM section because most of the heat dissipated there, and better heat transfer caused by forced convection.

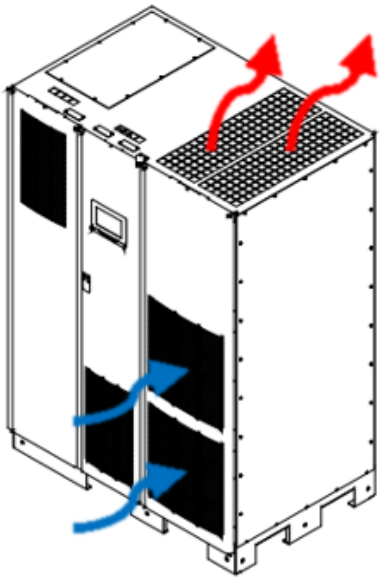

Figure 7. *Airflow through the UPM section.*

Main components for this study i.e., cooling fans are located at horizontal position at lower section inside the UPM. Fans create suction flow from front intake and blow out from top outlet. UPM components maximum temperature is specified by manufacturer and fans static pressure and airflow are dimensioned to keep volume flowrate high enough to keep components junctions and surfaces temperature in allowable limits.

Most of the static pressure is caused by components in way of airflow, but also air filter installed behind air intake. Filter is needed because accumulation of particulate contaminations of air which can cause e.g., obstruction of cooling airflow, interference with moving parts, abrasion, interconnect interference, deformation, corrosion, impedance changes and conductor bridging. (ASHRAE Inc., 2014, pp. 14-15)

4. THEORY

Following chapter 4 explains theory behind the study before next chapter number 5, where is explained how theories are applied to development process. Theory part is divided in to 5 sections and theories are represented in same order as they have been applied. These sections are Characteristics-Properties Modelling / Property Driven Development (CPM/PDD), Design Reasoning Pattern (DRP), thermal and flow modelling, Computational Fluid Dynamics (CFD) and Taguchi method.

4.1 Characteristics-Properties Modelling / Property-Driven Development (CPM/PDD)

CPM/PDD approach to development process is one way to manage development projects and product knowledge (Conrad, et al., 2008, p. 745). The CPM part of method is way to model product development. It's based on relation between characteristics and properties of the product. PDD part of method explains the development process based on CPM (Weber, 2007, p. 87). CPM/PDD is more like a framework to development work where developer can integrate any other methods and tools (Weber, 2014, p. 329).

As mentioned, PDD describes the development process. The process runs in iterative cycles where designer establishes product characteristics closer to required properties. Cycles can be divided to 4 steps, synthesis, analysis, individual deviation, and overall evaluation. The main driver of the process is overall evaluation (Conrad, et al., 2008, p. 747). PDD process starts with a list of required properties to product and 1 cycle steps runs as follows (Weber, 2007, p. 95):

1. Synthesis: create, change or modification of characteristics (C_i) based on last overall evaluation. In first cycle designer establishes first characteristics from required properties (PR_j). In this first cycle, just few major PR_j should take along to the cycle and add more PR_j in the next cycles.
2. Analysis: product properties (P_j) are determined and analysed from current characteristics. From the beginning of process, all relevant PR_j are analysed, not only those few PR_j which were taken along in earlier cycles.
3. Individual evaluation: analysis step's results are being evaluated individually to PR_j to find out deviations (ΔP_j) between P_j and PR_j.

4. Overall evaluation: designer goes through individual evaluation steps problems and short comings and decides how to proceed the development. Last step determines what methods and tools are being used in next step and in the beginning of process, decides what PR_j should take under inspection at the next cycle.

During the process there could appear new properties P_j on product behaviour or new required properties PR_j what final product needs. All appeared P_j and PR_j should be taken account and added to list (Conrad, et al., 2008, p. 747). PDD process beginning cycle ('cycle A') can be demonstrated as a flowchart as presented in Figure 8. Relations (R_j/R_j^{-1}) box in Figure 8 represents the known relations between PR_j, C_i, and P_j (Weber, 2014, p. 335).

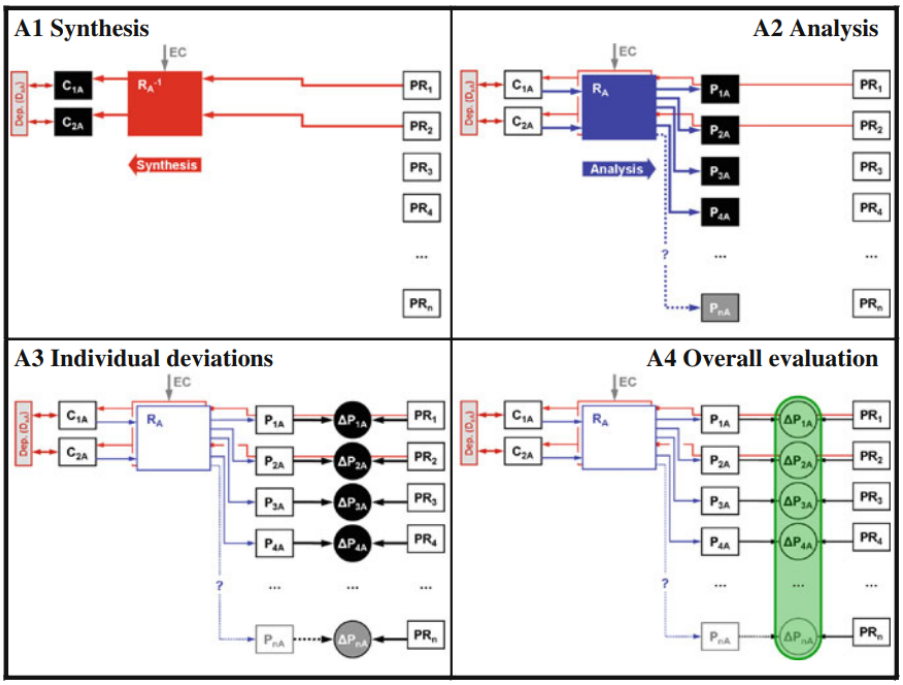

Figure 8. *PDD process steps (Conrad, et al., 2008, p. 5).*

Development process next cycle begin with synthesis step after overall evaluation, in situation where deviations (ΔP_j) between product properties (P_j) and required properties (PR_j) have been evaluated. PDD process next cycle ('cycle B') start is demonstrated in Figure 9. Process goes on like demonstrated in 'cycle B' until overall evaluation reaches satisfactory between P_j *and* PR_j. (Weber, 2014, p. 337)

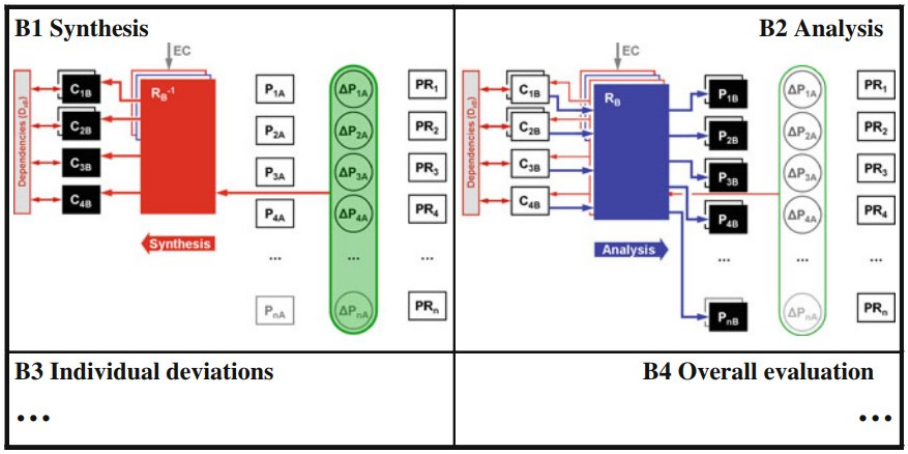

Figure 9. *PDD process next cycle (Weber, 2014, p. 338).*

CPM is the product modelling side of CPM/PDD approach, which defines product characteristics and properties (Weber, 2007, p. 87). PDD process is usually explained based on to CPM and no other way around as in this case (Weber, 2007) (Conrad, et al., 2008) (Weber, 2014). In CPM approach characteristics describe product's shape, structure, dimensions, materials, and all related parameters which designer could directly affect, modify, or determine. Properties are again product behaviour which designer can't directly affect. Properties describes products weight, safety, functions, costs, and maintenance etc. (Weber, 2014, p. 329)

CPM modelling, same as whole PDD process, starts with list of required properties (PR_j) or collecting such a list from users interviews, customer feedbacks, test reports, documentation etc. Structure of the list can be displayed like properties presented at right-hand side in Figure 10.

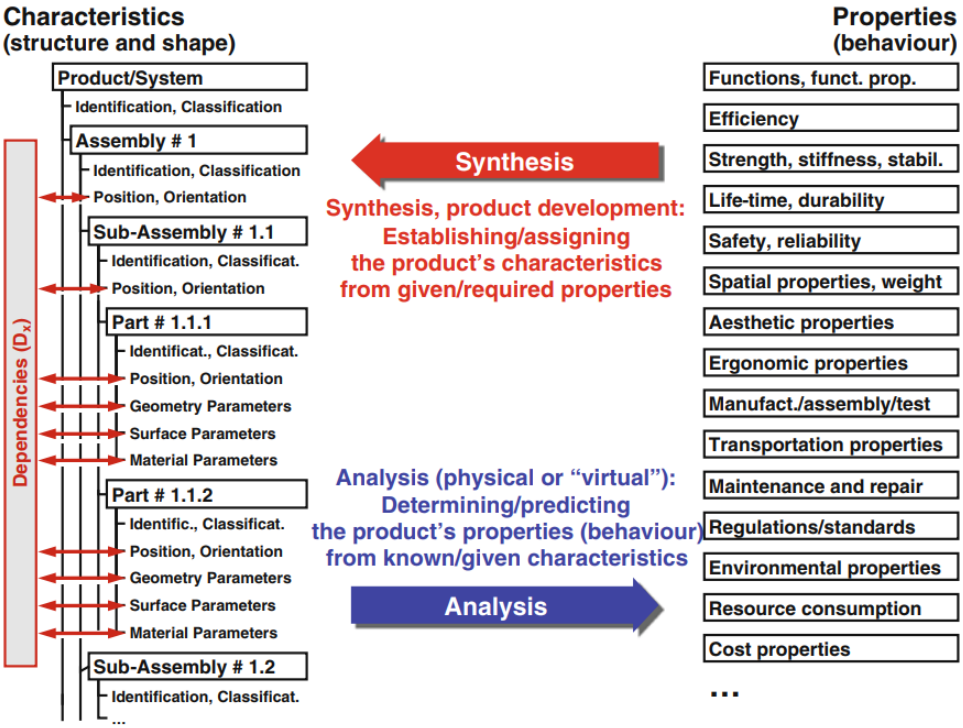

Figure 10. *Characteristics and properties list (Weber, 2014, p. 331).*

On the left-hand side of Figure 10 is presented characteristics list which is defined by product designer based on PR_j. Characteristics list includes all product's parts and their parameters. At the left-hand side of characteristics list, there is presented dependencies (D_x) box between different characteristics. These dependencies can reduce the number of characteristics and designer must go through them one by one. (Weber, 2014, p. 331)

CPM is, as its name suggests, product's characteristics and properties modelling. CPM product modelling determines products characteristics and properties and focuses on analysis and synthesis steps between them. In analysis all product's properties are predicted or determined from product's characteristics. Before physical product is made, properties are predicted from designer guesswork and experience or physical tests of single part, tables and diagrams, simplified calculations, and computer-based models/calculations. Different characteristics have relations (R_j) on different properties and all R_j must be analysed independently. Off course it doesn't mean that all relations are independent as shown in Figure 11. All relations have external conditions (EC_j) which can be example, external load, changing ambient conditions, manufacturability, and user cultural background. EC_j effects on product behaviour and designer should take them into account when analysing properties of product. In Figure 11 is presented simplified analysis model. (Weber, 2014, pp. 333-334)

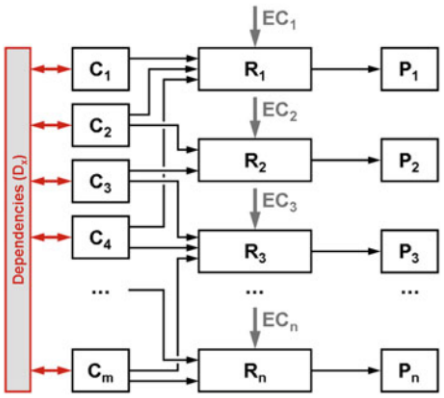

Figure 11. *Simplified analysis model (Weber, 2014, p. 333).*

Synthesis step is inversion from analysis step. In synthesis, properties or required properties of product have R_j^{-1}, which different EC_j effects, to characteristics. Synthesis step's purpose is to determine which properties are fulfilled on product's already selected characteristics and is there any conflicts. Conflicts are relations of different required properties which have influence in same characteristic which can be seen in Figure 12. Synthesis can be made with same tools and methods as analysis but inverted. Simplified synthesis model is represented in Figure 12. (Weber, 2014, pp. 334-335)

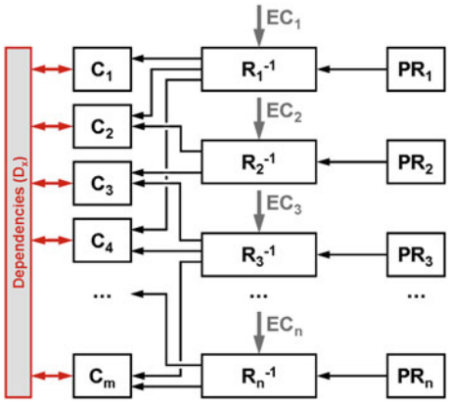

Figure 12. *Simplified synthesis model (Weber, 2014, p. 335).*

Well documented CPM modelling can increase product knowledge. Documented R_i/R_j^{-1} between PR_i/P_j and C_i shows links and context of different solutions of product and presents where these solutions effect and why. C_i documents can be technical drawings, CAD models, and part lists. Whereas PR_i/P_j can be required properties list, test reports, and analyses. Lists, charts, or tables of R_i/R_j^{-1} can fulfil data-information-knowledge in product development and helps further development when there is already information how characteristics effect on properties and other way around. (Conrad, et al., 2008, pp. 748-749)

4.2 Design Reasoning Pattern (DRP)

Design reasoning pattern in product development process aims to share information about the product with multidisciplinary development teams and knowledge for product's further development progress (Halonen, et al., 2014, pp. 702-703). DRP is, in very simplified view, a flow chart which maps design choices and their sequence. DRP models can be used in product development to map design reasoning, share knowledge between development teams, solve problems in industrial processes, handle material flow of manufacturing product or product family, and sequel production line assembly (Lehtonen, et al., 2016, pp. 392-394). Utilizing DRP in product development and making decision sequence explicit, it can help teams to share knowledge about product, individual developer to memorize development step and reasons behind decisions. All impacts of using DRP mapping in design decision sequence of development project are presented in Figure 13 (Halonen, et al., 2014, p. 703).

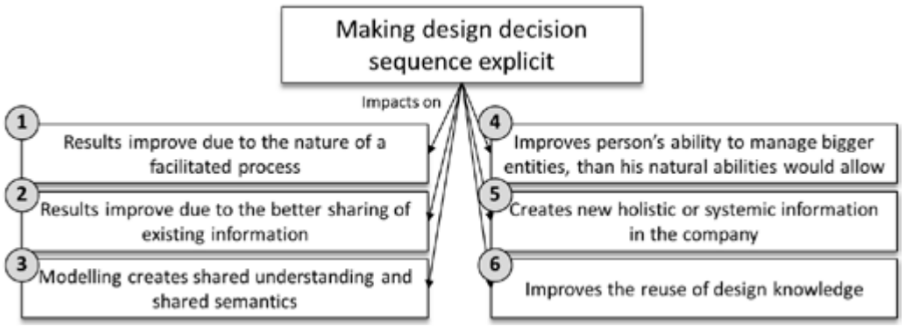

Figure 13. *Impacts of making design decision explicit (Halonen, et al., 2014, p. 703).*

This research focuses on product development and DRP is used to illustrate the design principles and product structure for further use in company where case study is produced. When mapping design decisions the goal is to make design principles understandable, explain reasons of decisions and share knowledge of the product. DRP map's starting point can include almost anything, depending on the contents of project and starting data, life cycle, customer, organisation, company's strategic, product family, and technical requirements. When mapping of design decisions DRP model can include design routines, reasons, rules, boundaries, and means in technical systems. (Halonen, et al., 2014, p. 706)

DRP models can be done as a timeline of the design decisions. Starting in requirements at the left, continuing to right to information of the design including initial information what different solutions of product needs. Level of details in map should be the same all through (Halonen, et al., 2014, p. 707). Information shouldn't be too detailed to avoid

DRP model becoming too large or uncontrollable. However, there are different ways to manage large and detailed models when needed to, example object-oriented modelling (Lehtonen, et al., 2016, p. 394). DRP map can be made for example answer to questions below (Halonen, et al., 2014, p. 707):

- Where development process starts?
- How to design great product?
- How design is made?
- What kind of information or deliverables are required to decision?
- Where information comes from?

Modelling process can be divided into 3 phases and 8 steps where designer or project organization decides why, how, and what will be modelled and models development work. Process for modelling is presented in Figure 14. Process is presented in linear order for simplicity but modelling of different phases can be done parallel order and after all modelling is iterative process. (Adlin, 2022, pp. 151-152)

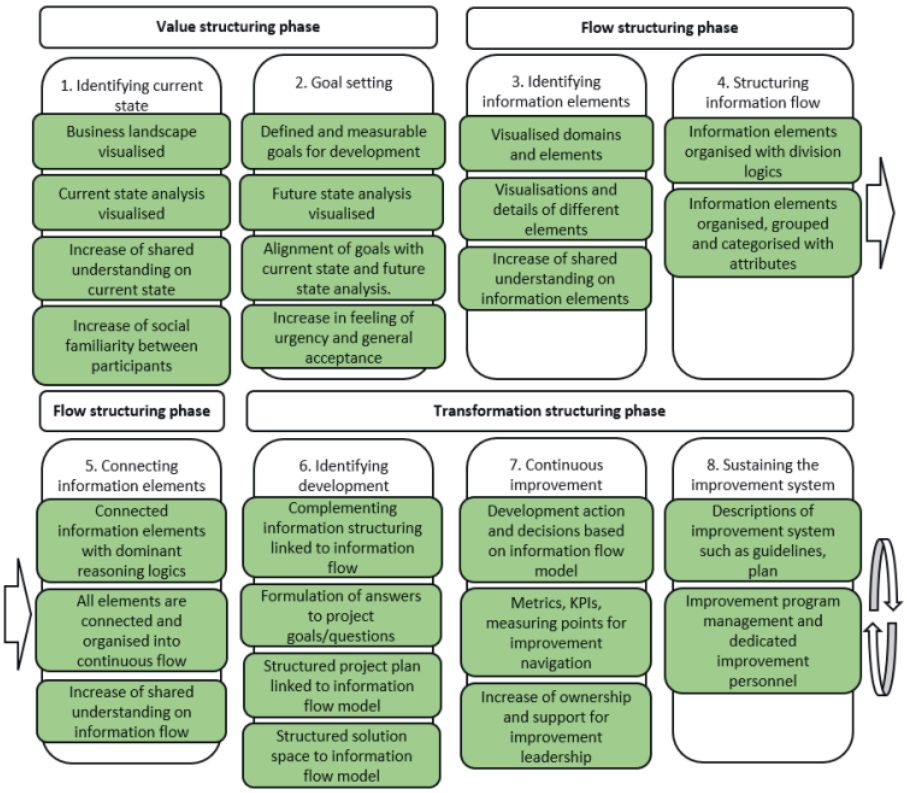

Figure 14. *Modelling phases (Adlin, 2022, p. 152).*

Figure 14 presents the DRP modelling as an Information Flow Modelling (IFM) because it comprises modelling method for all kinds of projects and situations. In this thesis IFM is presented as DRP because the focus is on designing and developing a product.

First phase, the value structuring phase, includes an identifying current state and goal setting steps. In identifying current state designers or project organization identifies start point of a project, finds why and how the modelling process should be done, and share the existing knowledge about company, market, product, manufacturing, and value generation. The goal setting step defines the goal of a design task or a project. In goal setting step designers or organization shares the understanding of project's start point identified in previous step, formulates a reasonable goal to development work and analyses the future state of a product and company. (Adlin, 2022, p. 153)

Second phase, the flow structuring phase, is the modelling phase. This phase's steps are identifying information elements, structuring information flow, and connecting information elements. In identifying information elements step the task is to find all information needed and form an understandable model for all designers and participants. Elements can include information and requirements of a product, interactions between different product families and environments, and information of workflow. In the structuring information flow step, goal is to arrange all information elements, for example, into phases of organization department or product development. Task in the connecting information elements step is to connect different information elements into reasonable, easy to follow and relational order. This collecting information elements step should expose the hidden relations, cause-effect patterns, and decision reasons behind the model. Second phase's steps are all iterative and should be done in parallel. (Adlin, 2022, pp. 154-155)

Third and last phase of modelling is transformation structuring phase. It includes identifying development, continuous improvement, and sustaining the improvement system steps. The identifying development step's goal is to extend model to formulate solutions and answers to the product development goals and identify which direction development project should go next. In the continuous improvement step variables, costs, time, product maturity deviations, and resources is marked up into model. This helps to coordinate further decisions of development project. Last step of modelling is sustaining the improvement system. In this sustaining the improvement system step the decisions of projects future resources, guidelines, and development activity as well as DRP models improvement plans are being make. (Adlin, 2022, p. 157)

4.3 Thermal and flow modelling

Main parameters, of this case, when dimensioning heat exchanger unit are usable back-pressure and heat load which are changing depending on UPS's electrical power load and environmental conditions. Electrical components cooling is fulfilled via forced convection done by fans inside the UPM. Increasing back-pressure decreases flow rate through UPM and lowers forced convection cooling impact which causes unwanted temperature to rise in operating components.

UPS heat losses can be calculated via its efficiency. According to the first law of thermodynamics, energy can't be created or destroyed. Energy just transforms from one form to another while total amount of energy remains constant (Yogendra & Pramod, 2012, p. 387). If we consider UPS a closed system where electrical energy has a certain input power and lower output power, difference between input and output energy must go somewhere. If electrical energy isn't stored in UPS batteries, it comes out as a heat energy, as a simplified point of view. If energy storage is disconnected, UPS covers are considered as system boundary and electrical energy is considered as a work, UPS thermodynamical equilibrium can be indicated like presented in Figure 15.

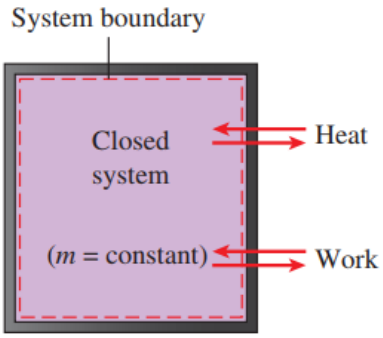

Figure 15. *Thermodynamical equilibrium (Çengel & Boles, 2015, p. 60).*

UPS efficiency can be computed from measured input and output power, when energy storage is disconnected, with equation (1)

$$\eta_{UPS} = \frac{P_{OUT}}{P_{IN}} = \frac{P_{OUT}}{P_{OUT} + P_{UPS}}, \tag{1}$$

where η_{UPS} is UPS efficiency, P_{OUT} is output power, P_{IN} is input power, and P_{UPS} power loss (Giuntini, 2011, p. 2). UPS power losses can be computed from efficiency calculated in equation (1) or measured input and output power with equation (2) (Giuntini, 2011, p. 2)

$$P_{UPS} = P_{IN} - \eta_{UPS} P_{IN} = P_{IN} - P_{OUT}. \tag{2}$$

Power loss from the UPS can be used as a heat load to the heat exchanger unit. Heat exchanger unit's dimensioning starts with calculating its heat exchanger's heat transfer area. Heat transfer area correlations are different depending on fin geometry and tube bank design (VDI e. V., 2010, pp. 1273-1275). This study uses correlations of staggered tube bank with rectangular fins. Heat transfer area A_{he} can be estimated with equation (4)

$$A_{he} = \frac{\dot{Q}}{k_{ht}\Delta\Theta_{LM}}, \tag{4}$$

where $\dot{Q}$ is heat flow, k_{ht} is overall heat transfer coefficient, and $\Delta\Theta_{LM}$ is logarithmic mean temperature difference (VDI e. V., 2010, p. 1273). Overall heat transfer coefficient k can be calculated with equation (5) and logarithmic mean temperature difference $\Delta\Theta_{LM}$ with equation (6).

$$\frac{1}{k} = \frac{1}{\alpha_v} + \frac{A_o}{A_{in}}\left(\frac{1}{\alpha_i} + \frac{d_0 - d_i}{2\lambda_t}\right), \tag{5}$$

where α_v is virtual heat transfer coefficient, A_o is total outer surface of fin and tube, A_{in} inside surface of tube, α_i heat transfer coefficient in the inner tube, d_o is outer diameter of tube, d_i inner diameter of tube, and λ_t is thermal conductivity of tube. (VDI e. V., 2010, pp. 1273-1276)

$$\Delta\Theta_{LM} = \frac{\Theta_{out} - \Theta_{in}}{ln\frac{\Theta_{tube} - \Theta_{in}}{\Theta_{tube} - \Theta_{out}}}, \tag{6}$$

where Θ_{out} is air temperature at outlet, Θ_{in} is air temperature at inlet, Θ_{tube} fluid temperature inside tube (VDI e. V., 2010, pp. 1275-1276). Virtual heat transfer coefficient α_v can be calculated with equation (7)

$$\alpha_v = \alpha_m \left[1 - \left(1 - \eta_f\right)\frac{A_f}{A_o}\right], \tag{7}$$

where α_m is mean heat transfer coefficient for tube and fin, η_f is fin efficiency, and A_f is fin surface area (VDI e. V., 2010, p. 1273). Mean heat transfer coefficient α_m can be calculated with equation (8) and fin efficiency with equation (9).

$$\alpha_m = \frac{Nu_d\lambda_{air}}{d_o}, \tag{8}$$

where Nu_d is Nusselt number for finned tube bank and λ_{air} is thermal conductivity of air (VDI e. V., 2010, p. 1276).

$$\eta_f = \frac{\tanh X}{X} = \frac{1}{X}\frac{e^X - e^{-X}}{e^X + e^{-X}}, \tag{9}$$

where *X* is operand which can be calculated with equation (10)

$$X = \varphi_{op} \frac{d_o}{2} \sqrt{\frac{2\alpha_m}{\lambda_f \delta_f}}, \tag{10}$$

where φ_{op} is operand, λ_f is thermal conductivity of fin, and δ_f is fin thickness (VDI e. V., 2010, pp. 1273-1274). Equation's (10) operand φ for rectangular fins can be calculated with equation (11)

$$\varphi_{op} = \left(\varphi'_{\mathrm{op}} - 1\right)\left(1 + 0.35 \ln \varphi'_{op}\right), \tag{11}$$

where φ'_{op} is operand (VDI e. V., 2010, p. 1274). The φ'_{op} operand can be calculated with equation (12)

$$\varphi'_{\mathrm{op}} = 1.28 \frac{b_f}{d_o} \sqrt{\left(\frac{l_f}{b_f} - 0.2\right)}, \tag{12}$$

where b_f is width of rectangular fin and l_f length of rectangular fin (VDI e. V., 2010, p. 1274). Nusselt number of equation (8) for finned tube banks can be calculated with equation (13)

$$Nu_d = C \cdot Re_d^{0.6} \left(\frac{A_o}{A_{t0}}\right)^{-0.15} Pr^{\frac{!}{3}}, \tag{13}$$

where *C* is factor (in-line arrangement: 1-3 rows *C=0.2*, 4≥ rows *C=0.22* and staggered arrangement: 2 rows *C=0.33*, 3 rows *C= 0.36*, 4≥ rows *C=0.38*), Re_d is Reynolds number for air side, A_{t0} is surface area of bare tube between fins, and *Pr* is Prandtl number of air (VDI e. V., 2010, p. 1275). Reynolds number Re_d for heat exchanger's air side flow can be calculated with equation (14)

$$Re_d = \frac{d_o w_{sT} \rho_{air}}{\nu_{air}}, \tag{14}$$

where w_{sT} is temperature corrected air velocity in the smallest cross section of heat exchanger, ρ_{air} is density of air, and ν_{air} is kinematic viscosity (VDI e. V., 2010, p. 1276). Temperature corrected smallest cross section velocity w_{sT} of heat exchanger air side can be calculated with equation (15)

$$w_{sT} = w_s \frac{\frac{1}{2}(\Theta_{in} + \Theta_{out})}{\Theta_{out}}, \tag{15}$$

where w_s is air velocity in the smallest cross section of heat exchanger (VDI e. V., 2010, p. 1276). Air velocity in the smallest cross section w_s can be calculated with equation (16)

$$w_s = w_0 \frac{A_0}{A_s}, \tag{16}$$

where w_0 is air inflow velocity to heat exchanger, A_0 is inflow cross-sectional area, and A_s is the smallest cross-sectional area of air flow (VDI e. V., 2010, p. 1276). Physical dimensions of heat exchanger depend on available space to use. If height and width of flow channel is limited, heat exchanger needs more tube rows to fulfil heat transfer area which is calculated with equation (4). Needed tube rows *NR* to fulfil necessary heat transfer area can be calculated with equation (17)

$$NR = \frac{A_{he}}{NC \cdot A_o}, \tag{17}$$

where NC is number of tube columns (VDI e. V., 2010, p. 1276). Smaller height and width increase number on tube rows and depth of heat exchanger and larger height and width vice versa.

4.3.1 Condensation

Condensation is when water vapor which is in gaseous state starts to turn into liquid state. Condensation happens when water vapor comes into contact with surface which temperature is below the temperature of its thermodynamic equilibrium. (VDI e. V., 2010, p. 905)

Normal air always contains some amount water vapor. Often air is divided as a dry air and water vapor to simplify calculations in air-conditioning applications. Pressure of saturated mixture of dry air and water vapor p_{tot} can be calculated within the idea-gas assumption with equation (18)

$$p_{tot} = p_{dry\ air} + p_{water\ vapor}, \tag{18}$$

where $p_{dry\ air}$ is partial pressure of dry air, and $p_{water\ vapor}$ is partial pressure of water vapor. Partial water vapor pressure is the pressure where it exists alone in certain temperature, volume, and pressure. (Çengel & Boles, 2015, p. 726)

When cooling air, its specific humidity remains the same, but relative humidity increases or in heating other way around. In cooling, condensation begins when heat exchanger's surface temperature is below water vapor dewpoint. Dewpoint is temperature where water is saturated, and it depends on the vapor's pressure and temperature. When relative humidity of ambient air is known, partial water vapor pressure can be calculated with equation (19)

$$p_{water\ vapor} = \frac{RH}{100} \cdot p_{sat.water}, \tag{19}$$

where *RH* is relative humidity and $p_{sat.water}$ is pressure of saturated water. The temperature where water is saturated and meets its dewpoint can be read from tables, example Çengel & Boles (2015, pp. 904-907). (Çengel & Boles, 2015, pp. 727, 740-741)

Cooling air with heat exchanger, cooling fluid's temperature is lower than air (Çengel & Boles, 2015, p. 738). Temperature of heat exchanger surface where water vapor meets its dewpoint, assumed that heat transfer coefficient and thermal conductivity remains the same through heat exchanger, can be estimated with equations (20) and (21)

$$\Theta_{surf} = \Theta_{in} - \frac{\frac{\dot{Q}}{A_{he}}}{\alpha_m}, \tag{20}$$

$$\Theta_{tube} = \Theta_{surf} - \frac{\left(\frac{Q}{A_{he}}\right)\frac{(d_o - d_i)}{2}}{\lambda_c}, \tag{21}$$

where Θ_{surf} is inside surface temperature of pipe, d_i is inside diameter of pipe, and λ_c is thermal conductivity of copper (Lienhard IV & Lienhard V, 2019, pp. 13-19).

In air cooling heat exchanger higher temperature moist air enters the cooling section where its temperature starts to decrease and relative humidity increases. When cooling section is long enough, air meets its saturation point, in other words air with 100 % relative humidity, and water vapor reaches its dewpoint. Because of the saturation of air, it cannot keep same amount of water vapor which it can hold in higher temperature. Condensation begins after air meets its saturation point and goes on until cooling is over. (Çengel & Boles, 2015, p. 741)

Amount of water m_w which exits from heat exchanger can be calculated with equation (22)

$$m_w = m_{air}(\omega_1 - \omega_2), \tag{22}$$

where m_{air} is flow rate of air and ω_n is specific humidity of air (Çengel & Boles, 2015, p. 741). Equation (22) specific humidity ω_1 and ω_2 can be calculated with equation (23) (Çengel & Boles, 2015, p. 728)

$$\omega_n = \frac{0.622RH \cdot p_{sat.water}}{p_{tot}p_{sat.water}}. \tag{23}$$

4.3.2 Pressure drop

Pressure drop depends on depth of finned tube heat exchanger, temperature change, and smallest flow channel's cross-sectional area. Fin and tube surface roughness cause

friction and obstacles in flow or transformation of flow channel's size, direction, etc. create resistance (Basu, et al., 2000, pp. 459-478). For fin tube heat exchanger pressure drop Δp_{tb} can be estimated with correlation in equation (24)

$$\Delta p_{tb} = K \frac{\rho_{air} w_{sT}^2}{2}, \tag{24}$$

where K is loss coefficient for cross flow (Basu, et al., 2000, p. 466). Loss coefficient K for staggered finned tube bank, where lateral and longitudinal pitch are 2 times tube diameter, in cross flow can be calculated with equation (25)

$$K = \left(2.7NR \cdot \sigma_f'^{-0.72}\right) Re_d^{-0.24} \sigma_f''^{0.45}, \tag{25}$$

where σ'_f is ratio of pitch of fin and diameter of tube and σ''_f is ratio of height of fin and diameter of tube (Basu, et al., 2000, p. 467). In heat exchanger unit the heat exchanger isn't the only object which causes pressure drop in flow.

If air flow path should be changed, cooling unit needs duct system to control flow. Changes in flow direction creates pressure drop due to fluid separation from channel walls and flow mixing vortexes (Çengel & Cimbala, 2018, pp. 380-383). Pressure drop in flow channel bends can be estimated with correlation equation (26)

$$\Delta p_{ml} = K_L \frac{1}{2} \rho_{air} w_0^2, \tag{26}$$

where K_L is loss coefficient for certain type of component (Çengel & Cimbala, 2018, p. 380). Loss coefficients K_L for duct system components is given in Figure 16.

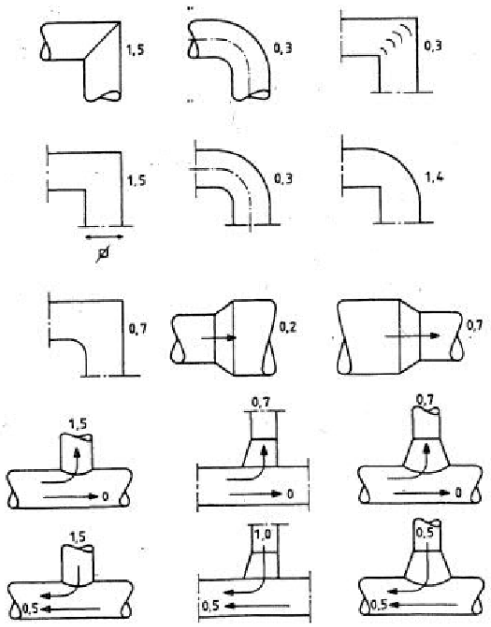

Figure 16. *Duct component loss coefficients (Seppänen, 1996, p. 100)*

Filter in air intake also causes pressure drop. Filter is needed to clean the dust from ventilation air to prevent problems mentioned in chapter 3.1. Filter's pressure drop Δp_{filter} can be estimated with correlation in equation (27)

$$\Delta p_{filter} = \left(\frac{m_{air}}{A_{ep}}\right)^{n_{fp}}, \tag{27}$$

where m_{air} is air flow rate, A_{ep} filter's effective pass area, and n_{fp} is filter specific pressure loss coefficient (Liu, et al., 2003, p. 590).

4.3.3 Axial fans

Fan is a "air-pump" which moves air to meet its requirements such as flowrate or pressure (Cory, 2005, p. 3). For a specific definition of a fan according to the Cory (2005, p. 21) is "A fan is a rotary-bladed machine which delivers a continuous flow of air or gas at some pressure, without materially changing its density". Fans have different types of shapes and sizes depending on its requirements. Main types of fans can be divided in to 5 different flows and they are propeller or axial flow, centrifugal or radial flow, mixed or compound flow, tangential or cross flow, and ring-shaped in which the circulation of fluid is helicoidal (Cory, 2005, pp. 21-22). Eaton uses axial fans in their UPS, so this study focuses on them.

Axial fans can also be divided to 3 types. Types of axial fans are ducted fan, ring mounted fan, and circulator fan (Cory, 2005, p. 26). At UPS there is a tube axial fan which is fan with impeller and casing. 2 different sizes of tube axial fans are represented in Figure 17.

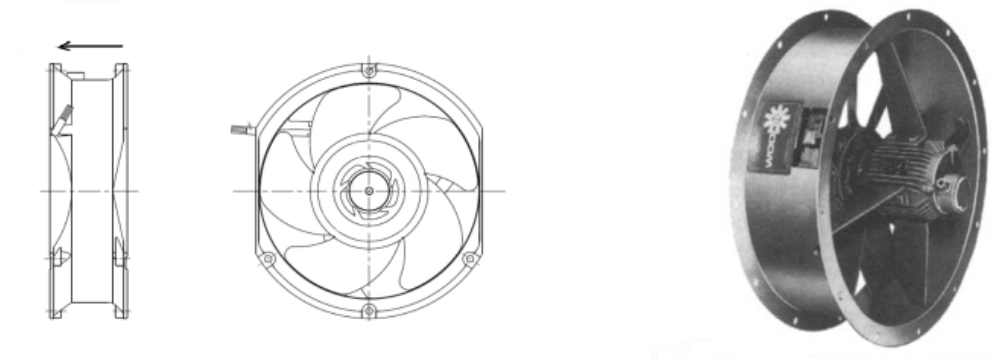

Figure 17. *2 sizes of axial fans (Eaton Corp., 2020, p. 1) (Cory, 2005, p. 27).*

Fans operation, such as air static pressure change or velocity, can be estimated with Bernoulli equation (Cory, 2005, p. 50). The Bernoulli equation can be used to couple pressure, velocity, and elevation in inlet and outlet of steady, incompressible, and frictionless fluid. Although there are no frictionless fluids, Bernoulli equation gives good,

approximated answer when viscous effects are negligibly small compared to inertia, gravitational, and pressure effects according to Çengel & Cimbala (2018, p. 203). Bernoulli equation to air is presented in equation (28) (Çengel & Cimbala, 2018, p. 205).

$$\frac{p_0}{\rho_{air}} + \frac{w_0^2}{2} + gz_0 = \frac{p_1}{\rho_{air}} + \frac{w_1^2}{2} + gz_1 \tag{28}$$

where p_0 is pressure at inflow, g is gravitational magnitude, z_0 inflows height from receiver point, p_1 is pressure at outflow, w_1 is velocity at outflow, and z_1 is outflows height from receiver point. In equation (28) first term in left-hand side is flow energy, second term is kinetic energy, and third term is potential energy at inlet. At the right-hand side terms are in same order but presented at outlet (Çengel & Cimbala, 2018, p. 206).

All fans are unique and have different operating characteristics, so manufacturer provides a fan curve based on test data to describe fans behaviour in different impeller rotation speed. Fan curve describes static pressure change what fan can produce in certain flow rate or other way around (Cory, 2005, p. 49). One example of fan's operational curve with 3 different impeller speed setting is presented in Figure 18.

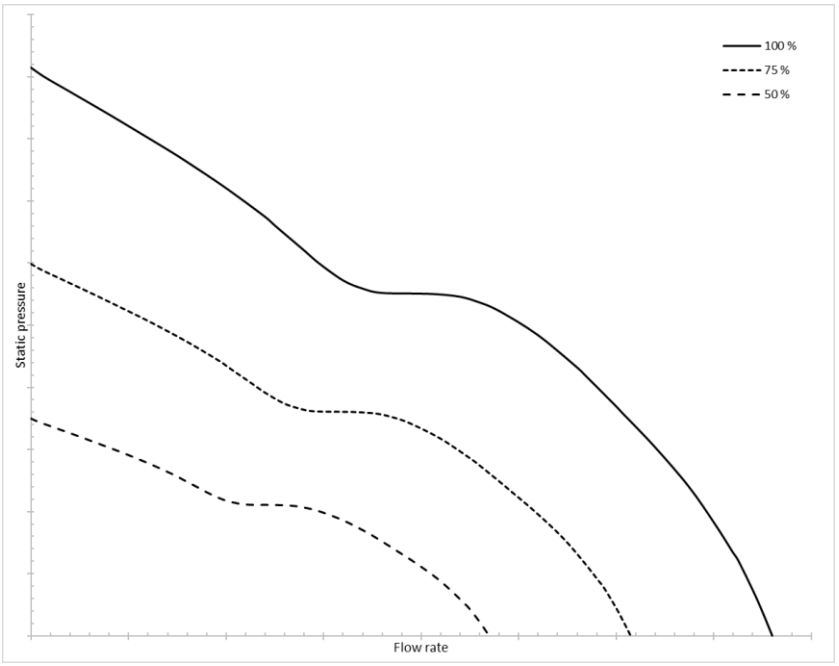

Figure 18. *Fan operation curve.*

4.4 Computational Fluid Dynamics (CFD)

CFD is a computer-based simulation or calculation which can be used to analyse fluid flow, heat transfer and phenomenon related to them, such as chemical reactions. Simu-

lation can be done in 2- or 3-dimensional geometry or fluid domain. Fluid physics is complex and non-linear, so CFD software calculate solution numerically. CFD calculation is done with numerical algorithms which are built in programming code behind CFD software's user interface. The code contains 3 main elements which are pre-processor, solver, and post-processor. (Versteeg & Malalasekera, 2007, pp. 1-4)

Pre-processing is comprising all tasks before solving mathematical problem in solver. Pre-processing starts at defining and modification of 2- or 3-dimensional geometry of problem under interest. Next is mesh (or grid) generation which divines fluid domain into smaller control volumes (CV). After mesh is ready, user selects physical and chemical phenomena that needs to be calculated and defines fluid properties. Last pre-processing task is to specify boundary conditions at edges of fluid and between edges of fluid and solid geometry. (Versteeg & Malalasekera, 2007, pp. 2-3)

Solver element as its name suggests a solver to numerical calculation. There are 3 general numerical calculation techniques which are finite difference, finite element, and spectral methods. This study focuses on Ansys Fluent software that is based on finite difference method and its finite volume formulation. In solver element is 3 main steps which are integration of base and selected governing equations to all over the CVs, converting integral equations to algebraic equations, and solving them iteratively. (Versteeg & Malalasekera, 2007, pp. 3-4)

Post-processing element contains all tasks which are needed to presenting calculation results into more understandable form. In post-processing state, results can be converted, for example, into vector and contour plots, particle tracks, and manipulate viewpoint of them. (Versteeg & Malalasekera, 2007, p. 4)

Pre- and post-processing elements of CFD code are more familiar from other softwares, excluding mesh generation from pre-processing element. Mesh generation and solver element is the most important part of software and especially solver's converting equations, so following subchapters are focused on them.

4.4.1 Mesh

Accuracy of solution depend highly on generated mesh (Versteeg & Malalasekera, 2007, p. 3). Generated mesh (or grid) looks like fish net. Mesh is the fluid domain divided into number of smaller sub-domains. Sub-domains are non-overlapping CVs (or cells) of mesh and in each CV, there is a node. Solution is calculated within each node using discretization. (Versteeg & Malalasekera, 2007, pp. 2-3)

Accuracy of solution can be governed by number of CVs. Generally, the more CVs, the more accurate solution (Versteeg & Malalasekera, 2007, p. 3). However, solution accuracy doesn't get any more accurate in some point or accuracy is seen only in decimals. It is desirable to start CFD simulation with coarse mesh and do a mesh independence test to avoid too fine mesh and long calculation times. For an accurate solution within shorter calculation time, it is desirable to simulate problem with a few or more meshes where each mesh is finer than previous. (Sadrehaghighi, 2021, pp. 44-45)

Ansys Fluent default measures of mesh quality are skewness and orthogonal quality (Ansys, Inc., 2018, pp. 358, 543). Skewness determines how close face or CV is to ideal equilateral or equiangular shape. Example of an ideal and skewed triangles and quadrilaterals faces is presented in Figure 19.

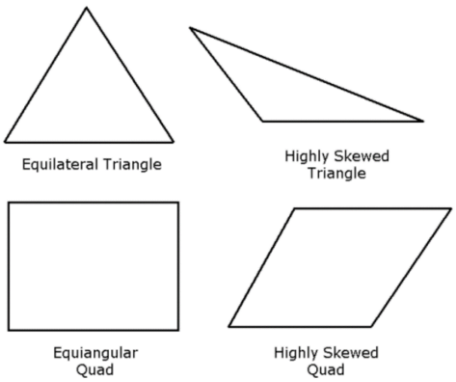

Figure 19. *Ideal and skewed triangle and equiangular faces (Ansys, Inc., 2018, p. 359).*

Skewness can be measured with 2 methods. For tetrahedra meshes skewness is based on equilateral volume and for all other CV and face shapes skewness is based on deviation from normalized equilateral angle. Equilateral-volume-based skewness is defined in equation (29) and normalized equiangular skewness in general is defined in equation (30)

$$Skewness = \frac{Optimal\ Cell\ Size - Cell\ Size}{Optimal\ Cell\ Size}, \tag{29}$$

$$\max\left[\frac{\theta_{max} - \theta_e}{180 - \theta_e}, \frac{\theta_e - \theta_{min}}{\theta_e}\right], \tag{30}$$

where Θ_{max} is largest angle in face or CV, Θ_{min} is smallest angle in face or cell, and Θ_e is angle for equiangular face or cell (60° for triangle, 90° for quad, etc.). (Ansys, Inc., 2018, pp. 359-360)

Orthogonal quality of mesh depends on cell type. Tetrahedra, prism, and pyramid type meshes orthogonal quality is the minimum of orthogonality, 1 minus skewness. For hexahedral and polyhedral meshes, orthogonal quality is same as orthogonality. Orthogonality is determined to all CV faces by calculating it with equations (31) and (32)

$$\frac{\overrightarrow{A_i} \cdot \overrightarrow{f_i}}{|\overrightarrow{A_i}||\overrightarrow{f_i}|}, \tag{31}$$

$$\frac{\overrightarrow{A_i} \cdot \overrightarrow{c_i}}{|\overrightarrow{A_i}||\overrightarrow{c_i}|}, \tag{32}$$

where A_i is normalized dot product of area vector of face, f_i is vector from centroid of CV to centroid of to that face, and c_i is vector from the centroid of the CV to the centroid of adjacent CV that shares that face. In Figure 20 is illustrated vectors to compute orthogonality. (Ansys, Inc., 2018, pp. 543-544)

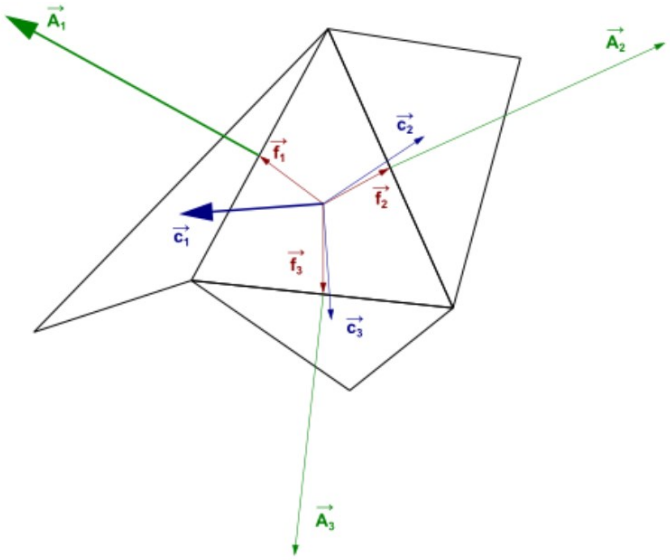

Figure 20. *Orthogonality vectors (Ansys, Inc., 2018, p. 544).*

Ansys Fluent reports skewness and orthogonal quality in range 0 to 1. Ansys (2018, pp. 356, 546) recommends that skewness maximum is less than 0.9 and average around 0.4 and orthogonal quality minimum is higher than 0.01 and average that is significantly higher than minimum. Finer the mesh is, lower the skewness and higher the orthogonal quality is. Skewness and orthogonal quality recommended ranges are presented in metrics spectrum in Figure 21.

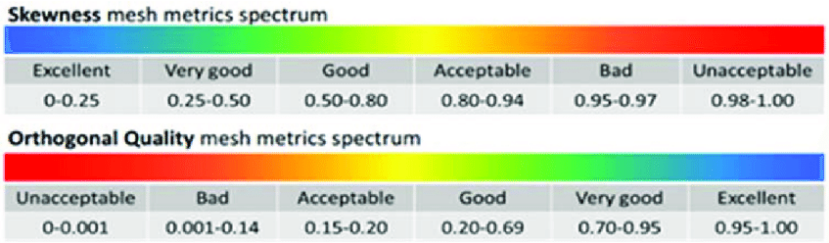

Figure 21. *Skewness and orthogonal quality mesh metrics spectrums (Fatchurrohman & Chia, 2017, p. 4).*

4.4.2 Governing equations

Governing equations of fluid flow are conservation of mass, conservation of momentum, and conservation of energy (Versteeg & Malalasekera, 2007, pp. 10-20). Conservation of mass, or continuity, to unsteady, 3-dimensional flow can be expressed as equation (33)

$$\frac{\partial \rho}{\partial t} + \nabla \cdot (\rho \vec{v}) = S_m, \tag{33}$$

where ρ is fluid density, t is time, v is velocity, and S_m is source term for added to continuous phase from dispersed second phase. Conservation of momentum can be expressed as equation (34)

$$\frac{\partial}{\partial t}(\rho \vec{v}) + \nabla \cdot (\rho \vec{v} \vec{v}) = -\nabla p + \rho \vec{g} + \vec{F}, \tag{34}$$

where p is static pressure and F is external body forces. Conservation of energy can be expressed as equation (35)

$$\frac{\partial}{\partial t}(\rho E) + \nabla \cdot \left(\vec{v}(\rho E_{ie} + p)\right) = -\nabla \cdot \left(\sum_j h_j J_j\right) + S_h, \tag{35}$$

where E_{ie} is internal energy, h_j is heat transfer coefficient, J_j is mass flux, and S_h is source term for added energy. (Ansys, Inc., 2018, p. 15)

4.4.3 Turbulence modelling

Turbulence is 3-dimensional unsteady and random fluid flow motion. Detailed turbulence modelling needs a lot of computational power from Central Processing Unit (CPU), because of the time dependent small-scale eddies evolving in turbulent flow. Small-scale eddies need very detailed mesh where smallest CV is smaller than smallest eddy in flow and needs to be solved by Direct Numerical Simulation (DNS). Calculating such a fine mesh with DNS is very time consuming and needs more computational power from CPU

than a normal engineering station can contain for any foreseeable future. (Ansys, Inc., 2018, pp. 1179-1180)

CFD calculations are nowadays done with averaging procedure to save time and computational power. Most well-known procedure for turbulence modelling is time-averaging Reynolds-Averaged Navier-Stokes (RANS) equations. Reynolds averaging divides variables into time-averaged mean and fluctuating components. Averaged variables for scalar velocity components u_i are calculated with equation (36) and for pressure and other scalar quantities φ with equation (37)

$$u_i = \overline{u_i} + u_i', \tag{36}$$

$$\varphi = \bar{\varphi} + \varphi', \tag{37}$$

where $\bar{u}_i$ is mean velocity, u'_i is fluctuating velocity, $\bar{\varphi}$ is mean component, and φ' is fluctuating component. Mean and fluctuating components of φ are pressure, energy, species concentration or such as scalar components. (Ansys, Inc., 2018, p. 39)

In Ansys Fluent, variable density flows Reynolds averaged velocity is changed to Favre-averaged velocity (Ansys, Inc., 2018, p. 40). The Favre-averaged density-weighted mean velocity $\tilde{u}$ is defined as equation (38) and instantaneous velocity u defined as equation (39)

$$\tilde{u} = \frac{\overline{\rho u}}{\bar{\rho}}, \tag{38}$$

$$u = \tilde{u} + u'', \tag{39}$$

where u'' is fluctuating velocity with effects of density fluctuations. (Versteeg & Malalasekera, 2007, pp. 376-377).

Substituting Favre averaged components to instantaneous RANS continuity (40), momentum (41) and scalar transport (42) equations for compressible flow can be written as

$$\frac{\partial \bar{\rho}}{\partial t} + \nabla \cdot (\bar{\rho}\tilde{u}) = 0, \tag{40}$$

$$\frac{\partial}{\partial t}(\bar{\rho}\tilde{u}_i) + \nabla \cdot \left(\bar{\rho}\tilde{u}_i\tilde{u}_j\right) = -\nabla\bar{p} + \nabla \cdot (\mu\nabla\tilde{u}_i) + \mathrm{S_m} + \nabla \cdot (-\overline{\bar{\rho}u_i''^2} - \overline{\bar{\rho}u_i''u_j''}), \tag{41}$$

$$\frac{\partial}{\partial t}(\bar{\rho}\tilde{\varphi}) + \nabla \cdot (\bar{\rho}\tilde{\varphi}\tilde{u}) = \nabla \cdot \left(\Gamma_\varphi \nabla\tilde{\varphi}\right) + S_\varphi + \nabla \cdot \left(-\overline{\bar{\rho}u''\varphi''}\right), \tag{42}$$

where Γ_φ is diffusion coefficient (Versteeg & Malalasekera, 2007, p. 79). Last term in equation (41) is Reynolds stresses and must be calculated to close the equation (Ansys, Inc., 2018, p. 40). To solve Reynolds stresses, CFD software uses turbulence models (Versteeg & Malalasekera, 2007, p. 66). Ansys Fluent provides turbulence models such

as Spalart-Allmaras, k-ε, k-ω, Reynolds stress, and many others (Ansys, Inc., 2018, p. 1180). In Ansys Fluent the stresses are solved using Boussinesq hypothesis in Spalart-Allmaras, k-ε, and k-ω turbulence models (Ansys, Inc., 2018, p. 41). Boussinesq hypothesis is defined as equation (43)

$$-\overline{\bar{\rho}u_i''u_j''} = \mu_t\left(\frac{\partial\tilde{u}_i}{\partial x_j}+\frac{\partial\tilde{u}_j}{\partial x_i}\right)-\frac{2}{3}\left(\bar{\rho}k+\mu_t\frac{\partial\tilde{u}_k}{\partial x_k}\right)\delta_{ij}, \quad (43)$$

where μ_t is turbulent viscosity, k turbulent kinetic energy, and δ_{ij} is Kronecker delta ($\delta_{ij}=1$ if $i=j$ and $\delta_{ij}=0$ if $i\neq j$ (Versteeg & Malalasekera, 2007, p. 67)) (Ansys, Inc., 2018, p. 41).This study mainly used Shear-Stress Transport (SST) k-ω model which is developed by Menter and it's based k-ε model (Versteeg & Malalasekera, 2007, p. 91). In Menter's SST k-ω model, Reynolds stresses and k-equation are same as in Wilcox k-ω model (Versteeg & Malalasekera, 2007, p. 91). Equation's (43) turbulent viscosity can be calculated with equation (44)

$$\mu_t = \frac{\rho k}{\omega}\frac{1}{\max\left[\frac{1}{\alpha^*},\frac{SF_2}{a_1\omega}\right]}, \quad (44)$$

where ω is specific dissipation rate, F_2 and α^* are coefficients, and a_1 is model specific constant (Ansys, Inc., 2018, p. 59). Coefficients F_2 can be calculated with equation (53) and α^* with equation (51). Turbulent kinetic energy k and specific dissipation rate ω can be obtained from transport equations (45) and (46)

$$\frac{\partial}{\partial t}(\rho k)+\frac{\partial}{\partial x_i}(\rho k u_i)=\frac{\partial}{\partial x_j}\left(\Gamma_k\frac{\partial k}{\partial x_j}\right)+G_k-Y_k+S_k, \quad (45)$$

$$\frac{\partial}{\partial t}(\rho \omega)+\frac{\partial}{\partial x_i}(\rho \omega u_i)=\frac{\partial}{\partial x_j}\left(\Gamma_\omega\frac{\partial \omega}{\partial x_j}\right)+G_\omega-Y_\omega+S_\omega, \quad (46)$$

where G_k is production of turbulence kinetic energy, G_ω is generation of ω, Γ_k and Γ_ω are effective diffusivity of k and ω, Y_k and Y_ω are turbulence dissipation of k and ω (Ansys, Inc., 2018, pp. 61-62). G_k and G_ω can be calculated with equations (47) and (48)

$$G_k = \mu_t S^2, \quad (47)$$

$$G_\omega = \frac{\alpha\alpha^*}{v_t}G_k, \quad (48)$$

where S is mean rate-of-strain tensor, α and α^* are coefficients, and v_t is turbulent kinematic viscosity (Ansys, Inc., 2018, pp. 62-63). Mean rate-of-strain tenson can be calculated with equation (49) and Coefficients α and α^* can be calculated with equations (50) and (51)

$$S = \sqrt{2S_{ij}S_{ij}}, \tag{49}$$

$$\alpha = \frac{\alpha_\infty}{\alpha^*}\left(\frac{\alpha_0 + \frac{Re_t}{R_\omega}}{1 + \frac{Re_t}{R_\omega}}\right), \tag{50}$$

$$\alpha^* = \frac{\beta_i}{3}, \tag{51}$$

Turbulent Reynolds number Re_t can be calculated with equation (52) and coefficient F_2, α_∞ and β_i can be calculated with equations (53), (54), and (55)

$$Re_t = \frac{\rho k}{\mu\omega}, \tag{52}$$

$$F_2 = \tanh(\Phi_2^2), \tag{53}$$

$$\alpha_\infty = F_1\alpha_{\infty,1} + (1 - F_1)\alpha_{\infty,2}, \tag{54}$$

$$\beta_i = F_1\beta_{i,1} + (1 - F_1)\beta_{i,2}, \tag{55}$$

where μ is dynamic viscosity, Φ_2, F_1, $\alpha_{\infty,1}$, and $\alpha_{\infty,2}$ are coefficients and $\beta_{i,1}$ and $\beta_{i,2}$ are model specific constants (Ansys, Inc., 2018, pp. 64, 62-63). Coefficients Φ_2, F_1, $\alpha_{\infty,1}$, and $\alpha_{\infty,2}$ can be calculated with equations (56), (57), (58), and (59)

$$\Phi_2 = \max\left[2\frac{\sqrt{k}}{0.09\omega y}, \frac{500\mu}{\rho y^2\omega}\right], \tag{56}$$

$$F_1 = \tanh(\Phi_1^4), \tag{57}$$

$$\alpha_{\infty,1} = \frac{\beta_{i,1}}{\beta_\infty^*} - \frac{\kappa^2}{\sigma_{\omega,1}\sqrt{\beta_\infty^*}}, \tag{58}$$

$$\alpha_{\infty,2} = \frac{\beta_{i,2}}{\beta_\infty^*} - \frac{\kappa^2}{\sigma_{\omega,2}\sqrt{\beta_\infty^*}}, \tag{59}$$

where y is distance to next surface, Φ_1 is Thiele modulus, and κ, β_∞^*, $\sigma_{\omega,1}$, and $\sigma_{\omega,2}$ are model specific constants (Ansys, Inc., 2018, pp. 62-64).

Equations (45) and (46) turbulence dissipation terms Y_k and Y_ω can be calculated with equations (60) and (61)

$$Y_k = \rho\beta^* k\omega, \tag{60}$$

$$Y_\omega = \rho\beta\omega^2, \tag{61}$$

where β^* and β are coefficients (Ansys, Inc., 2018, p. 63). Coefficients β^* and β can be calculated with equation (62) and (63)

$$\beta^* = \beta_i^*[1 + \zeta^* F(M_t)], \tag{62}$$

$$\beta = F_1\beta_{i,1} + (1 - F_1)\beta_{i,2}, \tag{63}$$

where β_i^* is coefficient, $F(M_t)$ is compressibility function and ζ^* is model specific constant (Ansys, Inc., 2018, pp. 60,63). Coefficient β_i^* can be calculated with equation (64) and Compressibility function $F(M_t)$ with equation (65)

$$\beta_i^* = \beta_\infty^* \left(\frac{\frac{4}{15} + \left(\frac{Re_t}{R_\beta}\right)^4}{1 + \left(\frac{Re_t}{R_\beta}\right)^4} \right), \tag{64}$$

$$F(M_t) = \begin{cases} 0 & M_t \leq M_{t0} \\ M_t^2 - M_{t0}^2 & M_t > M_{t0} \end{cases}, \tag{65}$$

where β_∞^*, R_β, and M_{t0} are model specific constants and M_t^2 is coefficient (Ansys, Inc., 2018, p. 60). Coefficient M_t^2 can be calculated with equation (66)

$$M_t^2 \equiv \frac{2k}{a^2}, \tag{66}$$

where a is coefficient (Ansys, Inc., 2018, pp. 60-61). Coefficient a can be calculated with equation (67)

$$a = \sqrt{\gamma RT}, \tag{67}$$

where γ is ratio of specific heats (c_p/c_v), R is gas-law constant, and T is temperature (Ansys, Inc., 2018, p. 61).

Equations (45) and (46) effective diffusivity terms Γ_k and Γ_ω can be calculated with equation (68) and (69)

$$\Gamma_k = \mu + \frac{\mu_t}{\sigma_k}, \tag{68}$$

$$\Gamma_\omega = \mu + \frac{\mu_t}{\sigma_\omega}, \tag{69}$$

where σ_k and σ_ω are turbulent Prandtl numbers (Ansys, Inc., 2018, p. 62). Turbulent Prandtl numbers σ_k and σ_ω can be calculated with equations (70) and (71)

$$\sigma_k = \frac{1}{\frac{F_1}{\sigma_{k,1}} + \frac{1 - F_1}{\sigma_{k,2}}}, \tag{70}$$

$$\sigma_\omega = \frac{1}{\frac{F_1}{\sigma_{\omega,1}} + \frac{1 - F_1}{\sigma_{\omega,2}}}, \tag{71}$$

where $\sigma_{k,1}$, $\sigma_{k,2}$, $\sigma_{\omega,1}$, and $\sigma_{\omega,2}$ are model specific constants (Ansys, Inc., 2018, p. 62).

4.4.4 Discretisation

Before solving equations of flow, CFD software converts scalar equations to an algebraic equation which can be solved numerically (Ansys, Inc., 2018, p. 690). Finite volume method discretisation starts by defining boundaries of each CV and placing nodes (or nodal points) in centre of CV boundaries. CV boundaries are faces of volume inside the fluid domain and defined boundary conditions at the edge of fluid domain. Principle of discretisation is easiest to explain in 1-dimensional steady state flow. In Figure 22 is presented part of 1-dimensional mesh where *P* represents general centre node, *W* west node, *E* east node, and *w* and *e* west and east faces of CV. (Versteeg & Malalasekera, 2007, p. 116)

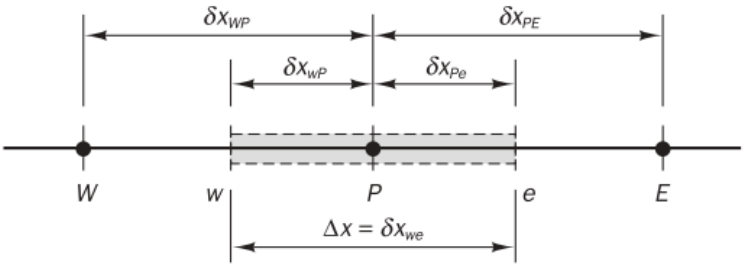

Figure 22. *Discretisation mesh (Versteeg & Malalasekera, 2007, p. 116).*

In Figure 22 distances between the nodes *P* and *W* or *E* is represented with δx_{WP} and δx_{PE}, distance from node *P* to *w* or *e* face with δx_{wP} and δx_{Pe}, and CV's width $\Delta x = \delta x_{we}$. (Versteeg & Malalasekera, 2007, p. 116)

Governing equations are integrated over every CV to yield discretised equations to centre node *P*. Discretisation over a mesh is presented in simplest governing equation, a 1-dimensional steady state heat conduction presented in equation (72)

$$\frac{d}{dx}\left(\Gamma_\varphi \frac{d\phi}{dx}\right) + S_{diff} = 0, \tag{72}$$

where Φ is diffusion of property and S_{diff} is source term of diffusion (Versteeg & Malalasekera, 2007, p. 115). Next, equation (72) is integrated over the mesh presented in Figure 22. Integrated equation is presented in equation (73)

$$\int_{\Delta V} \frac{d}{dx}\left(\Gamma_\varphi \frac{d\phi}{dx}\right) dV + \int_{\Delta V} S_{diff} dV = \left(\Gamma_\varphi A \frac{d\phi}{dx}\right)_e - \left(\Gamma_\varphi A \frac{d\phi}{dx}\right)_w + \bar{S}_{\mathrm{diff}} \Delta \mathrm{V} = 0, \tag{73}$$

where *A* is cross-sectional area of CV's face, ΔV is volume of CV, and $\bar{S}_{diff}$ is average value of diffusion source. Linearly interpolated diffusion coefficient Γ_φ can be calculated

in uniform grid with equation (74) to west side of centre node and with (75) to east side of centre node

$$\Gamma_{\varphi_w} = \frac{\Gamma_W + \Gamma_P}{2}, \tag{74}$$

$$\Gamma_{\varphi_e} = \frac{\Gamma_P + \Gamma_E}{2}, \tag{75}$$

where subscript *w* is west side face, *e* is east side face, *W* is west side node, *P* is centre node, and *E* is east side node (Versteeg & Malalasekera, 2007, p. 117). Equation's (73) right-hand side 2 first terms are diffusive flux terms. Diffusive flux term to west side node can be calculated with equation (76) and to east side node with equation (77)

$$\left(\Gamma_\varphi A \frac{d\phi}{dx}\right)_w = \Gamma_{\varphi_w} A_w \left(\frac{\phi_P - \phi_W}{\delta_{x_{WP}}}\right), \tag{76}$$

$$\left(\Gamma_\varphi A \frac{d\phi}{dx}\right)_e = \Gamma_{\varphi_e} A_e \left(\frac{\phi_e - \phi_P}{\delta_{x_{PE}}}\right), \tag{77}$$

where subscripts are the same as equations (74) and (75) (Versteeg & Malalasekera, 2007, p. 117). Source term, the last term of right-hand side in equation (73), can be approximated with equation (78) to dependent variable

$$\bar{S}\Delta V = S_u + S_P \phi_P, \tag{78}$$

where S_u is function of dependent variable (Versteeg & Malalasekera, 2007, p. 117).

Discretisation technique presented above can't be used directly to unstructured meshes. In unstructured meshes CVs can be in any shapes and has no specific co-ordinate system. With Gauss's divergence theorem discretisation can be done to any shape of CVs. Gauss's divergence theorem can be expressed as in equation (79)

$$\int_{CV} div\ \boldsymbol{a}_c\ dV = \int_A \boldsymbol{n}_{out}\ .\boldsymbol{a}\ dA\,, \tag{79}$$

where $\boldsymbol{a}_c$ is component vector and $\boldsymbol{n}_{out}$ is a normal of outward unit vector (Versteeg & Malalasekera, 2007, p. 313). For more information and derivation of equations check (Ansys, Inc., 2018), (Ansys, Inc., 2018), and (Versteeg & Malalasekera, 2007).

4.5 Taguchi method

Taguchi method is Dr. Genichi Taguchi's approach to improve quality and optimize processes in manufacturing industry. Taguchi methods cover product manufacturing from new product development to product manufacturing. The idea is to design and build quality into product, so it's immune to uncontrolled applications and environmental factors,

design manufacturing process to minimize variation around target values of quality and reduce costs by manufacturing high quality products. Taguchi has been developed 3 concepts to improve product quality and tackle unwanted influence of outer factors. His first concept to improve quality is to design products that are so robust, they can't be influenced to uncontrolled applications and environmental factors on manufacturing processes. Second concept is to specify critical target value of quality and develop manufacturing process to meet this target value with a minimized deviation around it. Third concept is to measure deviations from specified target value in terms of the overall life cycle costs of product, including warranty time. (Roy, 2010, pp. 10-12)

Taguchi methods of quality have been studied and implemented to chemical, electrical, and mechanical applications, but also to, software testing, on-line quality engineering and to human performance with Mahalanobis-Taguchi method (Taguchi, et al., 2005, pp. 57-122). This study focuses on Taguchi's approach to Design Of Experiments (DOE) and this subchapter goes through its principles.

Taguchi's design of experiments includes orthogonal arrays (OAs) to determine minimum number of tests and standardized method to analyse results of tests. When designing experiment, the number of tests can rise to countless numbers depending on factors and their levels. Full number of possible tests or designs *N* can be calculated with equation (80)

$$N = L^m, \tag{80}$$

where *L* is number of levels of each factor and *m* is number of factors (Roy, 2010, p. 3).

As the equation (80) suggests, full tests can easily get expensive and time consuming because of the high number of possible tests. Method to select limited number of tests which produce most information is well known, but there are no general guidelines how to do selection or analysing the result. Taguchi's method combines these two by defining general OAs and standard for analysing results. In Table 5 is comparison for total number of tests with all possible factors and levels and number of tests using Taguchi's OAs. (Roy, 2010, pp. 50-51)

Table 5. *Comparison between the full tests and Taguchi method (Roy, 2010, p. 51).*

Levels (*L*)	Factors (*m*)	Full test (*N*)	Taguchi method
2	2	4	4
2	3	8	4
2	7	128	8
2	15	32,768	16
3	4	81	9

Designing tests with Taguchi method should always satisfy 2 objectives, factors, and levels. Without determinizing number of factors and levels of each factor we couldn't identify how many trials it will need and selecting OAs is impossible (Roy, 2010, p. 53). Taguchi, et al. (2005, p. 1528) have been suggested following steps to designing and running tests:

1. *Define a problem*. Why tests should be done and what answers it should give
2. *Determine objectives*. Identify measurable input and output characteristics and how they can be measured
3. *Brainstorm*. Arrange all factors to control and noise factors and determine their levels and values
4. *Design the test*. Select appropriate OAs, list control factors and interactions to OA columns, and select OA for noise factors and assign them in columns
5. *Conduct tests and collect data.*
6. *Analyse data with Average response tables and graphs and Analysis Of Variance (ANOVA) or with Signal to Noise (SN) tables, graphs.*
7. *Interpret the results.* Select the optimum levels of control factors and predict results of optimal conditions
8. *Run confirmatory tests to verify predicted results of optimal conditions.* If confirmatory and predicted results match, tests are ready, but if test results aren't predicted or results are unsatisfactory, more tests should be done

Results to steps 1 to 3 at list above comes from experience of engineer/designer and product knowledge which aren't in Taguchi method scope and aren't discussed in this subchapter.

Selecting OAs are in centre of the method. As said earlier, Dr. Taguchi has been defined a set OAs which are sufficient for many different situations and tests. After determining factors and levels of test, next step is selecting appropriate OA. OA is marked as L_n, where subscript n stands for needed tests (or trials). For example, product has a 7 different possible design option, input energy, supply pressure etc. aka factors and each have lower and upper value, thus 2 levels for each. For this test appropriate OA is L_8 which test is run by Table 6 (Taguchi, et al., 2005, p. 1530). Numbers in top row indicates each factor, first column at left-hand indicates number of test and numbers 1 and 2 in the table indicates levels of each factor (Roy, 2010, pp. 51-52). More OAs are given in Taguchi, et al. (2005) appendix A and in Roy (2010) appendix A.

Table 6. *Array L_8 test run conditions (Taguchi, et al., 2005, p. 1530).*

Factor / Test no.	1	2	3	4	5	6	7
1	1	1	1	1	1	1	1
2	1	1	1	2	2	2	2
3	1	2	2	1	1	2	2
4	1	2	2	2	2	1	1
5	2	1	2	1	2	1	2
6	2	1	2	2	1	2	1
7	2	2	1	1	2	2	1
8	2	2	1	2	1	1	2

Test structure for L_8 is illustrated at full test table with Taguchi method test numbers in Table 7 (Roy, 2010, p. 52). Table 7 notation *F* is factor, its subscript *n* is factor number, and *m* is level of factor, and *T* is test and its subscript *n* stands for test number.

Table 7. *Test structure (Roy, 2010, p. 52).*

Factors (F_{nm})				**F_{11}**				**F_{12}**			
				F_{21}		**F_{22}**		**F_{21}**		**F_{22}**	
				F_{31}	**F_{32}**	**F_{31}**	**F_{32}**	**F_{31}**	**F_{32}**	**F_{31}**	**F_{32}**
F_{41}	**F_{51}**	**F_{61}**	**F_{71}**	T_1							
			F_{72}								
		F_{62}	**F_{71}**								
			F_{72}				T_3				
	F_{52}	**F_{61}**	**F_{71}**								
			F_{72}						T_5		
		F_{62}	**F_{71}**							T_7	
			F_{72}								
F_{42}	**F_{51}**	**F_{61}**	**F_{71}**								
			F_{72}							T_8	
		F_{62}	**F_{71}**						T_6		
			F_{72}								
	F_{52}	**F_{61}**	**F_{71}**				T_4				
			F_{72}								
		F_{62}	**F_{71}**								
			F_{72}	T_2							

It is desirable to run tests in random order in first test runs and in test repetition or confirmatory tests, if its anyhow possible. Random order prevents influence of test setup to results and in confirmatory tests, results are more reliable. (Roy, 2010, p. 56)

4.5.1 Analysis of results

Taguchi's approach to testing is only partial and it needs different type of analysing than a full tests. Providing tests confidence there is a standard statistical technique called ANOVA. It doesn't analyse the test data but determines variance of the data and measures confidence of tests via variance. ANOVA provides the variance of control and noise factors which can be used to predict optimum conditions. (Roy, 2010, p. 129)

In ANOVA, data of tests are analysed with many quantities by calculating and organizing them in standard format. Generalized format of ANOVA table is presented in Table 8. (Roy, 2010, pp. 130, 137)

Table 8. *ANOVA table (Roy, 2010, p. 137).*

Source of variation	Degrees of free-dom f	Sum of squares S	Variance (mean square) V	Variance ratio F	Pure sum of squares S'	Precent contribu-tion P
Factor (F_1)						
Factor (F_2)						
…						
Factor (F_n)						
Error (e)						
Total (T)						

Analysing starts with calculating total number of trials *n* with equation (81)

$$n = n_1 + n_2 + n_3 + \cdots + n_n, \tag{81}$$

where n_n is test (Roy, 2010, p. 130).

Next is calculating Degrees Of Freedom (DOF). Daintith and Rennie (2005, p. 60) define DOF is 'the number of independent parameters that are needed to specify the configuration of a system'. In ANOVA, DOF represents the effective sample size (Eisenhauer, 2008, p. 77). For OAs total DOF f_T can be calculated with equation (82), DOF for 1 factor with (83), DOF for interactions f_{Fn*Fm} with (84) and DOF of error term f_e for sum of squares with (85)

$$f_T = nr - 1, \tag{82}$$

$$f_{F_n} = n - 1, \tag{83}$$

$$f_{F_n \cdot F_m} = f_{F_n} \cdot f_{Fm}, \tag{84}$$

$$f_e = f_T - f_{F_1} - f_{F_2} - f_{F_3} - \cdots - f_{F_n}, \tag{85}$$

where *r* is number repetitions of each trial, and f_{Fn} and f_{Fm} is DOF for each factor (f_{Fn}=*L*-1) (Roy, 2010, pp. 62, 130).

Sum of squares mentioned in above paragraph is measure of deviation of the test data from mean value of the data. Sum of squares is used in calculating variance. Factor S_{Fn}, error S_e, and total S_T sum of squares for 2 and more factors with 2 and more levels can be calculated with equations (86), (87) and (88)

$$S_{F_n} = \sum_{k=1}^{L} \sigma_k^2 - C.F., \tag{86}$$

$$S_T = \sum_{i=1}^{n} (Y_i - Y_0)^2 - C.F., \tag{87}$$

$$S_e = S_T - (S_{F_1} + S_{F_2} + S_{F_3} + \cdots + S_{F_n}), \tag{88}$$

where σ_k^2 is general variance of test sample, *C.F.* is correlation factor, Y_i is measured value, and Y_0 is target value (Roy, 2010, pp. 141-147). General variance σ_k^2 can be calculated with equation (89) and correlation factor C.F. with equation (90)

$$\sigma_k^2 = \frac{1}{n} \sum_{i=1}^{n} (Y_i - \bar{Y})^2, \tag{89}$$

$$C.F. = \frac{[\sum_{i=1}^{n} (Y_i - Y_0)]^2}{n}, \tag{90}$$

where $\bar{Y}$ is average value of Y_i. Total sum of squares is valuable value for controlling the variations around the target value and developing process or design, especially in the manufacturing process. (Roy, 2010, pp. 132, 142)

Calculating variance exposes distribution of data from the mean value. Variance is calculated from all the sum of squares. Total V_T, 1 factor's V_{Fn} and error V_m variance can be calculated with equations (91), (92) and (93) (Roy, 2010, pp. 132,135)

$$V_T = \frac{S_T}{f_T}, \tag{91}$$

$$V_{F_n} = \frac{S_{F_n}}{f_{F_n}}, \tag{92}$$

$$V_e = \frac{S_e}{f_e}. \tag{93}$$

Next step for analysing data is calculate variance ratio. Variance ratio, more commonly known as *F* value, is ratio between calculated variance and error variance. According to Roy (2010, p. 138) *F* value is used to measure the significance of the factor under investigation with respect to variance of all the factors in calculated in error term. *F* value calculated from data is compared with standard *F* value from the *F*-table. *F* value from measured data to 1 factor F_{Fn} can be calculated with equation (94)

$$F_{F_n} = \frac{V_{F_n}}{V_e}, \tag{94}$$

To *F*-table DOF numerator f_1 is f_{Fn} and DOF denominator f_2 is f_e. If calculated *F* value is smaller than *F* value from the table of selected significance level, factor doesn't contribute within the confidence level and factors included to study contributes only calculated

percentage and the rest of error is from other factors that isn't included in study. *F* value tables can be found, for example in Roy (2010) at Appendix B. (Roy, 2010, pp. 138-144)

Pure sum of squares is used to calculate percent contribution, which is used to estimate the contribution of each factor to the results (Roy, 2010, pp. 138-139). Pure sum of squares to 1 factor S'_{Fn} and for error S'_e can be calculated with equations (95) and (96) (Roy, 2010, p. 139)

$$S'_{F_n} = S_{F_n} - f_{F_n} V_e, \tag{95}$$

$$S'_e = S_e + \left(f_{F_1} + f_{F_2} + \cdots + f_{F_n}\right) V_e. \tag{96}$$

Last step to complete the ANOVA table is calculate percent contribution. Percent contribution to 1 factor P_{Fn} and error P_e can be calculated with equations (97) and (98) (Roy, 2010, p. 139)

$$P_{F_n} = \frac{100 S'_{F_n}}{S_T}, \tag{97}$$

$$P_e = \frac{100 S'_e}{S_T}. \tag{98}$$

For more information of ANOVA is presented in Roy (2010, pp. 129-172) and Taguchi, et al. (2005, pp. 501-583).

4.5.2 Signal-to-Noise ratio (SN)

Signal-to-Noise ratio (SN) is originally used in electrical engineering field and its roots are in communication industry. SN name comes from voice as a signal transmitted in wave from broadcasting station to radio and radio is used as a measuring equipment. Signal transmitted mixes with audible noise in space and a good radio catches the signal which is not affected by noise. In such cases SN ratio is expressed as decibels, where example 10,000 times magnitude of input to the magnitude of noise is 40 decibels. The SN ratio express quality of a radio and larger the ratio is, better quality of a radio is. (Taguchi, et al., 2005, p. 224)

SN ratio is used to analyze the effect of uncontrollable factors in tests and make design so robust that those uncontrollable factors doesn't have effect on final product. SN ratio measures variation around target value where signal is the output value and the noise is uncontrollable factor (Roy, 2010, pp. 172-173). SN ratio in product testing helps to select optimized level of factors with least variability and closest to average around the target value, helps to compare test data sets with respect to variability and deviation of average around the target value and it linearises results of all nonlinear behaviour (Roy, 2010, pp. 174-175). SN ratio can be defined as in equation (99) (Taguchi, et al., 2005, p. 225)

$$SN\ ratio = \frac{Power\ of\ signal}{Power\ of\ noise} = \frac{(sensitivity)^2}{(variability)^2}. \quad (99)$$

As the equation (99) proposes, high value of SN ratio implicates that design of a product is so robust that noise factors don't effect on signal (Roy, 2010, p. 173).

SN ratio can be used to observe how different test conditions impacts on signal in experiments with two or more test runs (Roy, 2010, p. 182). SN ratio for measuring quality of product can be divided into three quality categories. Categories and their usability are nominal-is-the-best, which is used to reduce variability around the target, smaller-the-better is used to reduce average and variability around the target and larger-the-better is used to maximize average with minimal variability around the target. (Taguchi, et al., 2005, p. 236)

To use SN ratio, test results are converted to single number in 2 steps after deciding which quality category is the best for the product in question. First step is to calculate Mean Square Deviation (MSD) of collected test results. MSD to nominal-is-the-best can be calculated with equation (100), smaller-the-better with equation (101), and larger-the-better with equation (102). Second step is to calculate SN ratio from MSD with equation (103). SN ratio is linear because of the logarithmic equation which transforms every non-linear behaviour in to linear. (Roy, 2010, pp. 173-175)

$$MSD_{nom} = \frac{(Y_1 - Y_0)^2 + (Y_2 - Y_0)^2 + \cdots + (Y_n - Y_0)^2}{n}, \quad (100)$$

$$MSD_{small} = \frac{Y_1^2 + Y_2^2 + \cdots + Y_n^2}{n}, \quad (101)$$

$$MSD_{large} = \frac{\frac{1}{Y_1^2} + \frac{1}{Y_2^2} + \cdots + \frac{1}{Y_n^2}}{n}, \quad (102)$$

$$SN = -10 \log_{10}(MSD). \quad (103)$$

5. PRODUCT DEVELOPMENT PROCESS

This chapter presents how development methods and tools were applied to product development process. Chapter is divided for all different methods and tools to their own subchapters. However, because of the integration of methods and tools to CPM/PDD method, all subchapters are somehow linked to the first subchapter 5.1.

5.1 Product concept using CPM/PDD method

CPM/PDD method were used to guide the development process. PDD part of the method, as mentioned in subchapter 4.1, describes development process and guides it with product's required properties list. As Weber (2014, p. 329) proposes, many other methods and tools could be integrated to CPM/PDD method. All other methods were used to examine properties of product characteristics and do they fulfil required properties. CPM part of the method guided comparison between different characteristics and properties. Also, CPM part helped to find out which characteristic have dependencies and could those dependencies reduce the need of different characteristics.

In this study, PDD part of the method launched development process by collecting required properties list by interviewing Eaton PQ's management level staff which are in contact to company's product development, manufacturing, and customers. Headings and frame for interview which were used to define different perspectives for relevant properties were:

- Functional properties
- Efficiency
- Strength, Stiffness, Stability
- Life-time, Durability
- Safety, Reliability
- Spatial Properties, Weight
- Aesthetic Properties
- Ergonomic Properties
- Manufacturing, Assembly, Test Properties
- Transportation Properties

- Maintenance and Repair Properties
- Compliance with Regulations and Standards
- Resource Consumption
- Cost Properties

All perspectives weren't caught, and all required properties hasn't taken account in this study, because of boundaries and focus of the thesis. Full list of found required properties of cooling unit is presented in appendix A (Paananen, et al., 2021).

After required properties was collected and analysed, product development moved to find solutions to fulfil them. In this stage, development process moves to CPM part of the method. As explained in subchapter 4.1, CPM has an analysis and synthesis steps for comparing characteristics and properties of product. CPM process started taking few of *PR* along to synthesis steps and, as Weber (2014, p. 336) is convinced, piling known elements and solutions to characteristics list. First synthesis step of CPM/PDD method is illustrated in Figure 23.

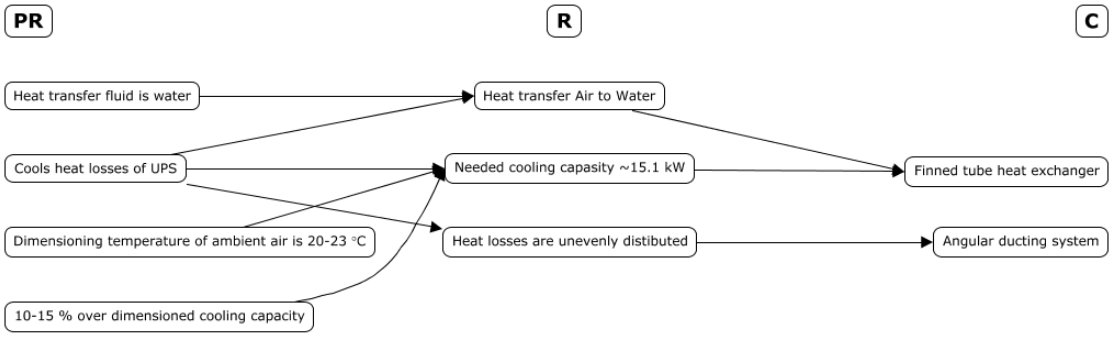

Figure 23. *First synthesis step of CPM/PDD method.*

At left-hand side of Figure 23 is few required properties *PR* taken from the required properties list, middle is the relations *R* and at the right-hand side is solution characteristic *C*. When all required properties, which have been taken into consideration, are fulfilled in ongoing synthesis step, process moves into analysis step. In analysis step, all properties of characteristics which have been determined so far are analysed individually. One analysis step is illustrated in Figure 24.

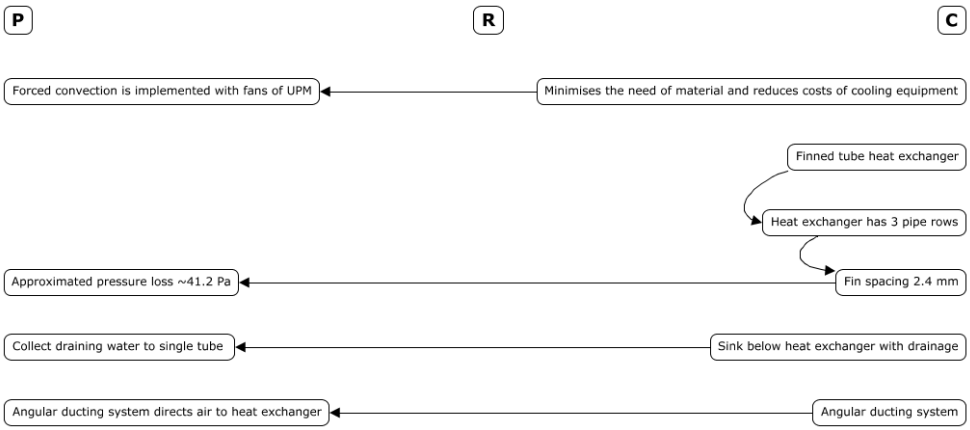

Figure 24. *Analysis step.*

At left-hand side of Figure 24 *P* is determined and predicted properties of characteristics. After the analysis step of CPM part of method is done, process moves back to PDD and its individual deviation step. In this step all properties determined in ongoing cycle were analysed from characteristics and compared to required properties and determine deviations between them. 1 individual step is illustrated in Figure 25.

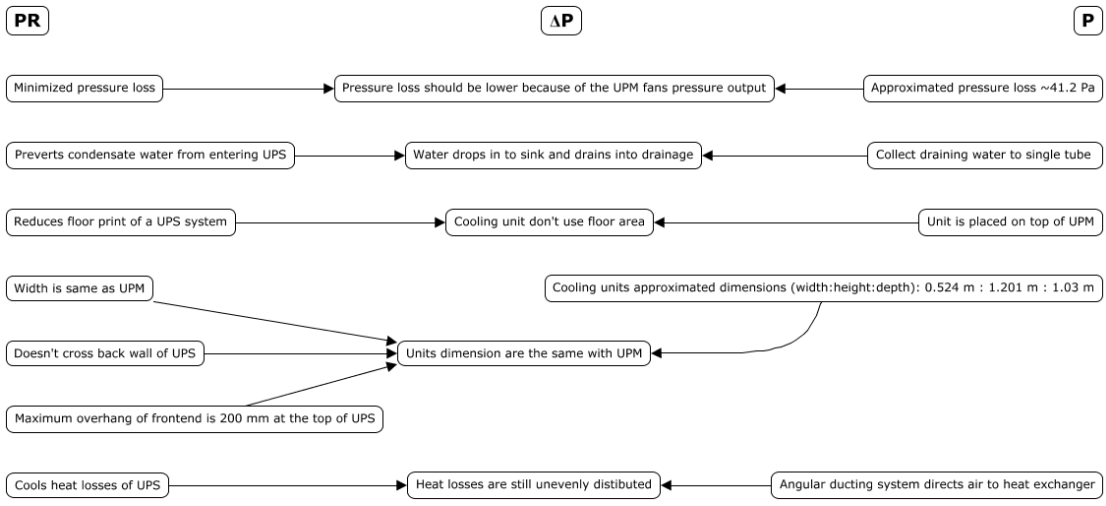

Figure 25. *Individual deviation step.*

In the middle of Figure 25 *ΔP* is deviation or non-deviation between properties of characteristics *P* and required properties *PR*. As seen in Figure 25, first and last individual deviation of required properties and properties have deviation between them, and they need more examination. Last step of PDD cycle is overall evaluation. It's almost the same as individual deviation step. In overall evaluation all determined properties were compared to all required properties, determine deviations between *P* and *PR* and examine wholly unheeded required properties. As told in subchapter 4.1, development process goes on until all required properties are fulfilled satisfactorily. This development project

doesn’t fulfil all required properties within the boundaries of thesis, because they were inconsistent with another required properties. In these situations, inconsistent properties were compared to each other and considered the importance of properties. More important properties in name of proofing a concept of heat exchanger unit were selected.

In this study, determining properties of characteristic were used approximate calculations with heat transfer and pressure loss, simulation of Computer-Aided Design (CAD) models with CFD, and prototype testing. Overall evaluations of properties and required properties were done with DRP method. Also, DRP were used to managed product knowledge and reasons behind the design solutions. Applying tools and methods to product development are opened in subchapters below.

5.2 Project planning and design reasoning with DRP

DRP method was used on research project planning and managing product knowledge and design reasons on product development. Objective to using DRP was to open projects outputs and intermediate steps when planning project and document product knowledge of designer to share and move forward. DRP models was made with Cmap Tools software which is developed to present concept maps (Fihmc, 2021).

5.2.1 Project planning

Project planning was started with deciding its objectives and objective relating topics. Project planning was done from end to start as reverse flow. To author, it’s easier to define an objective and move 1 step at time backwards examining what it needs to be done to get that particular output done and what are relations between different outputs. Off course, when doing thesis, the final objective is published thesis. Start point of project planning is presented from a part of entire project plan in Figure 26.

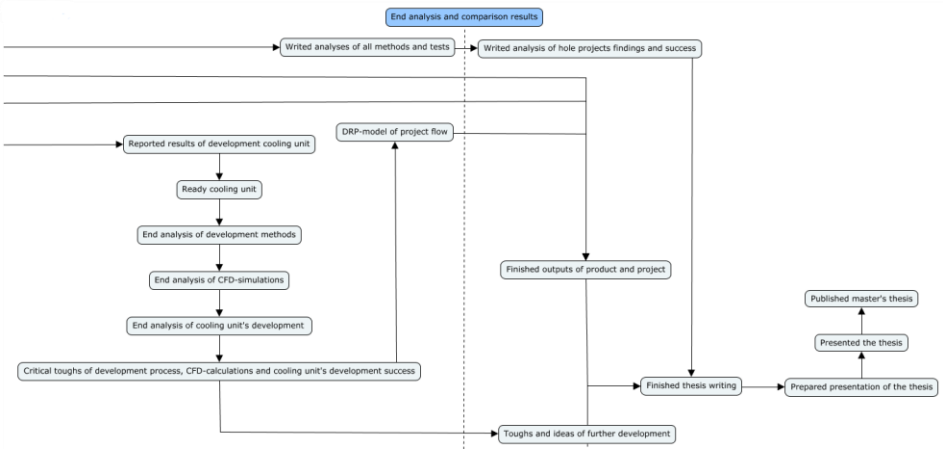

Figure 26. *Project’s final goal.*

As seen in Figure 26, DRP method used to illustrate the flow of project and rationalize what should be done and when. Project was also divided into intermediate steps to help seeing the big picture of project flow. Intermediate steps were implemented from thesis topics and outputs of these topics were placed inside them. Intermediate steps are illustrated with a light sky-blue boxes and dotted line in Figure 27.

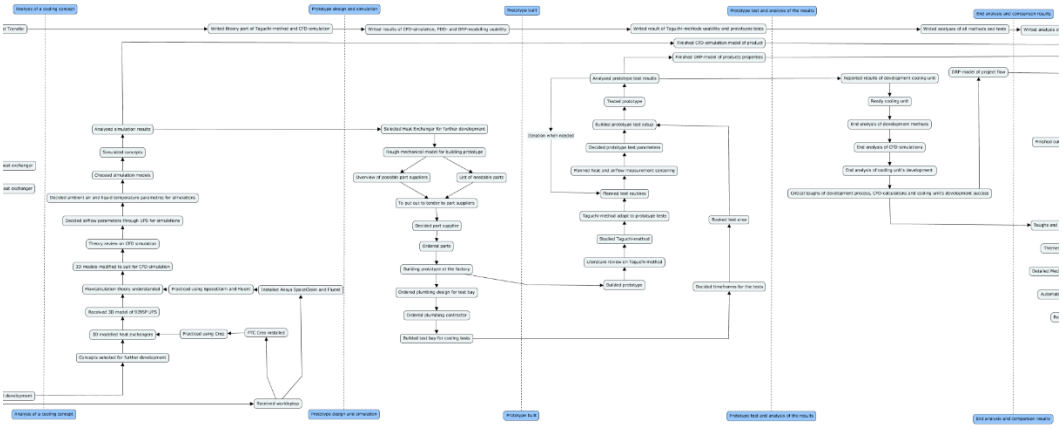

Figure 27. *Project's intermediate steps.*

5.2.2 Design reasoning

Design reasoning and product knowledge was modelled to illustrate the think flow of designer. DRP model was started on piling required properties of heat exchanger unit which were collected as a part of the CPM/PDD method. Start of DRP model from part of a ready DRP map is presented in Figure 28.

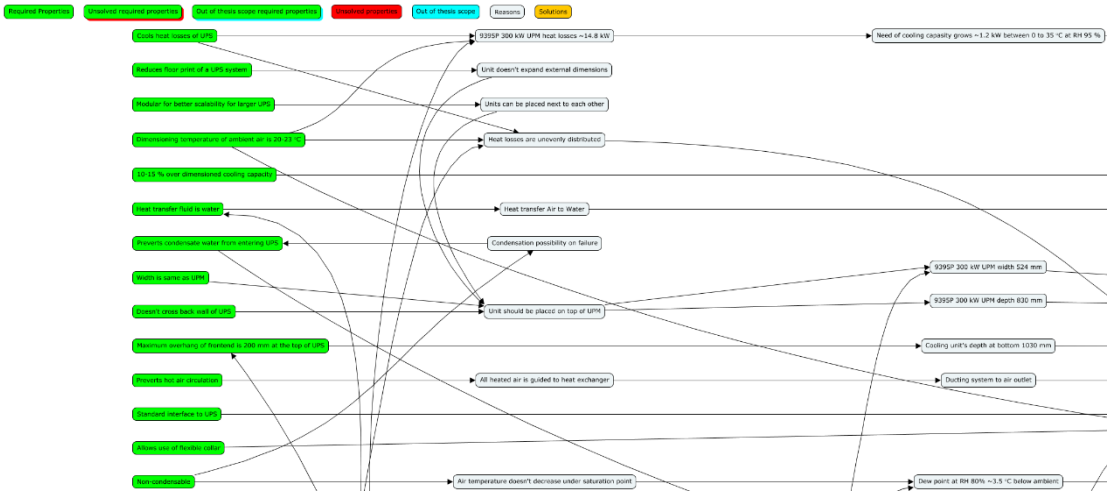

Figure 28. *Start of design reasoning.*

At left-hand side in Figure 28 the green boxes are required properties. At upper left corner are explanation of box colours. Colour lime is required properties, lime with red shadow is unsolved required properties, lime with cyan shadow is out of thesis scope

required properties, red is unsolved properties, cyan is out of thesis scope, alice blue is reason or initial information, and tangerine yellow is solution. To right from required properties are initial information behind design and design reasons. Flow map was done to answer few of the questions indicated in subchapter 4.2. Applied questions were:

- Where development process starts?
- How is design made?
- What kind of information or deliverables are required to decision?

Design reasoning map ended in the solutions after going through reasons and initial information. In Figure 29 is presented part of reasoning behind the solutions and solutions itself.

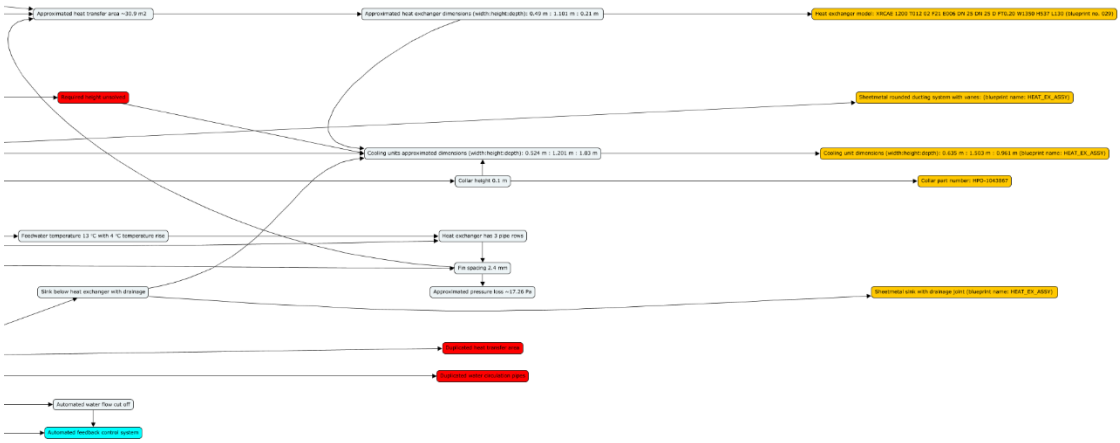

Figure 29. *Design solutions in DRP map.*

Lines between the boxes illustrate the dependencies and relations between different initial information and reasons. If some initial information could be solved with another solution or it depends on something, a line links them together. In DRP map, all boxes should have incoming and outgoing line, excluding required properties and solutions. Required properties could have only outgoing line and solutions could have only incoming line if another solution isn't depended on it. If box has no line at all, information inside the box is needless or something is missing from the design. With this kind of line rule, designer could be sure that all information has been considered (Adlin, 2022, p. 155).

5.3 Thermal and flow modelling

This subchapter more defines boundaries to modelling calculations than tells how equations are applied. Thermal and flow calculations were done because of 2 reasons. First, with calculations designer get approximate answers and initial scale of solution. Second,

with approximated calculations designer can get initial answers to characteristics of product and it's faster and cheaper than using CFD simulation or real prototype to iterative process. In this study, modelling calculations were made with Python programming language (Python Software Foundation, 2021) with using libraries such as CoolProp (Bell, et al., 2021) for fluid properties and Matplotlip (Hunter, 2021) for plotting.

Heat exchanger unit's characteristics dimensioning started with examining UPS heat losses and its operating boundary conditions. Standard (IEC, 2021) says that UPS shall perform as rated when operating in ambient temperature range of +15 °C to +30 °C and ambient humidity of 10 % to 75 % (non-condensing). Even though Eaton allows operating standard configuration of Power Xpert 9395P 300 kW UPS in ambient temperature range from 0 °C to +35 °C and relative humidity range from 5 % to 95 % (non-condensing) with minimum 1.0 °C difference to dry-bulb and wet-bulb temperatures (Eaton Corp., 2020, p. 1). This study uses ranges provided by Eaton in calculations.

UPS shall operate as rated in altitudes from sea-level and up to 1,000 m above without derating (IEC, 2021). Derating factors which standard gives to altitudes above 1,000 m from sea level are presented in Table 9 (IEC, 2021, p. 27)

Table 9. *Power derating factors (IEC, 2021, p. 27)*

Altitude	**Derating factor**	
m	Convention cooling	Forced air cooling
1,000	1.000	1.000
1,200	0.994	0.990
1,500	0.985	0.975
2,000	0.970	0.950
2,500	0.955	0.925
3,000	0.940	0.900
3,500	0.925	0.875
3,600	0.922	0.870
4,000	0.910	0.850
4,200	0.904	0.840
4,500	0.895	0.825
5,000	0.880	0.800

Eaton allows rated operating at maximum up to 1,000 m above sea level and up to 2,000 m above sea level with 1 % de-rating per 100 m above 1,000 m (Eaton Corp., 2020, p. 1). In calculations of this study maximum altitude 1,000 m above sea level is used.

Temperature and humidity ranges must be considered when dimensioning heat exchanger. Dry air itself doesn't affect a lot on cooling capacity, but relative humidity increases the need of cooling capacity. Like indicated in subchapter 4.3.1 increase of temperature and keeping the same relative humidity increases specific humidity of air. Increase of needed cooling capacity at relative humidity 95 % is presented in Figure 30.

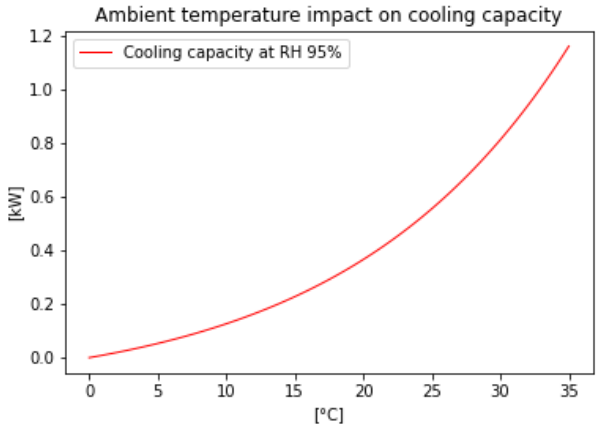

Figure 30. *Ambient temperature impact on cooling capacity.*

When using water as a heat transfer fluid, temperature range of usable water must be considered because water's specific heat is depending on temperature (Çengel & Boles, 2015, p. 175). So, feedwater's temperature has also effect on cooling capacity when dimensioning heat exchanger to be used in large temperature range. Impact of feedwater temperature at 10 °C temperature change in heat exchanger is presented in Figure 31.

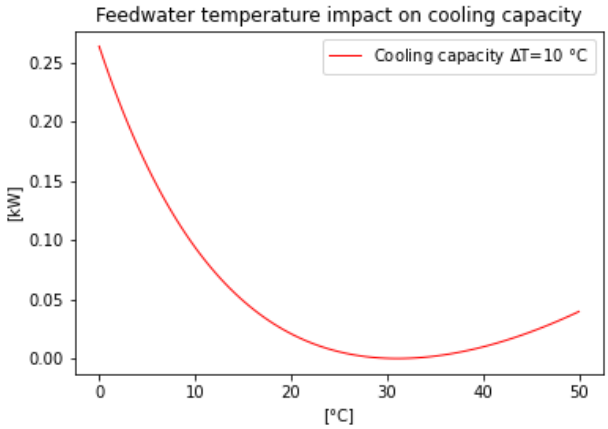

Figure 31. *Feedwater temperature impact on cooling capacity.*

UPS heat losses grows depending on the load. As indicated in first law of thermodynamics at subchapter 4.3, heat losses are always the same on specific power load. Electrical devices heat losses change some extent depending on environmental conditions. This study used in dimensioning only measured values from technical specifications. Heat loss on different loads is presented in Figure 32.

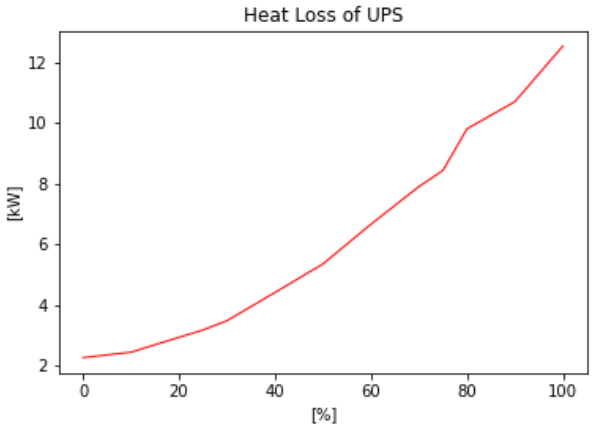

Figure 32. *Heat loss of 275 kW UPS in changing load.*

When considering condensation on cooling, level of relative humidity indicates the temperature where air meets its saturation point. Dewpoint of water vapor of saturated air is closer to the ambient temperature when relative humidity is high. In Figure 33 is presented water vapor dewpoints of saturated air from relative humidity 20 % to 95 %.

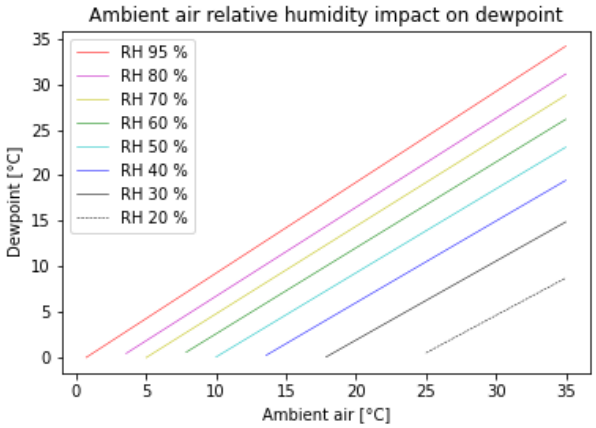

Figure 33. *Relative humidity impact on dewpoint.*

Heat load at the top of UPM is distributed. Heat exchanger's cooling capacity is almost the same through its whole area and air temperature decreases equal number of degrees everywhere if velocity is the same. Zeroth law of thermodynamics states, systems always strive to thermodynamic equilibrium. The outflow temperature equalizes over the time, but distributed temperature at outlet may cause higher temperature air recirculation and equal outflow temperature increases human comfort. Top view of air temperature distribution at the top of UPM is presented in Figure 34.

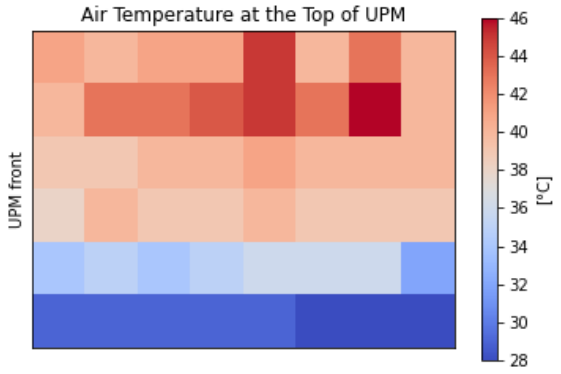

Figure 34. *Top view of air temperature distribution.*

Air velocity from the UPM is one of the main values when dimensioning heat exchanger. In free flow velocity defines how turbulent, or laminar, the flow is, and it affects the heat transfer area and usable correlations. Initial values for air velocity are presented in Figure 35.

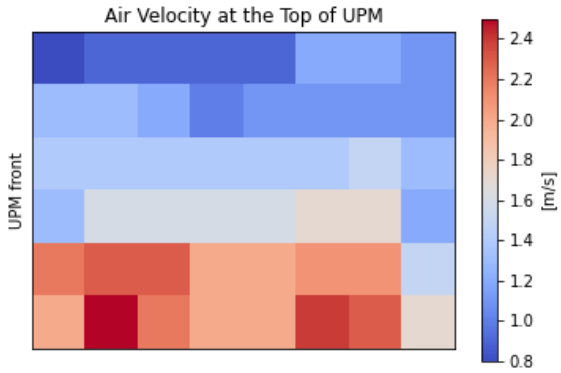

Figure 35. *Top view of air velocity from UPM.*

Air velocity and usable static pressure to cooling unit is done with fans. When more obstacles are inserted in the way of flow, pressure drop increases and volumetric airflow decreases as indicated in subchapter 4.3.3. UPM has its own fans inside to create forced convection to UPM cooling. The possibility is being examined, whether UPM own fans create enough pressure and airflow to UPM and heat exchanger unit, or should the number of fans be increased, or more powerful fans installed. At the start of project were decided 2 models of fans which can be used to this product development. In Figure 36 is presented fan manufacturer's provided operating curves.

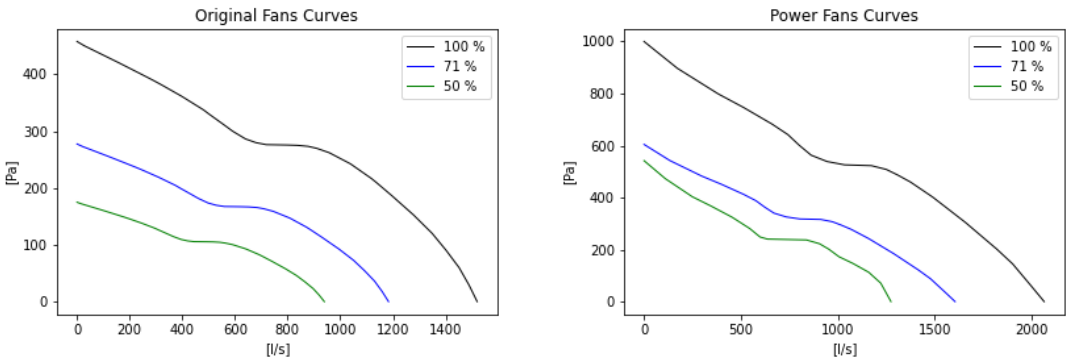

Figure 36. *Fans operating curves.*

5.4 CFD simulation

CFD simulation were used to certify properties of selected characteristics before building a prototype. Simulation models were done to the air flow in heat exchanger unit and heat exchanger's and UPM's pressure drop. All preparing for simulation of 3-dimensional CAD models were done with Ansys SpaceClaim which is simplified CAD software compared to traditional CAD systems (Ansys Inc., 2021). Meshing, fluid simulation and post-processing were done with CFD analysis software Ansys Fluent (Ansys Inc., 2021). This subchapter determines used CAD models, fluid simulation calculation methods, and boundary conditions to simulation models.

Model preparing included designing a suitable simulation model and simplification of detailed CAD models. The simplification of CAD models is one of the time-consuming tasks of CFD simulation. Too detailed model increases dramatically number of CVs in mesh. The greater number of CVs, the greater the need of computational power and calculation time. There is a general rule of thumb that simulation machine needs 2 to 2.5 GigaBytes (GB) of Random Access Memory (RAM) for 1,000,000 CVs to successfully solve the simulation (Autodesk Inc., 2014). CAD models for simulation were downsized, walls levelled, and small objectives deleted or merged to make the mesh size suitable for the computer to be used. After processing solid geometry that thought to be suitable for use, the geometry was turned into fluid domain before moving into meshing.

First model was heat exchanger which geometry was too large to simulate entirely. Because wanted simulation result was only airside pressure drop, sufficient geometry was only a small piece of the heat exchanger. Geometry which was simulated is presented in Figure 37.

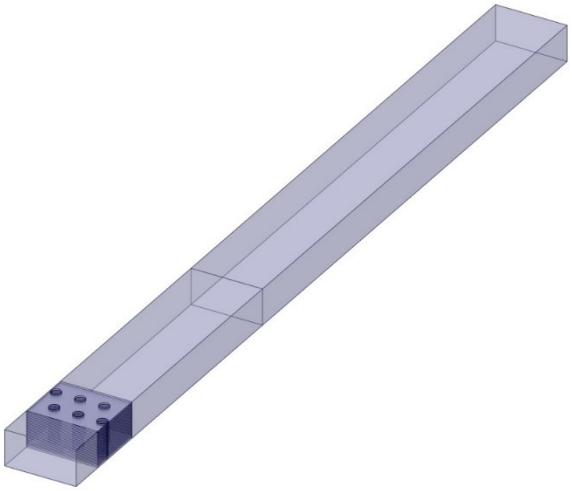

Figure 37. *Heat exchanger's pressure drop geometry.*

Next models were ducting system or a frame for heat exchanger unit. Results wanted of ducting system simulation were to examine temperature distribution on outlet and flow direction at the inside of duct. 3 different shapes were investigated which were angular, rounded and rounded with vanes. At Figure 38 is presented left to right simulation geometries of angular, rounded, and rounded with vanes ducting systems.

Figure 38. *Ducting systems geometries.*

The most time-consuming simulation model were the single UPM model. Results wanted from simulating UPM were system curve for volume flowrate and pressure coupling. Original CAD model of UPM contained around 1,500 detailed parts. After a heavy simplification of geometry, number of parts were around 20. In Figure 39 is presented UPM geometry for simulation.

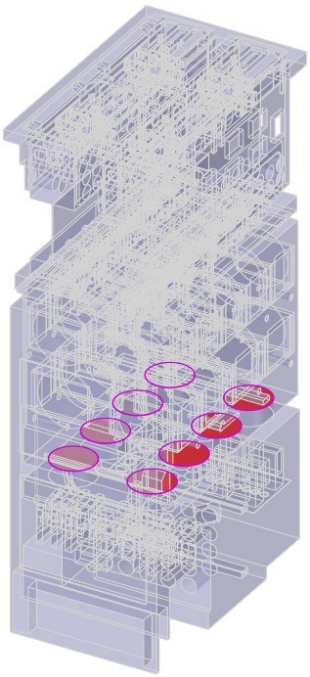

Figure 39. *UPM simulation geometry.*

After preparation of CAD models next task was mesh generation. The quality of mesh was targeted to orthogonal quality minimum ≥0.1. Mesh independent study was done to heat exchanger pressure model to obtain approximate level for mesh quality which can be used for other models. Yet, for more accurate solutions mesh independent study should be done to all geometries. Meshes were generated with Fluent's automated meshing tool. Models mesh type, size and quality are presented in Table 10.

Table 10. *Mesh types, sizes, and quality*

Model name	Mesh type	Mesh size (CVs)	Orthogonal quality
Heat Exchanger PD 1	poly-hexcore	1,984,994	0.142338
Heat Exchanger PD 2	poly-hexcore	4,327,998	0.102547
Heat Exchanger PD 3	polyhedra	3,854,234	0.127976
Angular Duct	poly-hexcore	1,511,440	0.100026
Rounded Duct	poly-hexcore	1,505,920	0.100011
Rounded Duct with Vanes	poly-hexcore	2,317,284	0.100136
UPM Flow	poly-hexcore	11,312,512	0.129091

Last task, before CFD simulation can be started, is defining boundary conditions and calculation methods. Velocities and temperatures were indicated in subchapter 5.3, ambient pressure was 101,325 Pa, and rest of defined boundary conditions are presented in Table 11.

Table 11. *Boundary conditions.*

Model name	Inlet	Interior	Wall	Outlet	Other
Heat exchanger PD 1/2/3	velocity-inlet	interior fluid (air ρ_{air} = 1.163 kg/m^3)	wall (aluminium, roughness 0.5)	pressure-outlet	inlet & outlet duct: symmetry wall
Angular Duct	velocity-inlet	interior fluid (air ρ_{air} = 1.225 kg/m^3)	wall (aluminium, roughness 0.5)	pressure-outlet	-
Rounded Duct	velocity-inlet	interior fluid (air ρ_{air} = 1.225 kg/m^3)	wall (aluminium, roughness 0.5)	pressure-outlet	-
Rounded Duct with Vanes	velocity-inlet	interior fluid (air ρ_{air} = 1.225 kg/m^3)	wall (aluminium, roughness 0.5)	pressure-outlet	-
UPM Flow	pressure-inlet	interior fluid (air ρ_{air} = 1.225 kg/m^3)	wall (aluminium, roughness 0.5)	pressure-outlet	fans: constant pressure (p_1=50, 200, 500 Pa)

All simulations were done steady-state calculation with a RANS based turbulence models and discretisation methods were chosen depending on the grid size in order to save time via faster calculation time. Calculation methods for all domains are presented in Table 12.

Table 12. *Calculation methods.*

Model name	Calculation models	Pressure-velocity coupling	Discretization
Heat exchanger PD 1/2/3	k-ω SST, Low-Re corrections	coupled	pressure: second order and rest: second order upwind
Angular Duct	k-ω SST, Low-Re corrections + energy	coupled	pressure: second order and rest: second order upwind
Rounded Duct	k-ω SST, Low-Re corrections + energy	coupled	pressure: second order and rest: second order upwind
Rounded Duct with Vanes	k-ω SST, Low-Re corrections + energy	coupled	pressure: second order and rest: second order upwind
UPM Flow	k-ω SST	coupled	pressure: second order, momentum: second order upwind and rest: first order upwind

5.5 Prototype tests with Taguchi method

Prototype tests with Taguchi method could save time and costs of testing, because of the decreased test runs. While theory of Taguchi method is indicated in subchapter 4.5, this subchapter opens the test factors, their levels and presents the testing table. In this

study, prototype tests were used for verification of calculation and properties of characteristics, simulation results and to proof concept's functionality.

Prototype tests were planned mainly with ranges indicated in subchapter 5.3. Tests could have been made with few or more heat exchangers, but Eaton PQ do not manufacture them. The heat exchanger has to be ordered from subcontractor and possibilities on influencing on product were limited. So, for economic reasons and lack of product variation the tests were decided to do with 1 pre-designed heat exchanger. Testing was planned to do with the 2 levels of each factor. Factors and levels of them are presented in Table 13.

Table 13. *Factors and levels of prototype test.*

Factor (number)	Level Low (1)	Level High (2)
UPS Power Load (1)	50 %	100 %
Fans (2)	Original fans	Power fans
Ambient Air Temperature (3)	20 °C	35 °C
Ambient Relative Humidity (4)	20 %	95 %
Water Temperature Change (5)	4 °C	10 °C

There are 5 factors with 2 levels (2^5). When calculating with equation (80) full tests needs 32 test runs. Full test structure is presented in Table 14.

Table 14. *Prototype test structure.*

Factor/Level			1/1		1/2	
			2/1	2/2	2/1	2/2
3/1	4/1	5/1				
		5/2				
	4/2	5/1				
		5/2				
3/2	4/1	5/1				
		5/2				
	4/2	5/1				
		5/2				

Nearest Taguchi OA for test with 5 factors and 2 levels is L_8. OA reduces the number of tests from 32 to 8. OA L_8 is designed to tests with 7 factors and 2 levels, but with a little modification on its table it's suitable for these tests. Modified L_8 table for these tests is presented in Table 15.

Table 15. *Orthogonal array L_8 of prototype tests.*

Factor / Test	1	2	3	4	5
1	1	1	1	1	1
2	1	1	1	2	2
3	1	2	2	1	1
4	1	2	2	2	2
5	2	1	2	1	2
6	2	1	2	2	1
7	2	2	1	1	2
8	2	2	1	2	1

6. RESULTS

In this chapter is presented results of product development and the product itself. Chapter is divided to development methods, thermal and flow, product design and prototype tests results. Also, leaning on the results is discussed what didn't go as planned and what could have been done better.

6.1 Product development methods

CPM/PDD product development method, as indicated in earlier chapters, was used to manage the development work. DRP method was used to model the project flow and think flow behind the designer decisions. Both of methods nature is a kind of same when illustrating development as seen in subchapter 5.1 and 5.2.

First, research project started with planning project steps. Project planning was made applying DRP method to model project flow. As indicated in subchapter 5.2.1 planning progressed from end to start. DRP method helped to plan project passage and find out what tasks could be done at same time, and which task needs a certain output from preceding task. With DRP modelled project's tasks could be done more efficiently and there was no need to jump back and forward. Whole research project plan map is presented in appendix B. In map, box colour alice blue is task and light sky blue is the name of intermediate step. Off course, project planning always could go deeper and done more detailed, but accuracy of this level found suitable for this project.

Main presentable result from CPM/PDD method was required properties list while development work and knowledge are presented in way of DRP model. CPM/PDD method's guidance to take different perspectives account when collecting required properties helped finding all related properties and punch of more that weren't in a scope of this thesis. List of perspectives (headings) and found required properties is in appendix A. CPM/PDD method seemed to suit for technical product's development project well. It guided to take account all relations between different characteristics and between properties and characteristics step by step. The whole process driver, overall evaluations, helped to keep in mind what are the main parameters and requirements of the product to be developed.

CPM/PDD method also aims to collect product knowledge with characteristics and properties relations. In this study, DRP method was integrated to CPM/PDD method to collect and present product knowledge. Integrating DRP to CPM/PDD helped to find relations

between the required properties and between the different characteristics. Using DRP modelling, with a line rule indicated in subchapter 5.2.2, as an overall evaluation step for CPM/PDD project collected the designer think flow and design knowledge to an easily readable format. DRP map of product development is in appendix C, where box colour lime is required properties, lime with red shadow is unsolved required properties, lime with cyan shadow is out of thesis scope required properties, red is unsolved properties, cyan is out of thesis scope, alice blue is reason or initial information, and tangerine yellow is solution. Map could be always more detailed or accurate but balancing between too simplified and precise information brought author to such a result.

From the required properties list, the height of heat exchanger unit and duplicated cooling weren't solved. Also, there were bunch of required properties which doesn't fit in for this thesis scope. Unsolved required properties may could be solved with heat exchanger with more pipe rows and with more powerful fans or additional fans, but these solutions affect the UPS electrical efficiency. Lower UPS efficiency is undesirable, and these solutions will need more examination if these required properties turn into a problem. Unsolved and out of thesis scope required properties from the last overall evaluation are presented in Appendix C where box colour lime with red shadow is unsolved required properties, lime with cyan shadow is out of thesis scope required properties, red is unsolved properties, cyan is out of thesis scope.

6.2 Thermal and flow results

Designing a heat exchanger to UPS there were a lot of things to consider. Heat load and allowable operating ranges of environmental conditions indicated in subchapter 5.3 were the primary parameters to consider in dimensioning. Heat exchanger should have enough cooling capacity at the end of environmental operating range. At the same time, it shouldn't increase back pressure of fans too much and increase the UPS inner temperatures. Usable pressure change was the most problematic value because minimizing pressure drop of heat exchanger increases the height and width of it. The required properties of size of a heat exchanger didn't solve mainly due to usable pressure change.

Heat exchanger's approximate dimensions and operational values was calculated with equations presented in subchapter 4.3. Heat exchanger's heat transfer area with 10 °C feedwater and ambient air difference, 4 °C water temperature change and 2.4 mm fin spacing was approximately 30.9 m^2. This area fills the needed cooling capacity of ~17.6 kW. Needed cooling capacity comes from UPS heat losses, allowable temperature, and relative humidity ranges (0 °C to 35 °C and 5 % to 95 %) and 10 % percent over dimensioning. Heat exchanger's approximate dimension are width 490 mm, height 1,101 mm

and depth 210 mm. Calculated pressure drop for this heat exchanger is approximately 24.7 Pa

Calculated minimum surface temperature on heat exchanger's pipe surface is ~13.2 °C and with a 23 °C and RH 95 % ambient air's saturation point is 22.22 °C. Pipe surface temperature is way below the saturation point, so at least film-like condensation can be expected. However, cooling is not dimensioned to cool down air below its saturation point. When estimating condensation flow with equation (22) there shouldn't be any condensation flow to drainage.

Ordering the heat exchanger was one of the first tasks after approximate calculations were ready. At that time, worldwide shortage of raw materials and Covid-19 pandemic (Consultancy.eu, 2021) made it difficult to get a heat exchanger in a reasonable time. Personalized design heat exchanger's delivery time could have been 6 to 12 months and because of that it was decided to order a standard size heat exchanger. Heat exchanger was selected with a manufactures dimensioning software and selected heat exchanger's heat transfer area was 31.1 m^2. Its fin spacing was 2.1 mm, pipe diameter 13.35 mm and it has 12 pipe columns in 2 rows. Pressure drop was also calculated with manufacturer's provided values to examine the accuracy of used equations. Manufacturer promised 19 Pa pressure drop to heat exchanger and with equations presented in subchapter 4.3.2 calculated pressure drop was ~17.3 Pa. Equations used for calculations are approximate, but in this case, they provided a good result.

CFD simulation to heat exchanger was decided to do with a manufacturer's values. With simulation setup presented in subchapter 5.4 pressure drop of heat exchanger was ~16.9 Pa. Pressure field of heat exchanger is illustrated in Figure 40.

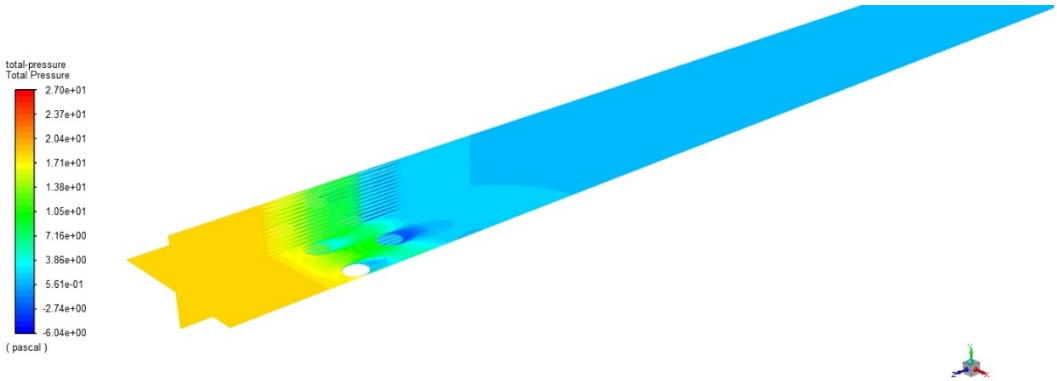

Figure 40. *Heat exchanger's pressure drop.*

The mesh independent study's results of a heat exchanger simulation were that pressure drop differed between 3 models ~0.11 Pa at maximum. Largest difference was between

the poly-hexcore and polyhedral meshes. Between 2 poly-hexcore meshes difference were ~0.007 Pa even though bigger mesh has 2 times more CVs. Mesh independent results are illustrated in Figure 41. With these results orthogonal quality 0.1 and poly-hexcore mesh was chosen to use in other simulations.

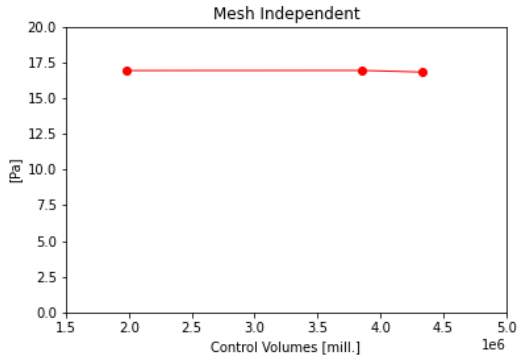

Figure 41. *Mesh independent study results.*

Ducting systems were designed to tackle the heat distribution and mix uneven temperatures before heat exchanger. Simulation results provided that round ducting system equalises temperatures most. It mixes distributed air and smoother the temperature field in outlet. Temperature results in outlet of ducting systems is presented in Figure 42. Ducting systems are presented from left to right in order of angular duct, rounded duct, and rounded duct with vanes.

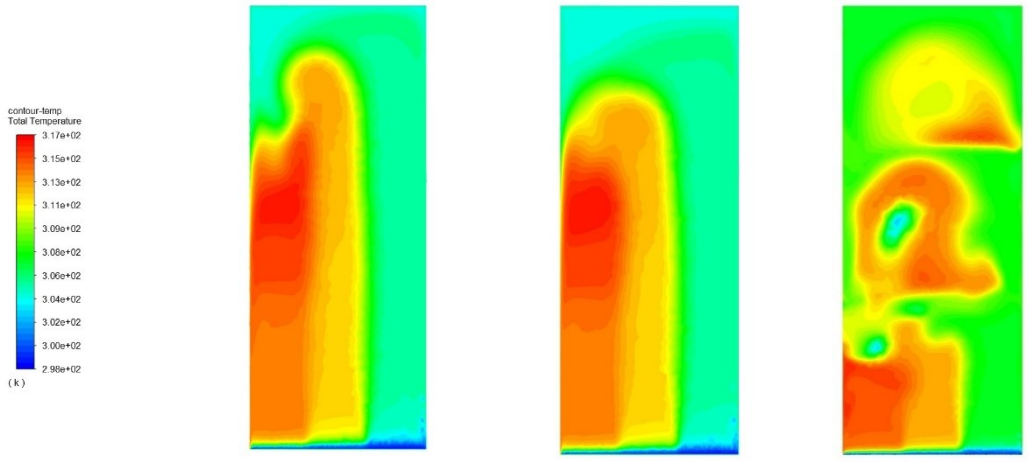

Figure 42. *Ducting systems temperature distribution.*

UPM system curve was formed with CFD simulation. Unluckily simplification was too heavy for the UPM, and simulation wasn't successful. Simulation results gave too much

pressure drop with certain volume flowrate when compared to initial information. Heaviest simplification was done to heatsinks which decreased CVs number more than 6,000,000. Including heatsinks geometry to simulation would have added the total number of CVs near 20,000,000. UPM model's refinement could not be done because simulation machine's computational power came against and starting a simulation crashed to memory deficiency. Unsuccessfully simulated system curve for UPM with power fans and original fans is presented in Figure 43.

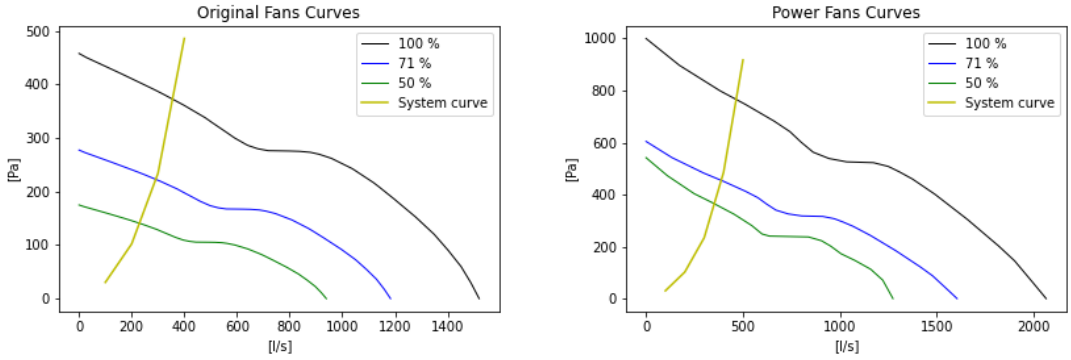

Figure 43. *Simulated system curve.*

6.3 Developed product

Prototype were built based on the results of thermal and flow calculations and CFD simulation. The most suitable solutions for standard configuration of UPM were pre-designed collar to UPM-Heat exchanger unit interface, rounded ducting system with vanes, condensation sink below heat exchanger, and standard size heat exchanger with 31.1 m^2 heat transfer area. Pressure drop for this heat exchanger is 19 Pa that manufacturer provides. Detailed part information is presented in DRP map at appendix C. The product's CAD model and prototype is presented in Figure 44.

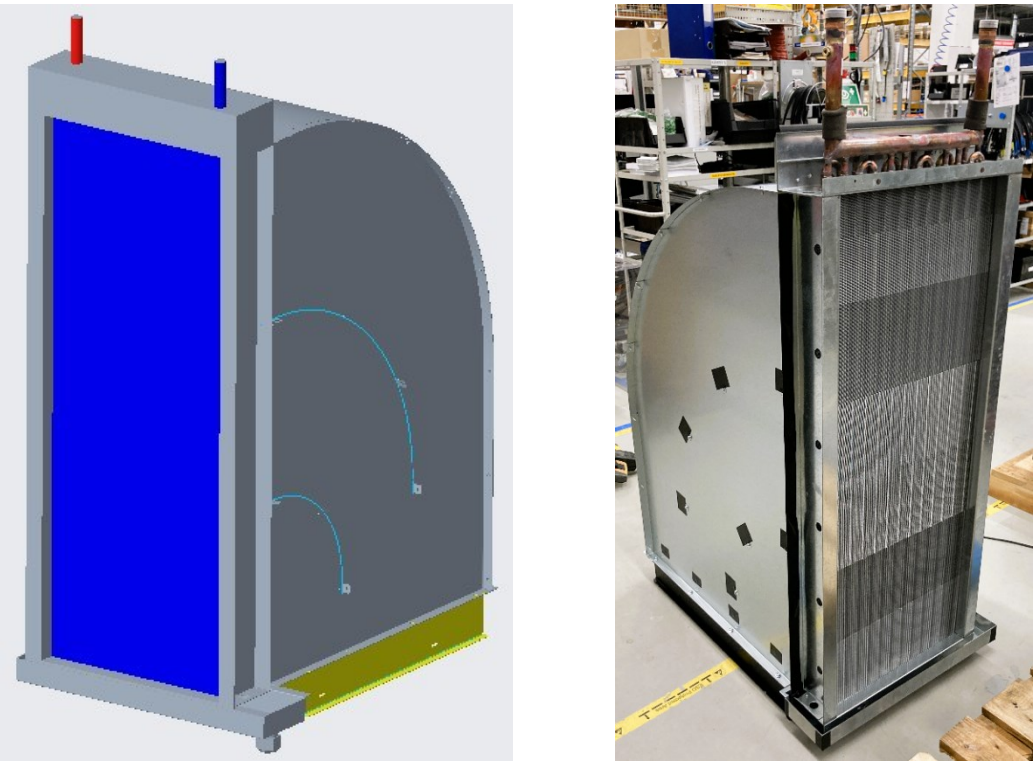

Figure 44. *Designed prototype.*

There was a consideration of a heat exchanger which leans in straight in front UPM's air outlet. Such a solution of heat exchanger was abandoned because there is a chance that condensation water forms and drops into inside UPM. This condensation problem is solvable by a droplet separator, but it increases pressure drop too much for original fans.

6.4 Prototype tests

Prototype tests were primarily planned to do with the Taguchi method. Unluckily Eaton's testing laboratory is built to electrical device tests because Eaton PQ manufactures electrical devices, and not heat transfer devices, there were not able to do planned changes in ambient conditions. For these reasons and reasons indicated in subchapter 5.5 Taguchi method couldn't be tested in real environment. At the paper the method seemed integrable to CPM/PDD method to defining properties and characteristics and properties relations of the product.

For these heat exchanger unit tests, whole testing process and equipment had to be designed from a scratch. Because designing a test bay is out of scope of this thesis, plans and detailed information of a test bay is left out.

Related to lack of test conditions for planned heat transfer tests, prototype was only tested in almost constant ambient temperature and relative humidity. So, factors of tests

decreased to 1 with 3 levels and 1 with 2 levels. Tests was done with UPS power load 50 %, 75 %, and 100 % and with original and power fans. Nearest Taguchi's OA for test number of 3^1x2^1 is L_8. With Taguchi method number of test do not really decrease on this level, so ANOVA analysis is unnecessary because analysis can be done more straightforward without it.

Test results were collected with measuring ambient air temperature at UPM inlet, temperature, and velocity at the UPM's outlet, and at heat exchanger unit's outlet. Illustration of measuring points at top of UPM and at front of heat exchanger unit is presented in Figure 45.

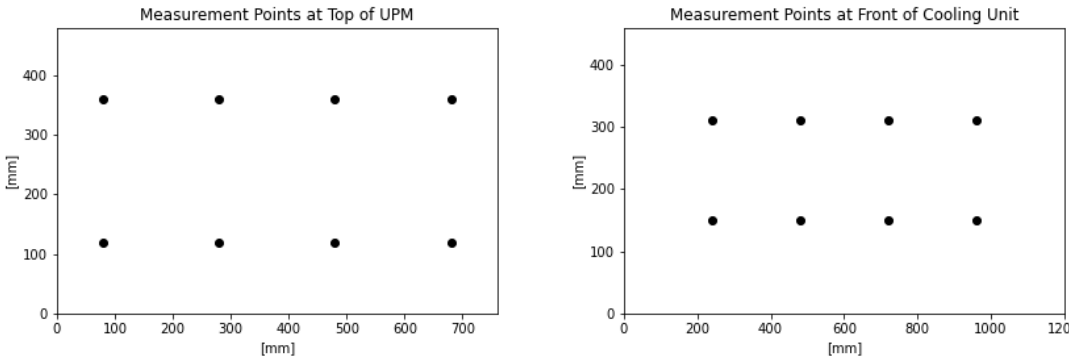

Figure 45. *Measurement points.*

Each test run was run until temperatures had levelled. Temperatures specified in preceding paragraph and inside the UPM were monitored to verify whole system is in steady state. One of the test runs monitored temperatures are presented in Figure 46, where different lines represent different measuring channels.

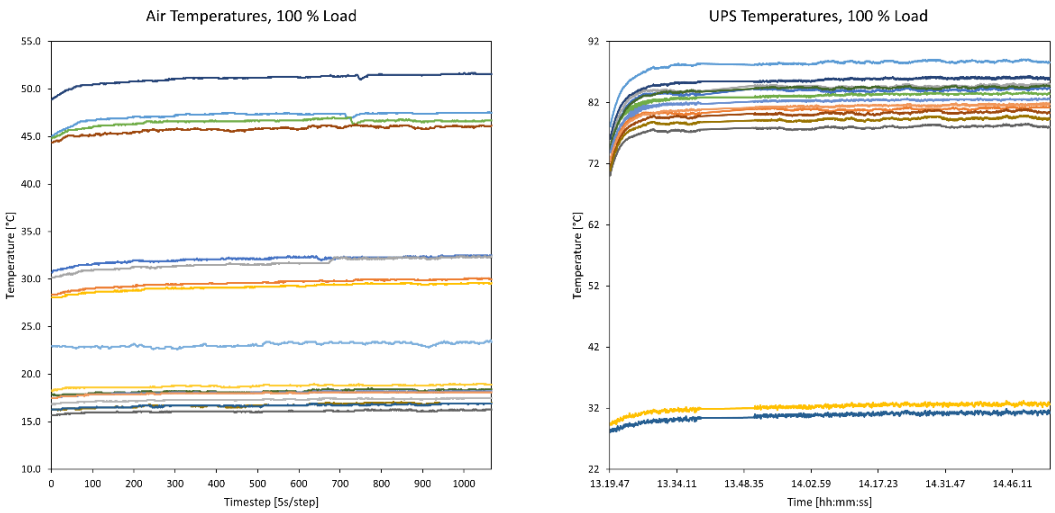

Figure 46. *Levelled temperatures.*

In measurements is also seen distribution of outflow temperature. As seen in left-hand side of Figure 46, temperatures differ from under 30 °C to just above 50 °C. Left-hand figure's lowest air temperatures are ambient air temperature at UPM's inlet and air temperatures after heat exchanger. Calculated results of prototype tests are averages of levelled measurements where temperature rise is omitted. Average of measured outflow temperatures and air velocities at 100 % UPS power load are presented in Figure 47. At top is measurements with original fans and under is with power fans.

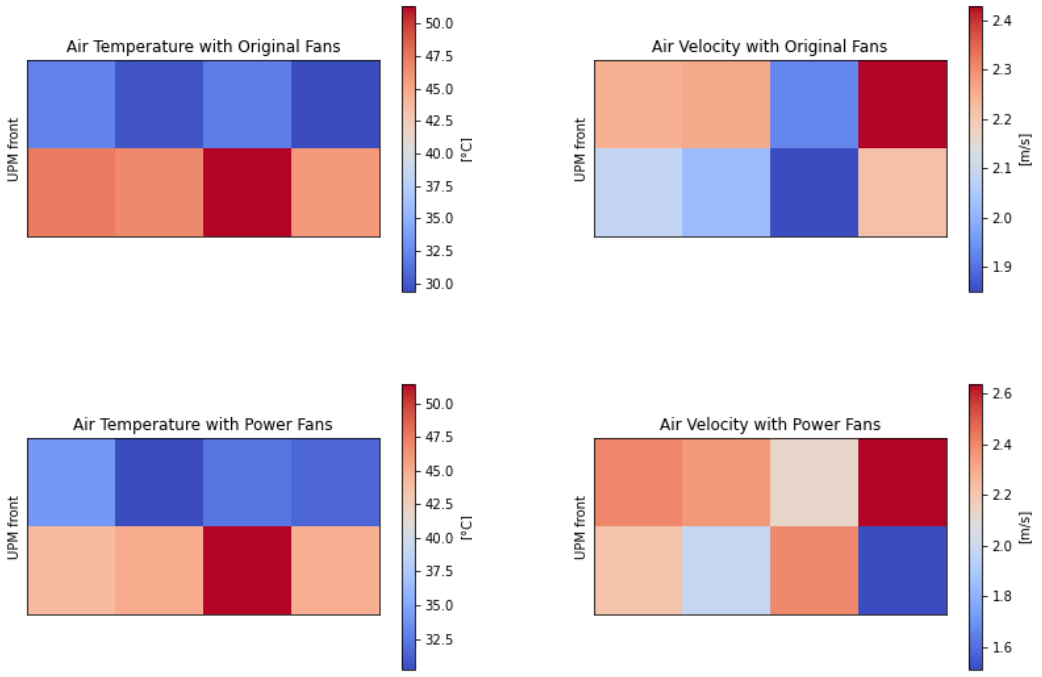

Figure 47. *Air temperatures and velocities measured in prototype tests.*

During the tests ambient air temperature was ~23 °C and relative humidity range was from 35 % to 40 %. Heat exchanger unit's outflow temperatures at 100 % UPS power load are presented in Figure 48. At the left-hand side is temperatures with original fans and at the right-hand side is with power fans.

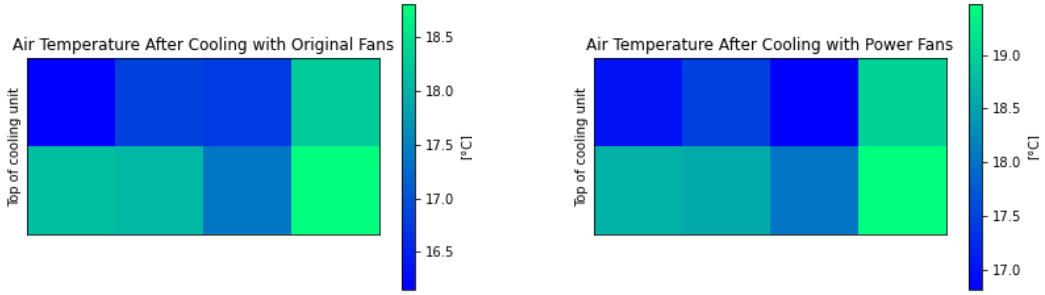

Figure 48. *Measured air temperatures after cooling unit.*

With test results, which some are presented above, heat exchanger unit's functionality can be calculated and analysed. Calculated cooling capacity of heat exchanger unit and thermal power of UPM with 2 different fans is presented in Figure 49.

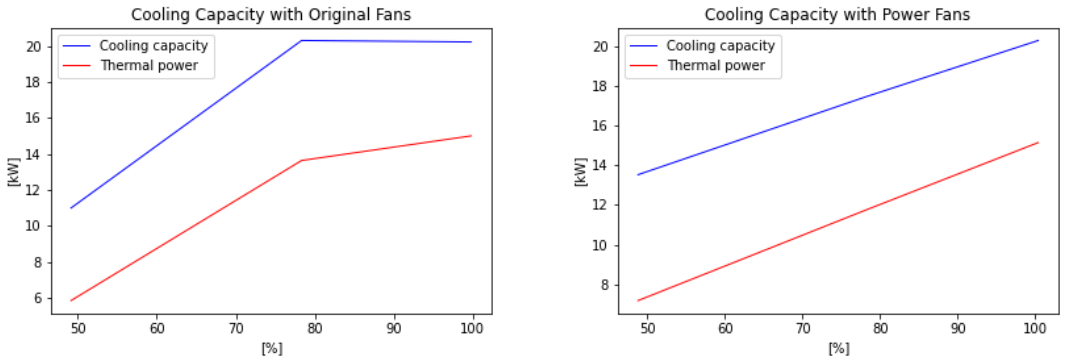

Figure 49. *Cooling capacity and thermal power.*

As seen in Figure 49, the cooling capacity of heat exchanger unit is very adequate when comparing it to thermal power of UPM. Cooling capacity jump with the original fans at ~75 % load is due to fans speed rose from low to medium. Similar jump isn't perceptible with the power fans because their speed stayed at the low level through the tests. Even though heat exchanger is dimensioned to UPS heat losses, it wasn't dimensioned to this large temperature difference of heated air and cooling water. Another point to this too large heat transfer surface is that heat exchanger was ordered as a standard size product. Standard size heat exchangers are always dimensioned to wide scale of conditions and thermal or cooling capacity is normally controlled with automated air or water flow regulation.

During the test, cooling water temperature was 7 to 8 °C and average air temperature from UPM at 100 % load was 36.8 °C. Water flow to different heat loads was calculated beforehand with dimensioned temperature change 4 °C in heat exchanger and flow was

adjusted by balancing valve. With this temperature difference suitable calculated heat transfer area to heat load is approximately 19.45 m^2. Prototype's heat exchanger at 100 % UPS power load with original fans the heat transfer area was ~60 % too large and its cooling capacity was ~35 % over dimensioned. Comparing to same load and power fans, heat exchanger's heat transfer area was ~70 % and cooling capacity was ~34 % over dimensioned.

Heat exchanger didn't produce droplet condensation during the tests, even though feed-water temperature was low. There were perceive some filmwise condensation on heat exchanger's surface, but because cool air temperature after heat exchanger unit wasn't under its saturation point droplets didn't form.

Heat exchanger unit's pressure drop was smaller than calculated with initial values. Maximum total pressure difference measured between the UPM outlet and heat exchanger unit outlet with original fans was ~14 Pa and with power fans ~24 Pa. Original UPM fans could manage this pressure drop, but it's almost in fan's stall region in 50 % and 100 % UPS's power load, which is undesirable. When system curve and fans operational curve intersect each other in stall region, it can cause pressure and volumetric flowrate fluctuations in fans (Seppänen, 1996, p. 134). Operating points, blue, magenta, and red dots, in different UPS loads are presented in Figure 50.

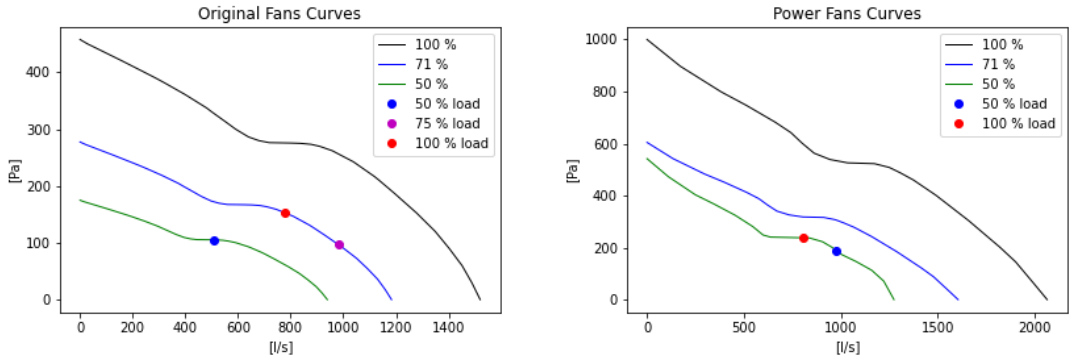

Figure 50. *Operating points with different UPS's power loads.*

Increasing the UPS's power load also increases temperature inside the UPM because of the higher thermal power of heat losses. Increase in outflow temperature causes increase of pressure drop, as seen in Figure 50 and indicated at subchapter 4.3.2.

6.5 Patent review

Reliable patent review search definitions and selection protocol is opened in subchapter 2.5. There were 644 patents found from database Espacenet with used keywords. 69 of them was related to UPS cooling and was selected to further examination.

Patents selected from patent review for further examination included UPS frame cooling (Liu, 2019) (Fan, 2021), whole UPS cooling systems (Huntgeburth, et al., 2019) (Darrelmann, et al., 2002), cooling device placements in UPS (Wang, et al., 2021) (Qin & Bao, 2020), UPS cooling with fans (Chen, et al., 2018), UPS container cooling (Lin, 2015) (Huang & Gao, 2018), and different types of cooling devices which are dimensioned to UPS (Hwan, 2021) (Xiangyang & Huili, 2021) (Ren, et al., 2020). More patents than cited were examined, but the amount of them where too large to cite all of them. None of the patents were directly related to this research's heat exchanger to be developed, but patent review gave good ideas how UPS device cooling could be made and what kind of solutions have been developed.

7. DISCUSSION AND CONCLUSIONS

The objective of research was to study how product development methods suits and integrate to each other in this kind of case study, but also develop a product for proof of concept. It can be said that this study has 2 partitions. One was to do research how to use development methods and study their propriety for a case study and another was to design a functioning heat exchanger unit. Author of thesis was responsible both of them and changing perspective between researcher, project manager, designer and a specialist in the subject's area was at times very challenging, but eye-opening.

7.1 Discussion

Research strategy was to do research on a case study. Case study is focuses just on 1 case and results of this research aren't necessarily expandable to all cases. Also, 1 person's findings may be limited and researcher's participation on development work may affect the results. If research is reproduced to a team, findings and results could be different or if researcher doesn't participate on development and development is done in multiple participants team. Also, there could be more suitable sources for this study which was not found because of the used keywords and databases or weren't noticed during the literature review.

At author's point of view research objectives were mainly achieved. First objective, integrating development methods to together wasn't successful for the part of Taguchi method at empirical part of study. However, in theoretical part of study integrating methods seemed promising and with different testing facilities, the methods could work together. Second objective, designing a functioning UPS integrated heat exchanger was successful in this extend. However, the technical objective of fulfilling all required properties weren't quite successful. Couple of required properties found during the product development process weren't achieved and bunch of required properties couldn't fit in the scope of thesis. Reasons and results behind unachieved objectives and required properties are opened in subchapters 6.1, 6.2, and 6.4.

Continuation of the UPS integrated heat exchanger development should focus findings of this thesis. Next step of development could take direction to developing a more compact heat exchanger to UPS, examine if condensation can be managed with a droplet separator and placing heat exchanger component directly at roof of UPS, and if installation of powerful fans is acceptable. Also, the heat exchanger unit need an automated

control which manages water flow on different heat loads if the unit's development is continued. When developing an automation control to the unit, there should be examined if UPS fan control and water circulation control could be synced together.

Continuation of the research should study if these methods are integrable at each other on different product development projects and more complex products. This thesis heat exchanger unit is at last quite simple product. Also, if study is reproduced, there could be examined possibility to do it to development teams with multiple participants. In the larger and complex projects, the CPM/PDD method could include some method to manage data of relations between characteristics and properties and dependencies between different characteristics. The presentation form of DRP method's is now mainly up to be decided by project organizations and designers. The DRP method's implementation could be helped, if it had a more standardized presentation habit.

7.2 Conclusions

Product development method CPM/PDD described the framework to development project, as Weber (2014, p. 329) is presented. For this kind of case study, the method suited well. It keeps the focus on the required properties during the development with its overall evaluations step and guides designer to stay on the path where the product meets its market desired properties. However, managing large number of required properties could produce difficulties to designer team of one. It might be advisable that product manager or such keeps fulfilled required properties on count and divides the task to designers or teams. Within this case of study, the number of characteristics and properties didn't grow large, and the amount were relatively small, so they were manageable to one designer. Investigating and managing all required properties helped to see the big picture of project. Author thinks that all designers should see the whole list of required properties before starting a development project and fulfilled required properties during the project to sufficient and efficient product development. Weber (2014, p. 329) has also proposed that CPM/PDD method is suitable for integrating any other product development methods and tools to methods process. Within this research to CPM/PDD process was integrated DRP method, approximative calculations and CFD simulation. Unluckily Taguchi method hasn't been able to integrate to CPM/PDD method during the development because of the reasons indicated in subchapter 6.4. However, it seemed integrable to CPM/PDD method in the same way as approximate calculations and CFD simulation because the method defines properties of characteristics of the product.

Nature of CPM/PDD and DRP is kind a same when presenting process flow and results. They both follow the box and arrow representation, but the difference between them that

CPM/PDD is more back and forward iterative presentation when DRP is flow type presentation. This study used DRP mapping to overall evaluation of CPM/PDD and collect product knowledge on easily readable format. When collecting and sharing product knowledge CPM/PDD method, without using any code or method to open decisions, more states that solutions are these and deviation between required properties and product properties are those. When using DRP mapping, it makes reasons and decisions behind solutions explicit. DRP map opens the designer's think flow, and it is easier to other designers to find why or on what stage solution or decision has been made. During this project, author was only member of design team, and it really needed some kind of product knowledge sharing format to use in possible further development. DRP map formed during project and determined questions which map answers opens the designer's think flow and makes design reasoning explicit, as Halonen et al. (2014, p. 703) has proposed. Map could always be more accurate and open every detail of designing and use a method to manage data to easily processable form as Lehtonen et al. (2016, p. 394) has suggested, but these methods were out of scope for this study. This study opened, on principle, reasons and relations between characteristics and required properties and tries to explain these on the map.

Approximate calculations and CFD simulation were used to determine the properties of characteristic. They both fit the CPM/PDD process very well and there wasn't any contradiction because the method is designed to take this kind of work account (Weber, 2014, p. 334). With approximate calculations there is always more accurate correlation on every situation and calculations can be done to cover every detail of product behaviour. The correlations presented in subchapter 4.3 were collected to cover main questions of product to be developed and give indicative answers. For those principles, correlations produced a sufficiently good results compared to results get from CFD simulated and measured values from build prototype. Even though calculations were firstly done to get initial scale of products behaviour which was used to validate the CFD simulation results. CFD softwares are complex and there is always possibility to forgot something so calculating initial scale of answer gives a better confidence to trust the simulation results. CFD simulation results were close to calculations results and measured from the prototype, excluding UPM pressure drop model. For scope of this development, heat exchanger's and ducting system's simulations gave sufficient answers and there wasn't need for more accurate answers. Unluckily the most time-consuming task, UPM pressure drop model, didn't succeed. Simplification of UPM were too heavy and still simulation time for each value was several days with used simulation machine. UPM system curve

for pressure and volume flowrate coupling can be done with computer with more computational power or using much more time to guess sufficient flow route's cross-sectional area.

Taguchi method was planned to use in prototype's testing to decrease the number of test runs. However, on this study, there wasn't need of decrease the test runs. Within the boundaries where test could be made there wasn't so many test runs that Taguchi method could have helped. With literature review and without a real experience how Taguchi method suits to CPM/PDD, author think that they will integrate each other well. Taguchi method decreases test runs, but also analyses the results and calculates variance between the results (Roy, 2010, p. 129). This helps defining the properties of product and find deviations of them to required properties and in conclusion it's an iterative method like CPM/PDD. Taguchi method seemed thorough approach to testing, and it would have been interesting to use it in real testing environment.

Author thinks that all used methods and tools suited well for the process and integrated to each other. They all covered a different area on development project and there wasn't really contradiction. However, as said before author was responsible for whole process and research, so there could be some perspectives that didn't come in mind or went unnoticed. One human's point of view is a small sample, and results could be different when research is reproduced or done in team.

REFERENCES

Adlin, N., 2022. *Formalisation of Information Flows to Support, Study of High-Variety, Low-Volume Manufacturing.* Tampere: Tampere University.

Alapassi, T., 2021. *Eaton UPS Liquid Cooling Concepts.* Espoo: Eaton Power Quality Oy.

Ansys Inc., 2021. *Ansys Fluent Fluid Simulation Software.* [Online] Available at: https://www.ansys.com/products/fluids/ansys-fluent [Accessed July 2022].

Ansys Inc., 2021. *Ansys SpaceClaim 3D Modeling Software.* [Online] Available at: https://www.ansys.com/products/3d-design/ansys-spaceclaim [Accessed July 2022].

Ansys, Inc., 2018. *Ansys Fluent Theory Guide.* Release 19.2 ed. Canonsburg: Ansys, Inc..

Ansys, Inc., 2018. *Ansys Fluent User's Guide.* Release 19.2 ed. Canonsburg: Ansys Inc..

ASHRAE Inc., 2014. *Particulate and Gaseous Contamination in Datacom Environments.* Second Edition ed. Atlanta: American Society of Heating, Refrigerating and Air-Conditioning Engineers.

ASHRAE Inc., 2015. *Heating, Ventilating, and Air-Conditioning Applications.* Atlanta: American Society of Heating, Refrigerating and Air-conditioning Engineers, Inc..

Autodesk Inc., 2014. *CFD Support and Learning.* [Online] Available at: https://knowledge.autodesk.com/support/cfd/learn-explore/caas/sfdcarticles/sfdcarticles/How-to-know-how-much-RAM-will-be-needed-for-a-Simulation-CFD-analysis.html [Accessed July 2022].

Basu, P., Kefa, C. & Jestin, L., 2000. *Boilers and Burners.* New York, Springer Science+Business Media, LCC.

Bell, I., Wronski, J., Quoilin, S. & Lemort, V., 2021. *CoolProp.* [Online] Available at: http://www.coolprop.org [Accessed June 2022].

Blessing, L., 2004. *DRM: A Design Research Methodology,* Berlin: Techical University of Berlin.

Çengel, Y. & Boles, M., 2015. *Thermodynamics An Engineering Approach.* Eighth edition ed. New York: McGraw-Hill Education.

Çengel, Y. & Cimbala, J., 2018. *Fluid Mechanics: Fundamentals and Applications.* Fourth Edition ed. New York: McGraw-Hill Education.

Chen, W. et al., 2018. *Cooling System of High -Power UPS Cabinet.* China, Patent No. CN207134861U.

Conrad, J., Köhler, C., Wanke, S. & Weber, C., 2008. *What is design knowledge from the viewpoint of CPM/PDD?.* Dubrovnik, Institute of Engineering Design/CAD, Saarland University.

Consultancy.eu, 2021. *Raw Material Prices and Supply Shortages skyrocket.* [Online] Available at: https://www.consultancy.eu/news/7143/raw-material-prices-and-supply-shortages-skyrocket-in-7-charts [Accessed July 2022].

Cory, W., 2005. *Fans & Ventilation: A Practical Guide.* Kidlington: Elsevier Science & Technology.

Daintith, J. & Rennie, R., 2005. *The Facts On File Dictionary of Mathematics.* Fourth Edition ed. New York: Marked House Books Ltd.

Darrelmann, H., Briest, R. & Ueffing, N., 2002. *Uninterruptible Power Supply (UPS) System with Primary Air Cooling.* United States, Patent No. US6424057B1.

Eaton Corp., 2011. *UPS Basics.* Raleigh: Eaton Corporation.

Eaton Corp., 2018. *Datasheet Power Xpert 9395P UPS 300-1200 kW.* Switzerland: Eaton EMEA Headquarters.

Eaton Corp., 2020. *P-151000047.* Espoo: Eaton Corporation, Electrical.

Eaton Corp., 2020. *Power Xpert 9395P 250-300 kVA UPS Technical Specification.* Rev009 ed. Espoo: Eaton Corporation.

Eaton Corp., 2020. *The Eaton UPS and Power Management Fundamentals Handbook.* Cleverland: Eaton Corporation.

Eaton Corp., 2022. *Eaton Power Xpert 9395 High Performance (9395P-300) UPS - 300kVA, 300kW Installation and Operation Manual.* Revision 08 ed. Raleigh: Eaton Corporation.

Eisenhauer, J., 2008. Degrees of Freedom. *Teaching Statistics,* 30(3), pp. 75-78.

European Patent Organisation, 2016. *Espacenet.* [Online] Available at: fi.espacenet.com [Accessed April 2022].

Fan, W., 2021. *UPS Power Supply Cabinet.* China, Patent No. CN213043294U.

Fatchurrohman, N. & Chia, S., 2017. *Performance of Hybrid Nano-micro Reinforced Mg Metal Matrix Composites Brake Calliper: Simulation Approach.* Pekan, IOP Publishing.

Fihmc, 2021. *Cmap.* [Online] Available at: https://cmap.ihmc.us/products/ [Accessed 8 July 2022].

Giuntini, L., 2011. *Modeling UPS Efficiency as a Function of Load.* Torremolinos, 2011 International Conference on Power Engineering, Energy and Electrical Drives.

Halonen, N., Lehtonen, T. & Juuti, T., 2014. *Impacts of Making Design Decision Sequence Explicit on NPD Project in Forest Machinery Company.* Espoo, NordDesign 2014.

Huang, J. & Gao, Y., 2018. *Special Vehicle Heat Dissipation System with UPS (Uninterrupted Power Supply) Device.* China, Patent No. CN107813752A.

Hunter, J., 2021. *Matplotlib: A 2D graphics environment.* [Online] Available at: https://matplotlib.org [Accessed July 2022].

Huntgeburth, J., Benke, T. & Ueffing, N., 2019. *Online UPS System with Combined Air and Water Cooling.* United States, Patent No. US20190379269A1.

Hwan, O. S., 2021. *UPS Self Cooling Device.* Korea, Patent No. KR20200127612A.

IEC, 2021. *IEC 62040-3.* Edition 3.0 ed. Geneva: International Electrotechnical Commission.

Lehtonen, T. ym., 2016. *Challeges and Opportunities in Capturing Design Knowledge.* Tampere, Springer, Cham.

Lienhard IV, J. & Lienhard V, J., 2019. *A Heat Transfer Textbook.* Fifth Edition ed. Cambridge: Phlogisto Press.

Lin, K., 2015. *Modularization UPS supply Vehicle.* China, Patent No. CN204701515U.

Liu, D., 2019. *UPS Uninterrupted Power Supply Water-Cooling Heat Dissipation Shell.* China, Patent No. CN209329773U.

Liu, M., Claridge, D. E. & Deng, S., 2003. *An air filter pressure loss model for fan energy calculation in air handling unit.* Chichester, John Wiley & Sons, Ltd.

Lähdesmäki, T. et al., 2009. *Menetelmäpolkuja humanisteille.* [Online] Available at: http://www.jyu.fi/mehu [Accessed 5 April 2022].

Paananen, J., Kärkkäinen, J. & Alapassi, T., 2021. *Required properties of cooling unit* [Interview] (August 2021).

Python Software Foundation, 2021. *Python.* [Online] Available at: https://www.python.org/downloads/windows/ [Accessed July 2022].

Qin, X. & Bao, Y., 2020. *UPS Power Box Convenient For Heat Dissipation.* China, Patent No. CN211209369U.

Ren, H., Chang, Y. & Li, Y., 2020. *UPS Power Supply Auxiliary Cooling Device.* China, Patent No. CN211880884U.

Roy, R., 2010. *A Primer on The Taguchi Method.* Second Edition ed. Dearborn: Society of Manufacturing Engineers.

Sadrehaghighi, I., 2021. *Mesh Sensitivity & Mesh Independence Study.* Mason: CFD Open Series.

Seppänen, O., 1996. *Ilmastointitekniikka ja sisäilmasto.* Espoo: Suomen LVI-liitto ry.

Taguchi, G., Chowdhury, S. & Wu, Y., 2005. *Taguchi's Quality Engineering Handbook.* Hoboken: Wiley & Sons, Ins..

VDI e. V., 2010. *VDI Heat Atlas.* Second Edition ed. Düsseldorf: Springer, Berlin, Heidelberg.

Versteeg, H. K. & Malalasekera, W., 2007. *An Introduction to Computational Fluid Dynamics,* Edinburgh: Pearson Education Limited.

Wang, H., Jia, Y. & Ma, L., 2021. *UPS Air Cooling Heat Dissipation Device.* China, Patent No. CN213152728U.

Weber, C., 2007. *Looking at "DFX" and "Product Maturity" from the Perspective of a New Approach to Modelling Product and Product Development Processes.* Germany, Institute of Engineering Design/CAD, Saarlanf University.

Weber, C., 2014. Modelling Products and Product Development Based on Characteristics and Properties. In: A. Chakrabarti & L. T. M. Blessing, eds. *An Anthology of Theories and Models of Design.* London: Springer, pp. 327-352.

Xiangyang, Y. & Huili, Y., 2021. *UPS (Uninterrupted Power Supply) with Efficient Heat Dissipation.* China, Patent No. CN215011275U.

Yin, R., 2018. *Case Study Research and Applications: Design and Methods.* Sixth Edition ed. Los Angeles: SAGE Publications.

Yogendra, J. & Pramod, K., 2012. *Energy Efficient Thermal Management of Data Centers.* First Edition ed. Atlanta: Springer.

APPENDIX A: REQUIRED PROPERTIES OF COOLING UNIT

Functional properties
Cools heat losses of UPS
Reduces floor print of a UPS system
Minimises the need of material and reduces costs of cooling equipment
Modular for better scalability for greater power UPS
Dimensioning temperature of ambient air is 20-23 °C
10-15 % over dimensioned cooling capacity
Heat transfer fluid is water
Prevents condensate water from entering UPS
Maintenance hatch which allows maintenance in top of UPS
Prevents hot air circulation
Serviceable from front
Standard interface to UPS
Allows hanging assembly to the roof
Allows use of flexible collar
Non-condensable

Efficiency
Cooling capacity can be controlled in the need of load, air and water temperature, and air humid
Minimized pressure loss
Better efficiency than CRAC unit

Strength, stiffness, stability
Sheet metal structure

Life-time, durability
Reduces the need of material compared to CRAC unit Lifetime expectation same as UPS (15-20 years)

Safety, reliability
Fault tolerant
Duplicated cooling
Connectable to remote control
Prevents leakage to entering UPS
Reliability is same than UPS alone
No need to move or lift heavy objects on maintenance
Prevents head knock

Spatial properties, weight
Width is same as UPM

Height with UPS is lower than 2500 mm
Doesn't cross back wall of UPS
Maximum overhang of frontend is 200 mm at the top of UPS

Aesthetic properties

Appearance is similar to the UPS's

Ergonomic properties

Can be installed at construction site

Manufacturing/Assembly/test properties

Parts operational tests in manufacturer
Operational tests can be done in Eaton factory
Product parts assembly in Eaton factory

Transportation properties

Has its own transport package
Transport package prevents dirt and dents
Minimized material of transport package

Maintenance and repair properties

Cleaning of unit can be done from front
Maintenance can be done from front
Maintenance can be done to 1 UPM per time

Compliance with regulations/standards

Complies with electrical safety regulations
Follows ASHRAE recommendations
Complies with ISO 9001 - Quality management standard
Complies with HVAC regulations
Complies with environmental standards
Complies with material and manufacturing standards

Environmental properties

Reduces environmental footprint
Does not contain hazardous materials and chemicals
Minimized material use
Favours local suppliers
Part manufacturing in countries with smaller environmental footprint
Uses recycled material

Resource consumption

Reduces the need of cooling capacity

Cost properties
Minimized manufacturing costs
Reduces costs compared to CRAC unit

APPENDIX B: PROJECT PLAN

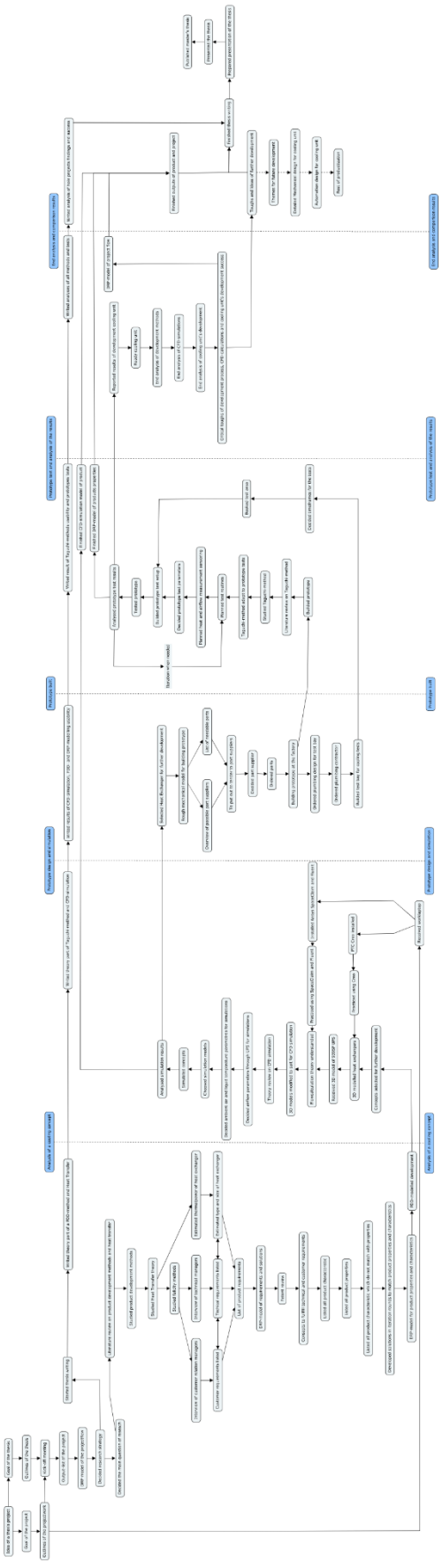

APPENDIX C: DRP MAP OF PRODUCT DEVELOPMENT